NUSC Technical Report 4683

# Operating Characteristics for Maximum Likelihood Detection of Signals in Gaussian Noise Of Unknown Level

## II. Phase-Incoherent Signals of Unknown Level

PETER G. CABLE
ALBERT H. NUTTALL
*Office of the Director of Science and Technology*


22 April 1974

NAVAL UNDERWATER SYSTEMS CENTER
*New London Laboratory*

## PREFACE

This research was conducted under NUSC Project No. A-752-05, "Applications of Statistical Communication Theory to Acoustic Signal Processing," Principal Investigator — Dr. A. H. Nuttall (Code TC), and Subproject and Task No. ZF 61 112 001, Program Manager — Dr. J. H. Huth (Chief of Naval Material, MAT-03L4).

The Technical Reviewer for this report was Dr. D. W. Hyde (Code TC1).

REVIEWED AND APPROVED: 22 April 1974

W. A. Von Winkle
Director, Science & Technology

The authors of this report are located at the New London Laboratory, Naval Underwater Systems Center, New London, Connecticut 06320.

UNCLASSIFIED

SECURITY CLASSIFICATION OF THIS PAGE (When Data Entered)

| REPORT DOCUMENTATION PAGE | | READ INSTRUCTIONS BEFORE COMPLETING FORM |
|---|---|---|
| 1. REPORT NUMBER<br>TR 4683 | 2. GOVT ACCESSION NO. | 3. RECIPIENT'S CATALOG NUMBER |
| 4. TITLE (and Subtitle)<br>OPERATING CHARACTERISTICS FOR MAXIMUM LIKELIHOOD DETECTION OF SIGNALS IN GAUSSIAN NOISE OF UNKNOWN LEVEL<br>II. PHASE-INCOHERENT SIGNALS OF UNKNOWN LEVEL | | 5. TYPE OF REPORT & PERIOD COVERED<br><br>6. PERFORMING ORG. REPORT NUMBER |
| 7. AUTHOR(s)<br>Peter G. Cable<br>Albert H. Nuttall | | 8. CONTRACT OR GRANT NUMBER(s) |
| 9. PERFORMING ORGANIZATION NAME AND ADDRESS<br>Naval Underwater Systems Center<br>New London Laboratory<br>New London, Connecticut 06320 | | 10. PROGRAM ELEMENT, PROJECT, TASK AREA & WORK UNIT NUMBERS<br>A-752-05, A-150-06<br>ZF 61 112 001, SF 43 452 001 |
| 11. CONTROLLING OFFICE NAME AND ADDRESS<br>Chief of Naval Material (MAT-03L4) and<br>Naval Ship Systems Command (SHP-037)<br>Washington, D. C. 20360 | | 12. REPORT DATE<br>22 April 1974<br>13. NUMBER OF PAGES<br>104 |
| 14. MONITORING AGENCY NAME & ADDRESS(if different from Controlling Office) | | 15. SECURITY CLASS. (of this report)<br>UNCLASSIFIED<br>15a. DECLASSIFICATION/DOWNGRADING SCHEDULE |

16. DISTRIBUTION STATEMENT (of this Report)

Approved for public release; distribution unlimited.

17. DISTRIBUTION STATEMENT (of the abstract entered in Block 20, if different from Report)

18. SUPPLEMENTARY NOTES

19. KEY WORDS (Continue on reverse side if necessary and identify by block number)

Detection and False Alarm Probabilities
Maximum Likelihood (ML) Detector
Noise-Level Estimation
Stationary Gaussian Noise

20. ABSTRACT (Continue on reverse side if necessary and identify by block number)

The detection and false alarm probabilities for maximum likelihood detection of nonfluctuating phase-incoherent signals in stationary Gaussian noise, where the received signal and noise levels are unknown, are derived and evaluated. This procedure is carried through for two cases involving different assumptions about the received signals. In the first case, the signal amplitudes in M potential-signal observations are assumed to be different and unknown values for each sample. In the second case, the signal amplitudes, although unknown, are assumed to be the same for all M observations.

DD FORM 1 JAN 73 1473 EDITION OF 1 NOV 65 IS OBSOLETE

UNCLASSIFIED

SECURITY CLASSIFICATION OF THIS PAGE (When Data Entered)

20. (Cont d).

Noise-level estimation in the maximum likelihood technique is improved if extra samples known to consist of noise-alone are available. For M observations of signal-plus-noise or noise and N observations of noise-alone, the performance of the maximum likelihood detector for assumed-unequal signal amplitudes can be obtained analytically, and curves of detection probability versus signal-to-noise ratio, with the false alarm probability as a parameter, are presented for M and N ranging, respectively, from 1 to 10 and 1 to 20. The performance of the maximum likelihood detector for assumed-equal signal amplitudes is not amenable to a closed-form solution, however, and simulation of receiver performance has been carried out in this second case for M and N covering the ranges referred to above.

Curves of signal-to-noise ratio required for 0.5 detection probability are presented for the unequal- and equal-amplitude processors for several specified values of false alarm probability. Detection performance for both maximum likelihood detectors generally improves noticeably as N is increased from unity. For very small false alarm probabilities, this improvement is maintained until N gets larger than 10.

# TABLE OF CONTENTS

## LIST OF TABLES



## LIST OF ILLUSTRATIONS

LIST OF ILLUSTRATIONS (Cont'd)

## LIST OF ILLUSTRATIONS (Cont'd)

LIST OF ILLUSTRATIONS (Cont'd)

## LIST OF ABBREVIATIONS

| | |
|---|---|
| ML | Maximum Likelihood |
| PDF | Probability Density Function |
| LR | Likelihood Ratio |
| GLR | Generalized Likelihood Ratio |
| UA | Unequal Amplitude |
| EA | Equal Amplitude |
| CFAR | Constant False Alarm Rate |

## LIST OF SYMBOLS

| | |
|---|---|
| $P_F$ | False alarm probability |
| $P_D$ | Detection probability |
| $H_1$ | Signal-present hypothesis |
| $H_o$ | Signal-absent hypothesis |
| M | Number of potential-signal samples |
| N | Number of noise-alone samples |
| $V_k(t)$ | Complex envelope of received waveform on k-th branch |
| $S_k(t)$ | Complex envelope of received signal on k-th branch |
| $N_k(t)$ | Complex envelope of received noise on k-th branch |
| $\tilde{V}_j(t), \tilde{N}_j(t)$ | Complex envelope of received noise on j-th noise-alone branch |
| $F_k(t), \tilde{F}_j(t)$ | Complex envelopes of receiver filters on the k-th potential-signal branch and j-th noise-alone branch |
| $z_k, \tilde{z}_j$ | Receiver filter outputs |
| $\sigma^2$ | Assumed filter output noise variance |

## LIST OF SYMBOLS (Cont'd)

| | |
|---|---|
| $\mathbf{R}$ | Observation vector |
| $p_k$ | Probability density under hypothesis $H_k$ |
| $A_k$ | Assumed amplitude of filter output signal component |
| $\psi_k$ | Assumed phase of filter output signal component |
| r | Scale factor in UA test |
| $\alpha$ | rM/N |
| $d_k^2/2$ | Branch signal-to-noise (power) ratio |
| $d_T^2/2$ | Total signal-to-noise (power) ratio |
| $R_{k\ell}$ | Noise correlation function |
| $E_k$ | Received signal energy on k-th branch |
| $N_d$ | Double-sided noise density level |
| ${}_1F_1$ | Confluent hypergeometric function |
| F | Hypergeometric function |
| $m, \tilde{m}$ | Sample means |
| $S, \tilde{S}$ | Sample powers |
| Var | Sample variance |
| $\gamma$ | Scale factor in EA GLR test |
| Carat | ML estimate |
| Overbar | Ensemble average |
| * | Conjugate |

# OPERATING CHARACTERISTICS FOR MAXIMUM LIKELIHOOD DETECTION OF SIGNAL IN GAUSSIAN NOISE OF UNKNOWN LEVEL

## II. PHASE-INCOHERENT SIGNALS OF UNKNOWN LEVEL

### INTRODUCTION

In the first report of this series on the operating characteristics for detecting unknown-level signals in Gaussian noise (reference 1), maximum likelihood (ML) detection of signals of known form in additive Gaussian noise of unknown level was analyzed. For the case of coherent signals corrupted by noise of unknown level, it was shown that the ML detector is optimum in the sense that, of all processors yielding a specified false-alarm probability $P_F$ without knowledge of absolute levels, the ML detector is uniformly most powerful.

In this report, the previous study is continued to cover two cases of ML detection of nonfluctuating, phase-incoherent signals in noise of unknown level. Again, as in the case of the previous study, the ML detectors will be shown to possess the important property of maintaining a specified $P_F$ irrespective of the actual noise level. However a major difference exists between the present and previous analyses. Whereas, for the coherent signals, the ML detector is optimum for the class of detectors invariant to level scaling, no such conclusion is possible for the phase-incoherent signals. Because of this inability to resolve the question of performance quality, we shall consider, but not thoroughly analyze, several reasonable, albeit, ad hoc processors. That is, we shall discuss and compare the performances of ML processors with other, heuristically obtained, processors. Relevant past work on this problem is furnished by reference 2 for the special case of a single signal sample.

In the analysis that follows, it is supposed that

1. sufficient knowledge of the signals is available to allow filtering the input to the receiving system, thereby removing noise outside the signal band, and

2. the sampled outputs of the system filters are statistically independent.

In order to restructure the originally nonparametric problem into a parametric form, it is further assumed that the noise is Gaussian and stationary.

In determining the ML detectors, the values of the unknown parameters are estimated by separately maximizing the probability density functions (PDFs) for the signal-present hypothesis $H_1$ and the signal-absent hypothesis $H_0$. It is reasonable to expect that the noise-level-estimation procedure is improved if extra samples consisting of noise-alone are available. This possibility which is of practical importance, is considered here. Indeed, in one case, the ML detector has meaning only if extra noise-alone samples are available.

The likelihood ratio (LR), formed using the ML estimates in the PDFs, results in a generalized likelihood ratio (GLR) test. In this report, the GLR procedure is used for two cases involving different assumptions about the signal. In the first case, the signal amplitudes, when signal is present, are assumed different and unknown from sample to sample. This will be referred to as the unequal amplitude (UA) case. In the second case, the signal amplitudes, although unknown, are assumed to be the same for all samples. This will be referred to as the equal amplitude (EA) case. In both cases, the signal amplitudes are nonfluctuating.

The performance characteristics of the ML detector for the UA case can be obtained analytically, regardless of the actual distribution of signal amplitudes, and extensive results are presented. For the EA case, these performance characteristics are not amenable to closed-form solution, however, and receiver-performance simulation has been conducted.

In the following sections, the problem is stated in detail, and ML detectors for the UA and EA cases are derived and discussed. The performance characteristics of the UA processor are derived, and a description of the simulation procedure for the EA processor is given. To ascertain the usefulness of the ML detectors, the detection performances of several ad hoc processors, whose $P_F$ is invariant to noise-level scaling, are also briefly considered.

## PROBLEM STATEMENT

It is supposed that a detection system performs M observations of a received signal-plus-noise or noise-alone process having waveforms

$$\mathrm{Re}\left\{V_k(t)\ \exp(i2\pi f_k t)\right\}, \quad 1 \le k \le M\ , \tag{1}$$

where

$$V_k(t) = \begin{cases} S_k(t) + N_k(t)\ , & H_1 \\ N_k(t)\ , & H_o \end{cases}\ , \quad 1 \le k \le M\ . \tag{2}$$

In (2), $S_k(t)$ and $N_k(t)$ are the complex envelopes of the received signal and Gaussian noise waveforms, respectively, for the k-th observation, and, in (1), $f_k$ is the center frequency used in the k-th observation. We note that the M observations referred to above may denote, for example, successive observation intervals in time, simultaneous observations either in different frequency bands or in different spatial locations, or, indeed, combinations of these. These M observations are called the potential-signal observations.

Further, it is assumed that N additional observations are available in which it is known that only noise is present. For these latter observations, the received waveforms are

$$\mathrm{Re}\left\{\tilde{V}_j(t)\ \exp(i2\pi\tilde{f}_j t)\right\}, \quad 1 \le j \le N, \tag{3}$$

where

$$\tilde{V}_j(t) = \tilde{N}_j(t), \quad 1 \le j \le N, \tag{4}$$

for both $H_1$ and $H_0$.

Following standard procedures (reference 3), receiver processing consists of computing the complex quantities

$$\int dt\ F_k(t)\ V_k(t) \equiv z_k = x_k + iy_k, \quad 1 \le k \le M, \tag{5}$$

and

$$\int dt\ \tilde{F}_j(t)\ \tilde{V}_j(t) \equiv \tilde{z}_j = \tilde{x}_j + i\tilde{y}_j, \quad 1 \le j \le N. \tag{6}$$

(Integration is over the range of nonzero integrand.) $\{F_k(t)\}$ and $\{\tilde{F}_j(t)\}$ are filters that need not be optimum (matched) in any sense. This generality in filter specification allows for mismatch in frequency or in time, or both, between transmission source and receiver. Because $\{N_k(t)\}$ and $\{\tilde{N}_j(t)\}$ are Gaussian processes, $\{z_k\}$ and $\{\tilde{z}_j\}$ are complex Gaussian random variables. They are proportional to samples of the complex envelopes at the filter outputs.

At this point, we restrict attention to the case where the M + N filter outputs are statistically independent of each other and of equal (but unknown) variance $\sigma_0^2$ (see appendix A). The above restriction, for example, would be pertinent when the receiver filters are disjoint in time or frequency and of equal gain, and when the noise spectrum is substantially flat over the entire detection system filter bank.

To summarize the discussion thus far, we are considering an observation vector $\mathbf{R}$ of independent Gaussian random variables:

$$\mathbf{R}^T = \left[x_1\ y_1 \cdots x_M\ y_M\ \tilde{x}_1\ \tilde{y}_1 \cdots \tilde{x}_N\ \tilde{y}_N\right]. \tag{7}$$

On the basis of $\mathbf{R}$, we are to decide between hypotheses $H_1$ (signal present in $\{x_k, y_k\}$) and $H_o$ (signal absent in $\{x_k, y_k\}$). The variance $\sigma_o^2$ associated with $\mathbf{R}$ is unknown; nevertheless we wish to consider processing of $\mathbf{R}$ that will ensure a specified $P_F$ irrespective of the magnitude of $\sigma_o^2$. As already noted, the ML technique is used to estimate all unknown parameters, and the GLR (references 3,4) is used to determine a test statistic. This procedure is discussed in the next section.

## ML ESTIMATION PROCEDURE AND ML DETECTOR

Under hypothesis $H_o$, the PDF of observation $\mathbf{R}$, conditioned on an assumed value of noise variance $\sigma^2$, is (appendix A)

$$p_o\left(\mathbf{R}\middle|\sigma^2\right) = \prod_{k=1}^{M}\left\{\frac{1}{2\pi\sigma^2}\exp\left[-\frac{x_k^2+y_k^2}{2\sigma^2}\right]\right\}\prod_{j=1}^{N}\left\{\frac{1}{2\pi\sigma^2}\exp\left[-\frac{\tilde{x}_j^2+\tilde{y}_j^2}{2\sigma^2}\right]\right\}. \tag{8}$$

The ML estimate, denoted by carats, of $\sigma_o^2$ under hypothesis $H_o$ is that value of $\sigma^2$ which maximizes (8), namely,

$$2\hat{\sigma}^2 = \frac{\sum_{k=1}^{M}\left(x_k^2+y_k^2\right)+\sum_{j=1}^{N}\left(\tilde{x}_j^2+\tilde{y}_j^2\right)}{M+N} = \frac{\sum_{k=1}^{M}\left|z_k\right|^2+\sum_{j=1}^{N}\left|\tilde{z}_j\right|^2}{M+N}, \tag{9}$$

which is proportional to the total sample power over all $M+N$ samples. Substitution of (9) in (8) yields

$$\max_{\sigma^2} p_o\left(\mathbf{R}\middle|\sigma^2\right) = \left(e\pi\frac{\sum_{k=1}^{M}\left|z_k\right|^2+\sum_{j=1}^{N}\left|\tilde{z}_j\right|^2}{M+N}\right)^{-(M+N)}. \tag{10}$$

Under hypothesis $H_1$, the PDF of $\mathbf{R}$, conditioned on assumed values of signal means and $\sigma^2$, is (appendix A)

$$p_1\left(\mathbf{R}\middle|\sigma^2,\mathbf{A},\psi\right)=\prod_{k=1}^{M}\left\{\frac{1}{2\pi\sigma^2}\exp\left[-\frac{\left(x_k-A_k\cos\psi_k\right)^2+\left(y_k-A_k\sin\psi_k\right)^2}{2\sigma^2}\right]\right\} \tag{11}$$

$$\cdot\prod_{j=1}^{N}\left\{\frac{1}{2\pi\sigma^2}\exp\left[-\frac{\tilde{x}_j^2+\tilde{y}_j^2}{2\sigma^2}\right]\right\},$$

where, denoting ensemble averages on the noise by overbars, the means are (from (A-4))

$$\bar{z}_k=\bar{x}_k+i\bar{y}_k\equiv A_k\exp\left(i\psi_k\right),\quad 1\le k\le M, \tag{12}$$

and

$$\mathbf{A}\equiv\left[A_1\cdots A_M\right]^T,\quad \psi\equiv\left[\psi_1\cdots\psi_M\right]^T. \tag{13}$$

The ML estimate $\hat{\sigma}^2$ obtained under hypothesis $H_1$ is (from (11))

$$2\hat{\sigma}^2=\frac{\sum_{k=1}^{M}\left|z_k-A_k\exp\left(i\psi_k\right)\right|^2+\sum_{j=1}^{N}\left|\tilde{z}_j\right|^2}{M+N}. \tag{14}$$

Substituting (14) in (11), we obtain

$$\max_{\sigma^2}p_1\left(\mathbf{R}\middle|\sigma^2,\mathbf{A},\psi\right)=\left(e\pi\frac{\sum_{k=1}^{M}\left|z_k-A_k\exp\left(i\psi_k\right)\right|^2+\sum_{j=1}^{N}\left|\tilde{z}_j\right|^2}{M+N}\right)^{-(M+N)} \tag{15}$$

This function, which pertains to hypothesis $H_1$, can be further maximized by choice of assumed signal amplitudes $\mathbf{A}$ and phases $\psi$. To proceed with this program, we distinguish two cases pertaining to different assumptions about the signal amplitudes $\{A_k\}$. The first case, UA, will apply to the situation

where each $\{A_k\}$ is allowed to be different; the second case, EA, will apply to the situation where each $\{A_k\}$ is assumed to be the same unknown value; that is, $A_k = A$, $1 \le k \le M$.

For the UA case, the ML estimates of signal amplitudes and phases are, upon use of (15),

$$\hat{A}_k = |z_k| , \quad \hat{\psi}_k = \arg(z_k) , \quad 1 \le k \le M . \tag{16}$$

Substitution of the ML estimates, (16), in (15) gives

$$\max_{\sigma^2, \mathbf{A}, \psi} p_1(\mathbf{R}|\sigma^2, \mathbf{A}, \psi) = \left( e\pi \frac{\sum_{j=1}^{N} |\tilde{z}_j|^2}{M+N} \right)^{-(M+N)} . \tag{17}$$

A GLR test,

$$\frac{\max_{\sigma^2, \mathbf{A}, \psi} p_1(\mathbf{R}|\sigma^2, \mathbf{A}, \psi)}{\max_{\sigma^2} p_o(\mathbf{R}|\sigma^2)} \underset{H_o}{\overset{H_1}{\gtrless}} \text{threshold} , \tag{18}$$

where hypothesis $H_1$ is declared true if the upper inequality is satisfied, and hypothesis $H_o$ is declared true if the lower inequality is satisfied, can now be constructed. For the UA case, GLR test (18) is expressible as

$$\frac{1}{M} \sum_{k=1}^{M} |z_k|^2 \gtrless r \frac{1}{N} \sum_{j=1}^{N} |\tilde{z}_j|^2 , \quad M \ge 1, \; N \ge 1 , \tag{19}$$

where $r (\ge 0)$ is a constant. The test states that the sums of squared-envelope samples at the filter outputs for potential-signal samples and noise-alone samples be compared.

Test (19), which when implemented is the UA processor, depends explicitly on the availability of noise-alone samples; that is, if $N = 0$, a test different from the one above must be formulated. It is noted that implementing the UA processor, (19), results in a constant false alarm rate (CFAR) receiver, since both sides of the test can be scaled arbitrarily for noise-alone without changing the result of the test.

The EA case can be handled similarly. The ML estimates of the signal amplitude and phases, which are available from (15), follow:

$$\hat{A} = \frac{1}{M}\sum_{k=1}^{M}|z_k|\,, \tag{20}$$

which is the average envelope for the potential-signal samples, and

$$\hat{\psi}_k = \arg(z_k)\,, \quad 1 \le k \le M\,. \tag{21}$$

Substituting ML estimates (20) and (21) in (15), we obtain

$$\max_{\sigma^2,\mathbf{A},\boldsymbol{\psi}} p_1\left(\mathbf{R}\middle|\sigma^2,\mathbf{A},\boldsymbol{\psi}\right) = \left(e\pi\frac{\sum_{k=1}^{M}|z_k|^2 - \frac{1}{M}\left(\sum_{k=1}^{M}|z_k|\right)^2 + \sum_{j=1}^{N}|\tilde{z}_j|^2}{M+N}\right)^{-(M+N)} \tag{22}$$

The GLR in this case then becomes

$$\mathrm{GLR} = \left(\frac{\sum_{k=1}^{M}|z_k|^2 + \sum_{j=1}^{N}|\tilde{z}_j|^2}{\sum_{k=1}^{M}|z_k|^2 - \frac{1}{M}\left(\sum_{k=1}^{M}|z_k|\right)^2 + \sum_{j=1}^{N}|\tilde{z}_j|^2}\right)^{M+N}, \tag{23}$$

and the GLR test can be written in the form

$$\left(\sum_{k=1}^{M}|z_k|\right)^2 \gtrless \gamma\left(\sum_{k=1}^{M}|z_k|^2 + \sum_{j=1}^{N}|\tilde{z}_j|^2\right), \quad M \ge 1,\ N \ge 0\,, \tag{24}$$

where $\gamma$ is a threshold (scale factor). The left side of (24) is the square of the sum of envelopes at the potential-signal filter outputs. The right side is proportional to the sum of squared envelopes of all the filter outputs.

Test (24), which when implemented is the EA processor, is a CFAR test. It becomes meaningless for the situation $M = 1$, $N = 0$, and, of course, no realization of a CFAR processor is possible in this instance. The test is

similar in form to the GLR test obtained for phase-coherent signals in Gaussian noise of unknown level (reference 1). The difference between the tests for the phase-coherent and the phase-incoherent cases is that, in the former test, phase information is preserved in the samples, while in the latter test, (24), only the sample envelopes are used.

We may note one further point: For the situation $M = 1$ $(N \geq 1)$, the UA processor, (19), and the EA processor, (24), treat the available observations identically. This observation is important because not only is the $M = 1$ situation of considerable practical interest, but also, as will be shown in the next section, performance for $M = 1$ for the EA processor is thereby amenable to a complete analytical treatment. (The UA processor analysis is tractable for all values of M and N.)

## EVALUATION OF UA AND EA PROCESSOR PERFORMANCES

The evaluation of the performance of the GLR test, (19), for the UA case, although tractable, is lengthy, and the derivation is carried through in detail in appendix B. One form for the probability of detection $P_D$ obtained in appendix B is

$$P_D = 1 - \left(\frac{\alpha}{1+\alpha}\right)^M \exp\left(-\frac{d_T^2}{2}\,\frac{1}{1+\alpha}\right) \sum_{k=0}^{N-1} \binom{M-1+k}{k} (1+\alpha)^{-k}\, {}_1F_1\left(-k; M; -\frac{d_T^2}{2}\,\frac{\alpha}{1+\alpha}\right), \quad (25)$$

where ${}_1F_1$ is the confluent hypergeometric function and $\alpha \equiv rM/N$. The total signal-to-noise ratio (power) parameter $d_T^2/2$ appearing above is given by

$$\frac{1}{2}\,d_T^2 \equiv \sum_{k=1}^{M} \left|\frac{1}{2}\,d_k^2\right| = \sum_{k=1}^{M} \frac{\left|\int dt\, F_k(t)\, S_k(t)\right|^2 / 2}{\frac{1}{2}\iint dt\, du\, F_1(t)\, F_1^*(u)\, R_{11}(t-u)}\,, \quad (26)$$

where $S_k(t)$ is the actual received signal complex envelope on the k-th observation, and

$$\overline{N_k(t)\, N_\ell^*(u)} = R_{k\ell}(t-u)\,, \quad 1 \leq k, \ell \leq M\,, \quad (27)$$

is the actual complex-envelope noise crosscorrelation on the potential-signal samples. In (26), $F_k(t)$ is the complex envelope of the receiver filter employed on the k-th potential-signal branch.

For the special case of white noise and equal-gain* matched filters,

$$R_{11}(\tau) = 4N_d\,\delta(\tau)\ , \quad F_k(t) = S_k(t)/E_k^{1/2}\ , \quad 1 \le k \le M\ , \tag{28}$$

where $E_k$ is the received signal energy on the k-th observation and $N_d$ is the double-sided noise power density spectral level. In this instance, there follows

$$\frac{1}{2}\,d_k^2 = \frac{\left|\int dt\,|S_k(t)|^2\right|^2 \Big/ (2E_k)}{\frac{1}{2}\int dt\left(|S_1(t)|^2/E_1\right)4N_d} = \frac{E_k}{2N_d} \tag{29}$$

and

$$\frac{1}{2}\,d_T^2 = \frac{1}{2N_d}\sum_{k=1}^{M} E_k \equiv \frac{E_T}{2N_d} = \frac{E_T}{N_o}\ , \tag{30}$$

where $N_o$ is the single-sided noise power density spectral level. The quantity $d_k^2/2$ can be interpreted as the output signal-to-noise ratio of the filter on the k-th potential-signal branch; it is proportional to the received signal power on the k-th branch. Also, $d_T^2/2$ can be interpreted as the total system output signal-to-noise ratio; since $d_T^2/2$ is proportional to the total received signal energy $E_T$, then $10\log\left(d_T^2/2\right)$ can be used as a decibel measure of performance. A difference in the required decibel level between two processors (for example, different M and/or N) measures directly the difference in input signal-to-noise ratio in decibels required for the two processors to realize the same $P_F$ and $P_D$.

From (30), we note that the exact way that the total received signal energy $E_T$ is actually fractionalized into the observation branches is not important; only $E_T$ affects UA processor performance. Thus the UA processor is robust with respect to actual signal energy fractionalization; it represents an attainable level of performance regardless of the exact conditions.

---

*The normalization in (28) makes the filter gains, as measured by $\int dt\,|F_k(t)|^2$, independent of k and makes $\sigma_{kk}^2$ independent of k, as required by (A-13).

When $d_T$ is set equal to zero in formula (25) for $P_D$, we obtain

$$P_F = 1 - \left(\frac{\alpha}{1+\alpha}\right)^M \sum_{k=0}^{N-1} \binom{M-1+k}{k} (1+\alpha)^{-k} . \tag{31}$$

An alternative form for $P_D$ is obtained in appendix B and is given by

$$P_D = 1 - \frac{\alpha}{1+\alpha} \exp\left(-\frac{d_T^2}{2}\frac{1}{1+\alpha}\right) \sum_{k=0}^{N-1} (1+\alpha)^{-k} \, {}_1F_1\left(-k;1;-\frac{d_T^2}{2}\frac{\alpha}{1+\alpha}\right)$$

$$+ (1+\alpha)^{-N} \exp\left(-\frac{d_T^2}{2}\frac{1}{1+\alpha}\right) \sum_{k=1}^{M-1} \binom{N-1+k}{k} \left(\frac{\alpha}{1+\alpha}\right)^k {}_1F_1\left(1-N;k+1;-\frac{d_T^2}{2}\frac{\alpha}{1+\alpha}\right) . \tag{32}$$

For $d_T = 0$, we obtain from (32)

$$P_F = (1+\alpha)^{-N} \sum_{k=0}^{M-1} \binom{N-1+k}{k} \left(\frac{\alpha}{1+\alpha}\right)^k . \tag{33}$$

Comparison of the alternative expressions for $P_F$ indicates that, computationally, (31) is more efficient for $M > N$, whereas (33) is better suited for $N > M$. Also (33) possesses only positive terms.

For the UA processor, as $N \to \infty$, the expressions (25), (31), (32), and (33) for $P_D$ and $P_F$ tend to the corresponding forms obtained for envelope-squared detection with known-noise level (reference 3), as indeed they must, because ML estimators are consistent (see appendix B).

Let us consider now the EA processor. It has already been noted that the EA and UA processors are identical for the situation $M = 1$ and any $N \geq 1$. Thus the $P_D$ and $P_F$ formulas, assembled above, also are applicable to the EA processor performance for $M = 1$. One other analytical result for the EA processor has been obtained: In appendix C, it is shown that for $M = 2$ and arbitrary N

$$P_F = \left\{ \begin{array}{ll} \dfrac{\Gamma\left(\frac{3}{2}\right)\Gamma(N+2)}{\Gamma\left(N+\frac{3}{2}\right)} (2\gamma)^{1/2} \left(1-\frac{\gamma}{2}\right)^{N+1/2} , & 1 \leq \gamma \leq 2 \\ (1-\gamma)^N (1+N\gamma) + N(N+1)\frac{\gamma^2}{3}\left(1-\frac{\gamma}{2}\right)^{N-1} F\left(1-N,\frac{3}{2};\frac{5}{2};\frac{\gamma}{2-\gamma}\right), & 0 \leq \gamma \leq 1 \end{array} \right\} , \tag{34}$$

where $\gamma$ is the scale factor in EA GLR test (24), and F is the Gaussian hypergeometric function. The factor $\gamma$ need take values only in the range (0, M); see appendix C for the argument for M = 2.

Since, for general M and N, $P_D$ and $P_F$ can not be analytically evaluated for the EA processor, a simulation approach to determine performance was adopted. Specifically, in order to determine $\gamma$ in GLR test (24), which realizes specified $P_F$ values of .01 and .001, 40,000 independent trials were conducted for the EA processor. The method of estimating the .99 and .999 quantiles is discussed in appendix D.

Since the determination of $\gamma$ for a specified $P_F$ was accomplished by a simulation based on 40,000 independent trials, the estimate of $\gamma$ has a nonzero standard deviation, which was also estimated by simulation. In the next section, the detection characteristics for the EA processor are associated with the estimated $\gamma$, and are themselves based on 10,000 independent trials. Therefore, in order to determine the reliability of the plotted curves, $P_D$ has also been determined when the estimated $\gamma$ is changed by $\pm 1$ standard deviation, as determined above. Additionally, the standard deviation of the estimate of $P_D$, as a result of statistical fluctuations based upon 10,000 independent trials, has been added. Specifically, when the true value of the detection probability is $P_D$, the standard deviation of the simulation estimate is $\left(P_D(1 - P_D)/10,000\right)^{1/2}$. The resultant uncertainty is indicated in the EA processor performance plots by broken lines parallel to the central curve. We may note that the detection characteristics need not be confined to the uncertainty region described; rather, this ribbon describes where $P_D$ lies with fair confidence, though it may actually deviate beyond the ribbon.

## RESULTS

Required values of scale factor r in UA test (19) are presented in table B-1 for $P_F = 10^{-n}$, n = 2, 3, 4, 6, 8, when M and N are varied as follows: M = 1, 2, 3, 4, 5, 10 and N = 1, 2, 3, 4, 6, 10, 20, $\infty$. The performance of the UA processor is shown in figures 1-30, where $P_D$ is plotted versus $d_T$ (which is a voltage measure of the total signal-to-noise ratio), with $P_F$, M, and N as parameters. Each figure in this sequence depicts performance over the range of N, indicated above, for a given $P_F$ and M. The entire sequence of figures illustrates performance for $P_F = 10^{-n}$, n = 2, 3, 4, 6, 8, and M = 1, 2, 3, 4, 5, 10. The curves for N = $\infty$ (known-noise level) have also been included for comparison.

Over the range of $P_F$ considered, UA processor performance degrades sharply when N is too few (typically, fewer than about 10 noise-alone samples). Because of the extremely high threshold scale factors r required to ensure low $P_F$, this degradation becomes increasingly severe as $P_F$ is lowered. This is illustrated for the UA processor with N = 1, where the required threshold (scale factor) r is well approximated by

$$r \cong \frac{1}{P_F} - \frac{M+1}{2M} \quad (N = 1) \tag{35}$$

when $P_F << 1$. Thus small values of $P_F$ require exceedingly large r. For example, $P_F = 10^{-6}$ requires r approximately equal to $10^6$. (See table B-1 for other values of N.)

The improvement attainable in UA processor performance by increasing N is more obvious in figures 31-36. These figures are plots of required $d_T$ in decibels (that is, $10 \log\left(d_T^2/2\right)$) to realize $P_D = .5$, with $P_F$ and M as parameters, versus N. The horizontal tic marks at the right edge of these figures show the required value of $d_T$ in decibels for $N = \infty$ and are, therefore, the asymptotes of the curves. These figures also indicate that, to achieve a given $P_D$ for a specified $d_T$, N must be increased as $P_F$ is lowered.

If the required $P_D$ is increased, the necessary values of signal-to-noise ratio $d_T$ in figures 31-36 would increase also. However, to a first approximation, the decibel difference between the values of $d_T$ required at finite N versus those required at $N = \infty$ are relatively independent of $P_D$, at least for $N \geq 6$. Thus, for a range of $P_D$ including approximately (.5, .99), the additional signal-to-noise ratio required at moderate values of N versus those required at $N = \infty$ depends only on N, M, and $P_F$. If the curves in figures 1-30 were straight lines emanating from a common intersection on the ordinate, this behavior would be precisely correct. Although this is not true for figures 1-30, an extended region of $P_D$, where extrapolations of the curves back to $d_T = 0$ approximately satisfy this requirement, is evident; in this region, the decibel difference discussed above is relatively independent of $P_D$. No other independencies of N, M, or $P_F$ have been observed.

It is apparent from figures 1-36 that UA processor performance steadily degrades as the signal energy fractionalization increases, that is, as M increases, for fixed $d_T$. For example, for $P_F = 10^{-2}$, $P_D = .5$, and N = 2, the required value of $d_T$ is 10.4 for M = 5 versus 5.4 for M = 1, a 5.7-dB increase. The situation is somewhat alleviated for larger N; for

example, at $P_F = 10^{-2}$, $P_D = .5$, and $N = 10$, the required value of $d_T$ is 4.8 for $M = 5$ versus 3.2 for $M = 1$, only a 3.5-dB increase. Also the degradation is not quite so severe for smaller $P_F$; for example, at $P_F = 10^{-8}$, $P_D = .5$, and $N = 20$, the required values of $d_T$ for $M = 5$ versus $M = 1$ differ by 3.1 dB.

When comparing the results of this report with those in reference 1, note that a direct overlay does not constitute a valid comparison. For example,* figure 17 in reference 1, when overlaid upon figures 31-36 here, yields curves that intersect for some values of N. The reason is that N, when specified here, corresponds to 2N degrees of freedom in the random variable on the right side of test (19); on the other hand, the variable N in reference 1 corresponds to only N degrees of freedom. Before a valid comparison is drawn, this factor of 2 difference in the interpretation of N in the two reports must be accounted for. This observation is also consistent with the fact that the envelope of the output of a narrowband filter need be sampled only half as often as a low-pass process with the same (positive-frequency) bandwidth as that of the narrowband filter. If the potential-signal (matched) filter outputs are each sampled once, as indicated in (5), only this correction is needed in translating results. It will then be found that the curves in reference 1 lie everywhere below those of figures 31-36; that is, phase-coherent operation yields better performance than phase-incoherent operation, as is to be expected.

Estimated values of the threshold $\gamma$ for the EA processor are given in table D-1. As noted in the previous section, the values must be estimated by simulation and, thus, are not exact (except for $M = 2$, which is treated in appendix C).

Simulated performance of the EA processor is shown in figures 37-46; there $P_D$ has been plotted versus $d_T$ for $P_F = 10^{-2}$ and $10^{-3}$, with M and N as parameters. It should be emphasized that, for a given $d_T$, all the M signal amplitudes were taken to be equal in the simulation. The performance curves for $M = 1$ have not been presented because, for this case, the UA and EA processors are equivalent; for $M = 1$, figures 1-5 define the performance of the UA and EA processors. Figures 37-46 present EA processor performance for $M = 2, 3, 4, 5, 10$ and $N = 1, 2, 3, 4, 6, 10, 20$. (An analytical method of determining performance for $N = \infty$ is described in appendix D; it was not pursued here, however.)

---

*Notice that the decibel definition of signal-to-noise ratio in reference 1, eq. (17) et seq., differs from that adopted here.

Consistently, EA processor performance is superior to that of the UA processor.* It is to be noted that the smaller the N, the greater the superiority of the EA processor. The principal reason for this performance difference (other than the equal signal amplitudes used in the simulation) can be seen in the forms of the EA and UA tests, (24) and (19), respectively. The EA test (except for M = 1) also uses the potential-signal samples being tested to help form a better noise-level estimate, that is, the right side of (24); the UA processor restricts itself by using noise-alone samples to form a noise-level estimate, that is, the right side of (19). For small N, the use of M+N samples significantly improves the noise-level estimates. As N is made larger, the potential-signal samples become less important in estimating the noise level.

Another example of this effect is evident from the performance of the EA processor for fixed $P_F$ and $d_T$, say $10^{-2}$ and 10, respectively. Then, for N = 0, as M increases from 2 to 4, for example, $P_D$ improves from .04 to .18. For N = 1, the change in $P_D$ is from .53 to .62; for N = 2, $P_D$ decreases from .95 to .925; and for N > 2, performance degrades as M increases from 2 to 4. The reason for this effect is that for large N, where a good estimate of noise power results, fractionalization of a fixed total amount of signal energy into more channels hampers EA processor performance because the recombination of signal energy is incoherent. However, for N = 0, where a noise-alone power estimate is not available, fractionalization of a fixed total-signal energy into more channels affords some (albeit poor) estimate of the noise power, thereby establishing a threshold for specified $P_F$. (Probably if too large an M is chosen, the fractionalization will be too great and performance will degrade with increasing M.) For intermediate N, such as N = 1, a transition between these two effects takes place.

The improvement in performance of the EA processor, as the number of noise-alone samples is increased, is shown explicitly in figures 47-51, where the $d_T$ (in decibels) required to realize $P_D = .5$ versus N, with $P_F$ and M as parameters, is plotted. The curve for M = 1 is not presented since it is identical to figure 31, as noted earlier. The comments given above concerning the use of potential-signal samples on both sides of the GLR test are illustrated in figures 50 and 51. In these plots, for N significantly smaller than M, the leveling off of the curves shows that the potential-signal samples in these instances are more important than the noise-alone samples in establishing stable noise-level estimates.

---

*We reiterate that the signal amplitudes have been set equal to each other in the simulation for the EA processor. This will be discussed again later.

## DISCUSSION

Operating characteristics for detecting phase-incoherent signals in Gaussian noise of unknown level have been presented. The two processors considered were ML detectors realized under different assumptions about signal amplitudes. In the first case, the signal amplitudes were assumed unequal and unknown from sample to sample. In the second case, the signal amplitudes were assumed equal, though unknown. Since the GLR tests contain no claims to optimality, it may be questioned whether other processors obtained from different and, presumably, ad hoc tests might outperform the processors considered here. In order to partially answer this question, a number of other tests, in addition to the UA and EA GLR tests, were compared by means of simulation. We shall now very briefly consider some reasonable ad hoc tests and the results of the simulations of their performance.

To facilitate the discussion, we define the following quantities in terms of previously used notation:

$$m \equiv \frac{1}{M}\sum_{k=1}^{M}|z_k|, \qquad \tilde{m} \equiv \frac{1}{N}\sum_{j=1}^{N}|\tilde{z}_j|,$$
$$S \equiv \sum_{k=1}^{M}|z_k|^2, \qquad \tilde{S} \equiv \sum_{j=1}^{N}|\tilde{z}_j|^2. \tag{36}$$

Recall that $|z_k|$ and $|\tilde{z}_j|$ are envelope samples at the outputs of the potential-signal and noise-alone filters, respectively. Using the above definitions, we can write the total-sample variance as

$$\text{Var} = \frac{S - Mm^2 + \tilde{S} - N\tilde{m}^2}{M + N - 2}. \tag{37}$$

Then the UA test in the new notation can be written as

$$\frac{S}{M} \gtrless c\,\frac{\tilde{S}}{N}, \tag{38}$$

where $c\ (>0)$ is a scaling constant, and the EA test can be written as

$$m \gtrless c\left(\frac{S+\tilde{S}}{M+N}\right)^{1/2} . \tag{39}$$

The additional ad hoc tests considered here are indicated in table 1. All the tests considered are invariant to level scaling; that is, they yield CFAR processors.

Table 1. Examples of Ad Hoc Processors Invariant to Level Scaling

| Case | Processing |
|---|---|
| (a) | $m \gtrless c\,(\text{Var})^{1/2}$ |
| (b) | $m - \tilde{m} \gtrless c\,(\text{Var})^{1/2}$ |
| (c) | $m - \tilde{m} \gtrless c\left(\frac{S+\tilde{S}}{M+N}\right)^{1/2}$ |
| (d) | $m \gtrless c\,(\tilde{S}/N)^{1/2}$ |
| (e) | $m \gtrless c\tilde{m}$ |
| (f) | $m - \tilde{m} \gtrless c\,(\tilde{S}/N)^{1/2}$ |
| (g) | $Mm - N\tilde{m} \gtrless c\left(\frac{S+\tilde{S}}{M+N}\right)^{1/2}$ |
| (h) | $Mm - N\tilde{m} \gtrless c\,(\tilde{S}/N)^{1/2}$ |

Note: If the upper inequality is satisfied, $H_1$ is declared true. If the lower inequality is satisfied, $H_0$ is declared true.

Case (b) in table 1 is an estimate of the usual deflection criterion (reference 5) compared with threshold c. Cases (c) and (d) are modifications of the EA processor, and, analogously, case (a) may be thought of as a modification of the deflection criterion. Case (f) is suggested by a comparison of cases (c) and (d). Cases (g) and (h) are extensions of cases (c) and (f), where the sample means have been weighted according to the number of samples used. Finally, case (e) is a straightforward comparison of sample means.

The processors in table 1 and the EA and UA processors were compared by simulating their performance over a wide range of values of M, N, and $d_T$. When equal signal amplitudes were used, the EA processor outperformed all others. For unequal received signal amplitudes, it has already been noted that the performance of the UA processor is unaffected as long as $d_T$ is kept constant. In fact, the UA processor performed best for some examples of unequal signal energy fractionalization used in the simulation, such as 0 in one of the M potential-signal branches. As an example, the EA processor for $M = 4$ was subjected to unequal signal amplitudes, namely, zero strength in one channel and equal signal strength in the remaining channels. (A related situation was treated in reference 2.) The detection characteristics for $P_F = 10^{-2}$ and $10^{-3}$ are given in figures 52 and 53. Comparison with figures 41 and 42 shows the degradation to be significant, especially for small values of N. Thus the EA processor is sensitive to the exact received signal energy fractionalization amongst branches, whereas the UA processor is completely insensitive to this effect. In all the cases studied, one of the two ML processors (EA or UA) outperformed all the other processors in table 1.

In the foregoing discussion, we considered the EA processor performance when unequal signal energy fractionalization occurred in the M potential-signal branches. We have also noted that UA processor performance is unaffected by the manner in which the received signal energy is fractionalized. Alternatively, if $\{d_k\}$ are considered to be random variables with known PDFs, the present results can be averaged over the given PDFs to obtain the average $P_D$ for fluctuating signal amplitudes. For the EA processor, graphical integration is required for this averaging procedure; for the UA processor, analytical evaluation is possible for some PDFs. The case of $d_T^2/2$ having a chi-squared PDF will be considered in part III of this sequence of technical reports (reference 1).

When the threshold $\gamma$ is varied by $\pm 1$ standard deviation away from its estimated value for a specified $P_F$, large percentage changes in $P_D$ for the EA processor sometimes occur. This is particularly true for small N and $P_F$. In these cases, the EA processor is very sensitive to its precise threshold setting and is not a viable processor. The UA processor is less sensitive to threshold setting because the M potential-signal samples are not in-bred; that is, they are used only on the left side of the GLF test. However, no analysis of the sensitivity to the threshold was conducted for either processor.

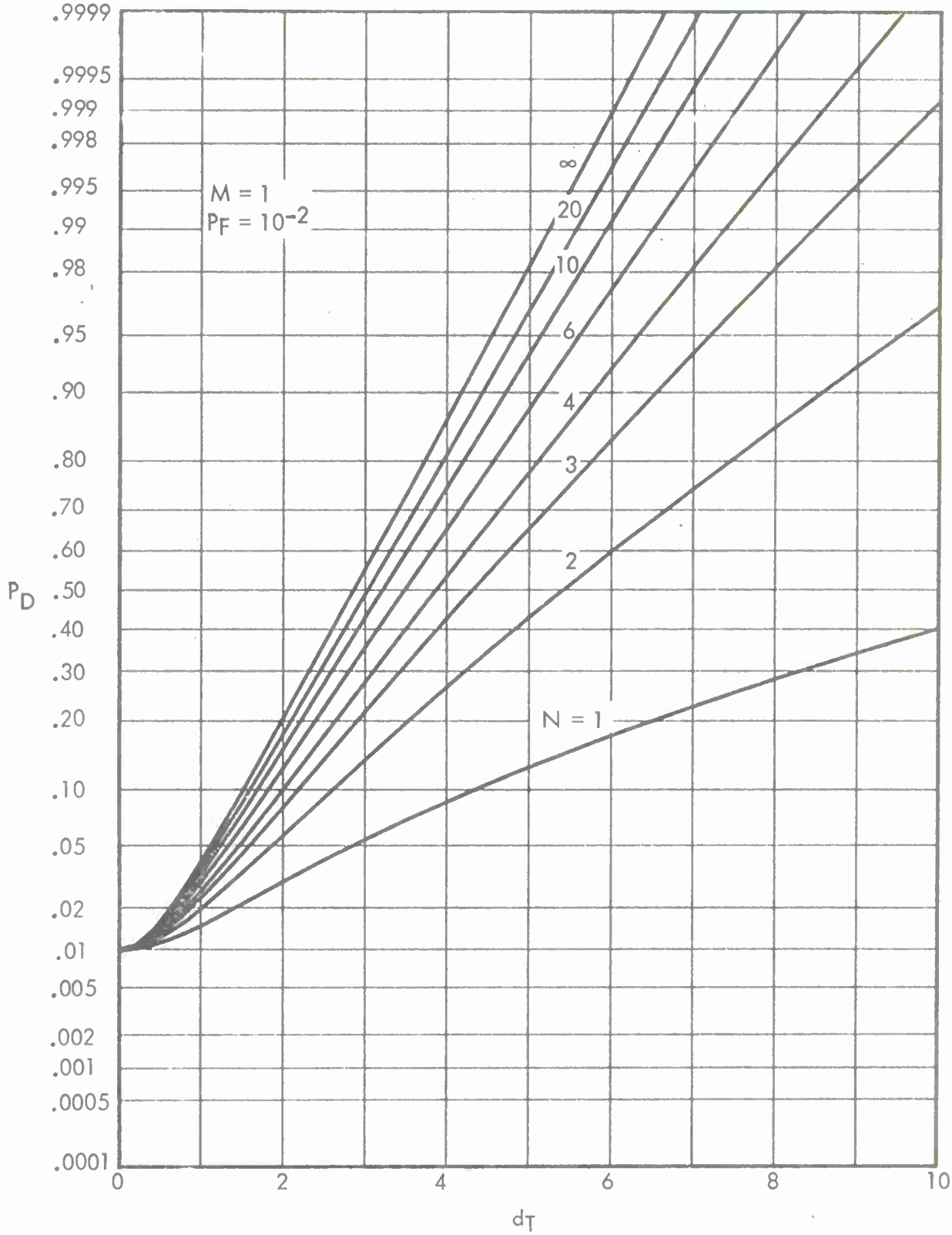


Figure 1. Detection Characteristics for UA Processor; M = 1, $P_F = 10^{-2}$

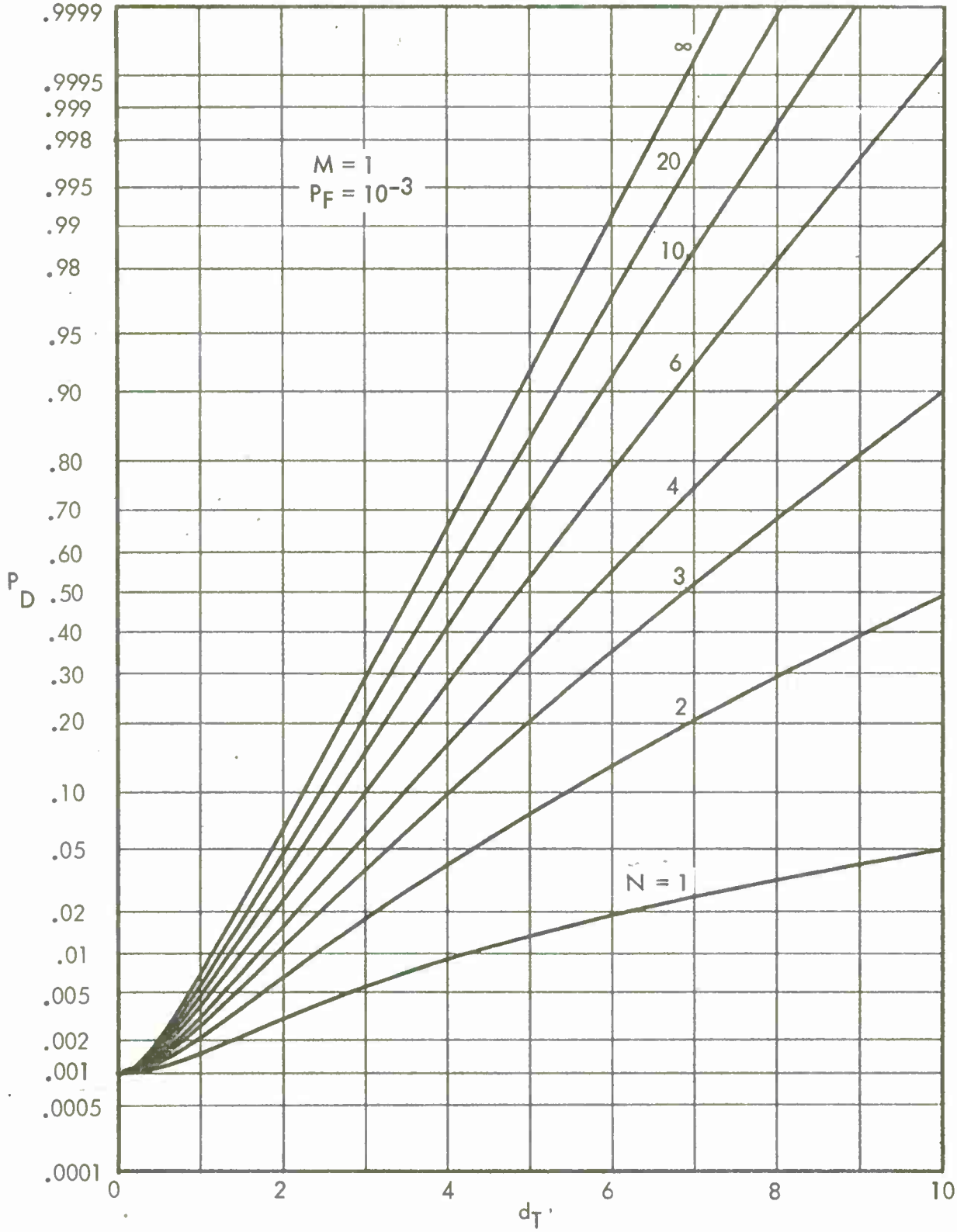


Figure 2. Detection Characteristics for UA Processor; M = 1, $P_F = 10^{-3}$

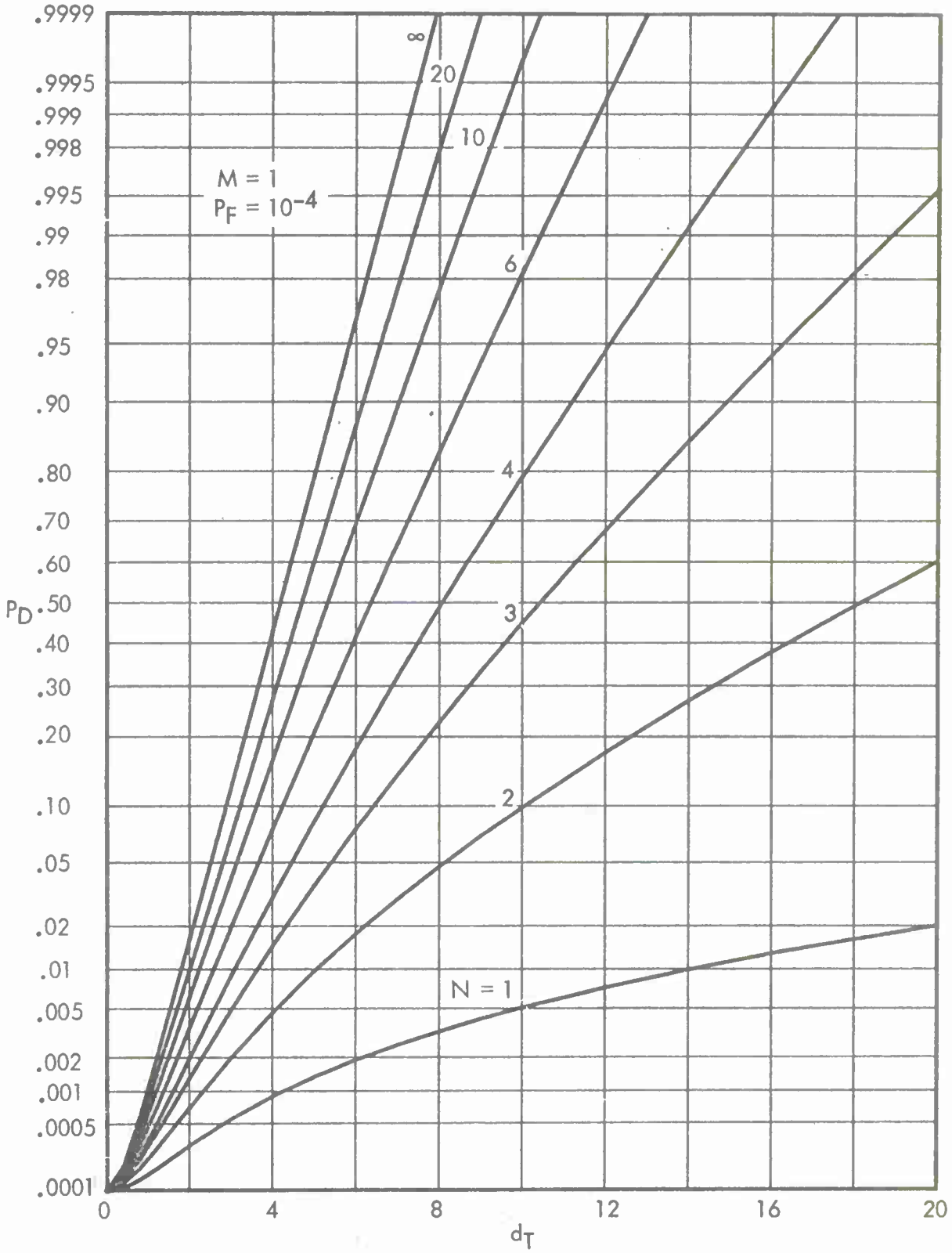


Figure 3. Detection Characteristics for UA Processor; M = 1, $P_F = 10^{-4}$

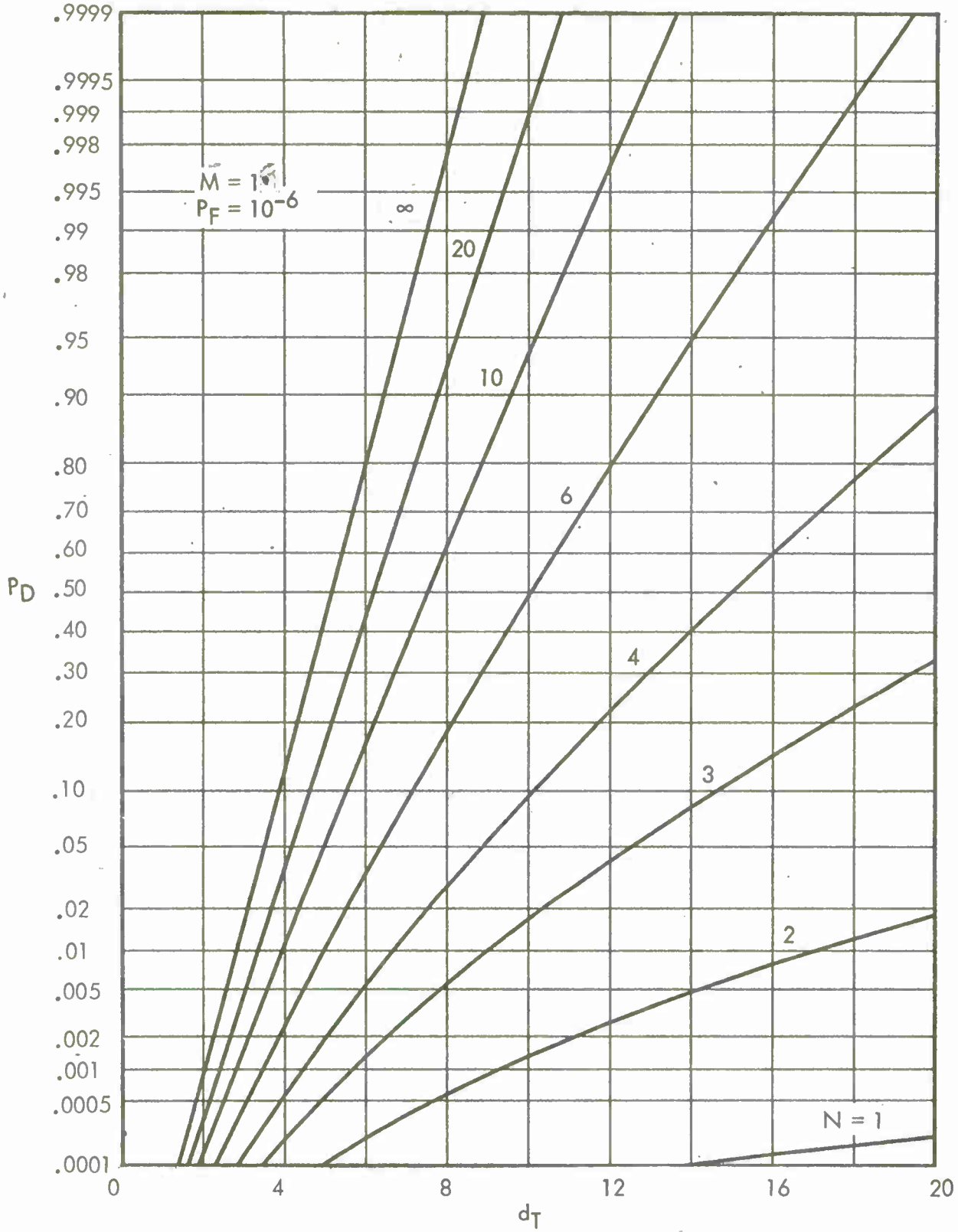


Figure 4. Detection Characteristics for UA Processor; M = 1, $P_F = 10^{-6}$

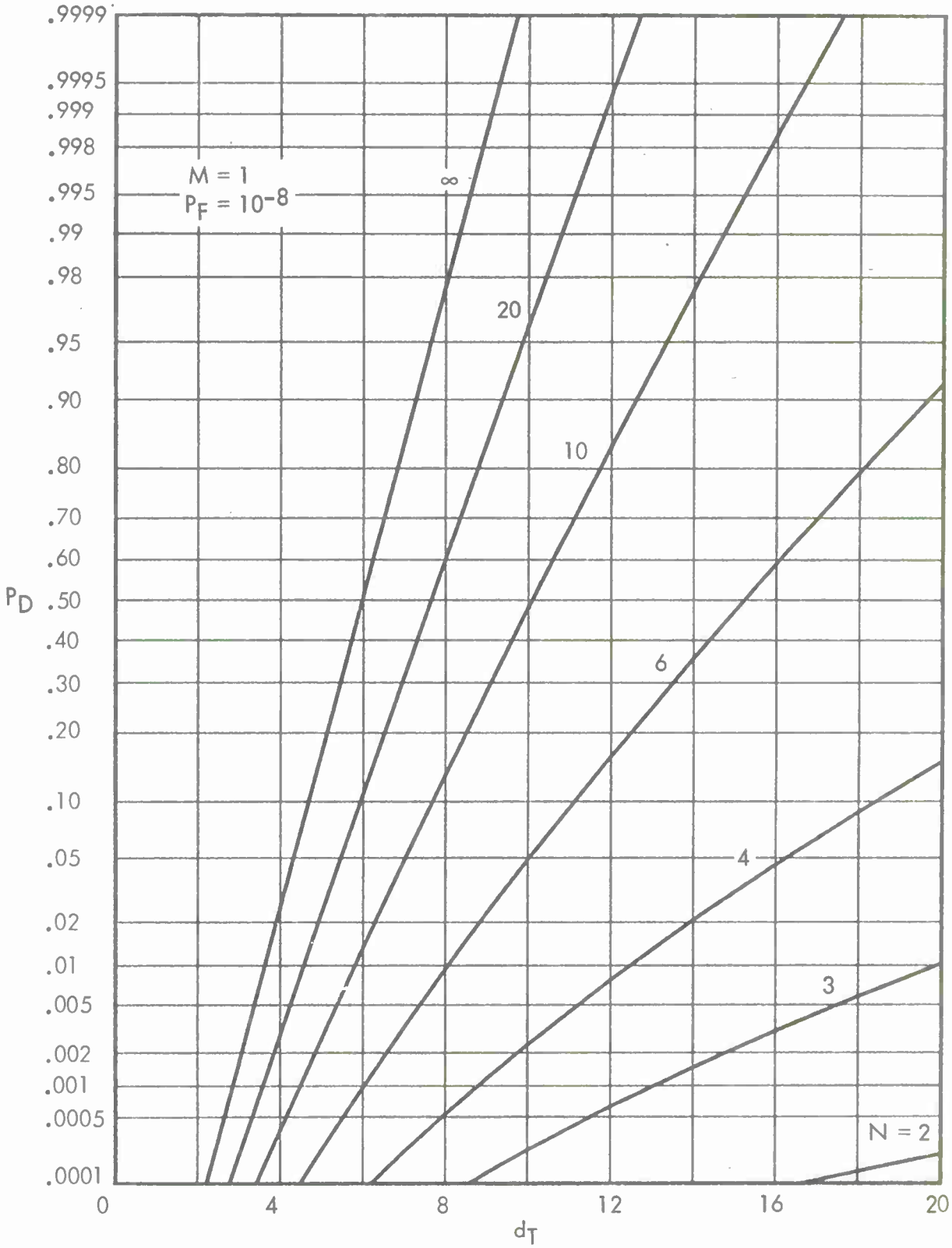


Figure 5. Detection Characteristics for UA Processor; M = 1, $P_F = 10^{-8}$

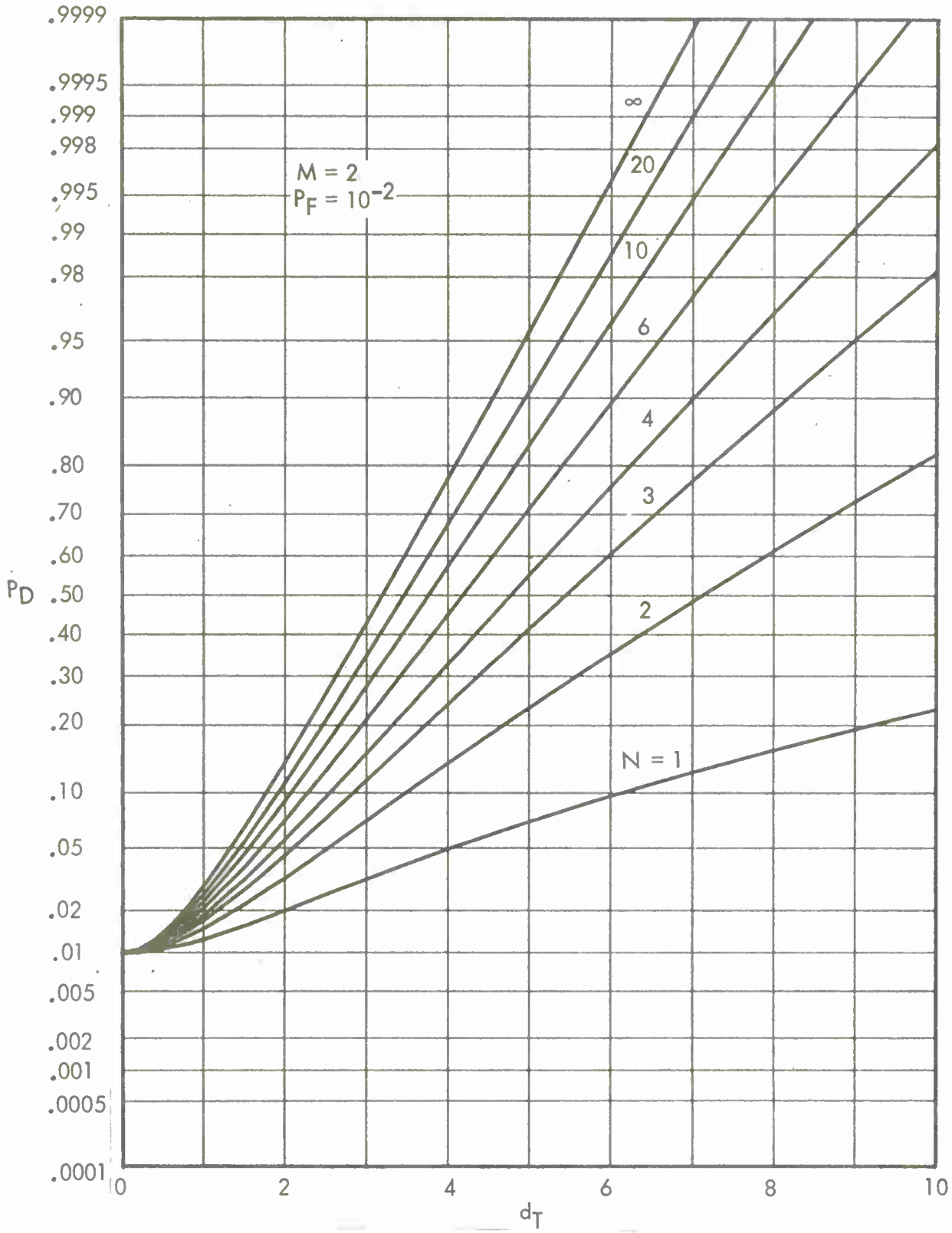


Figure 6. Detection Characteristics for UA Processor; M = 2, $P_F = 10^{-2}$

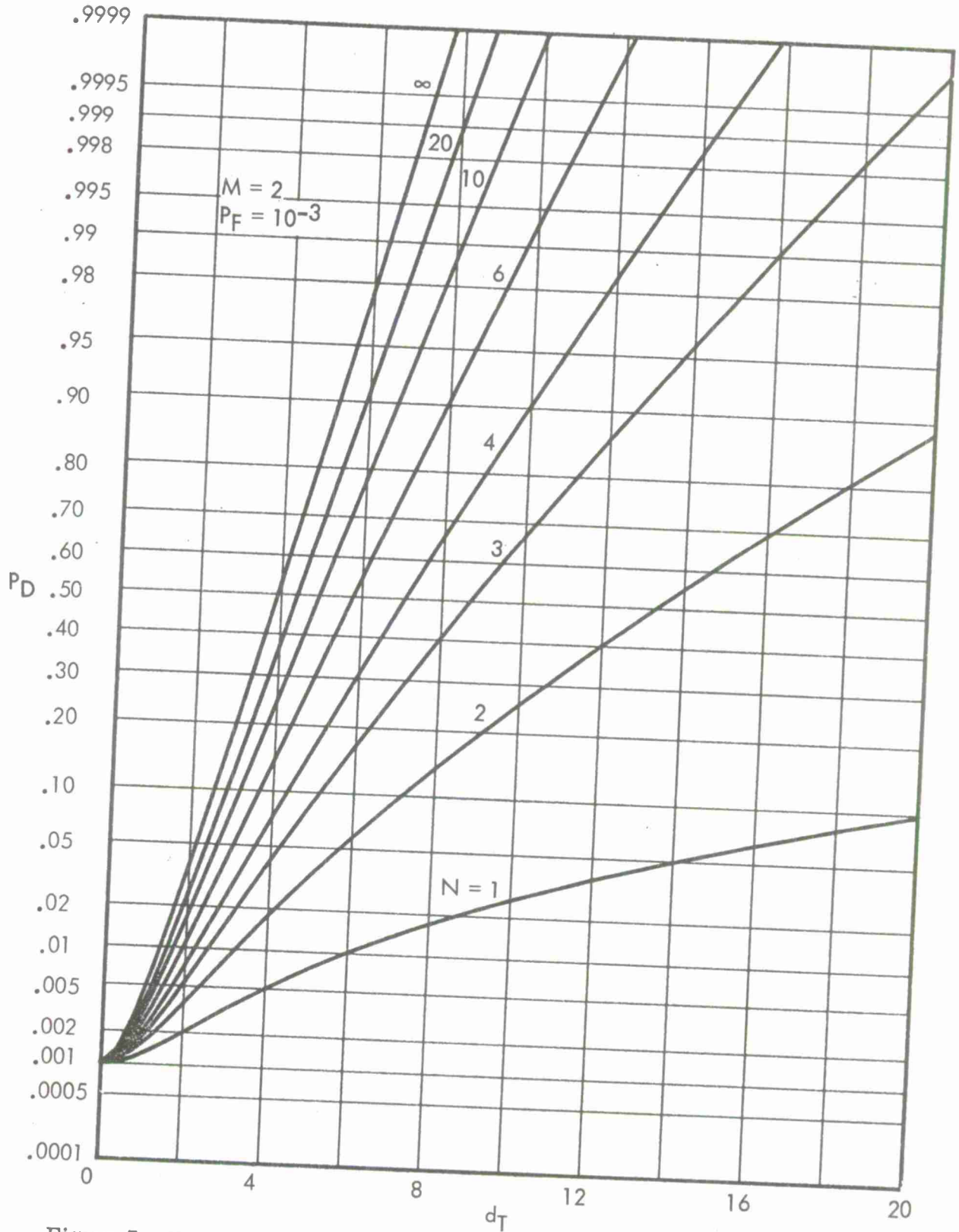


Figure 7. Detection Characteristics for UA Processor; M = 2, $P_F = 10^{-3}$

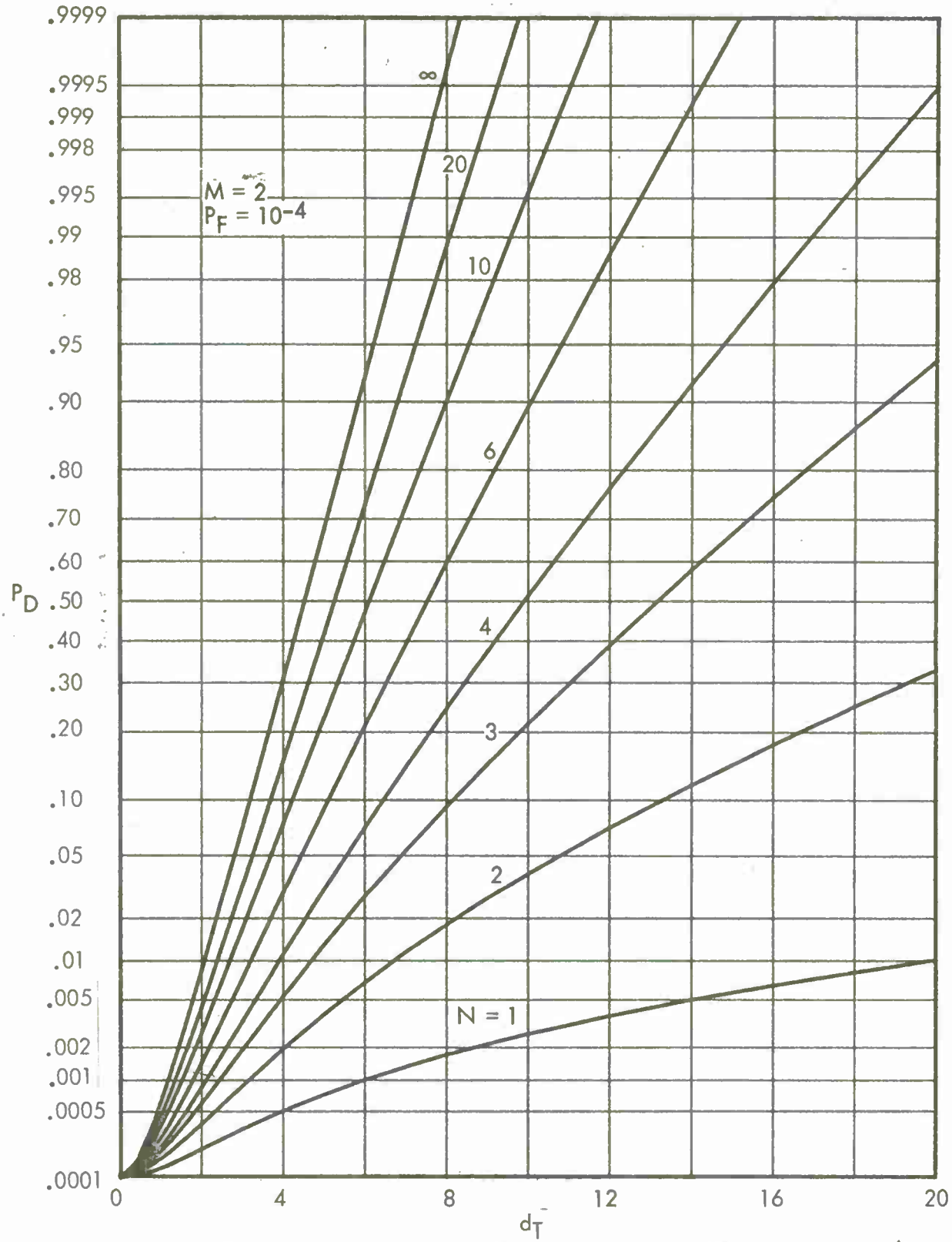


Figure 8. Detection Characteristics for UA Processor; M = 2, $P_F = 10^{-4}$

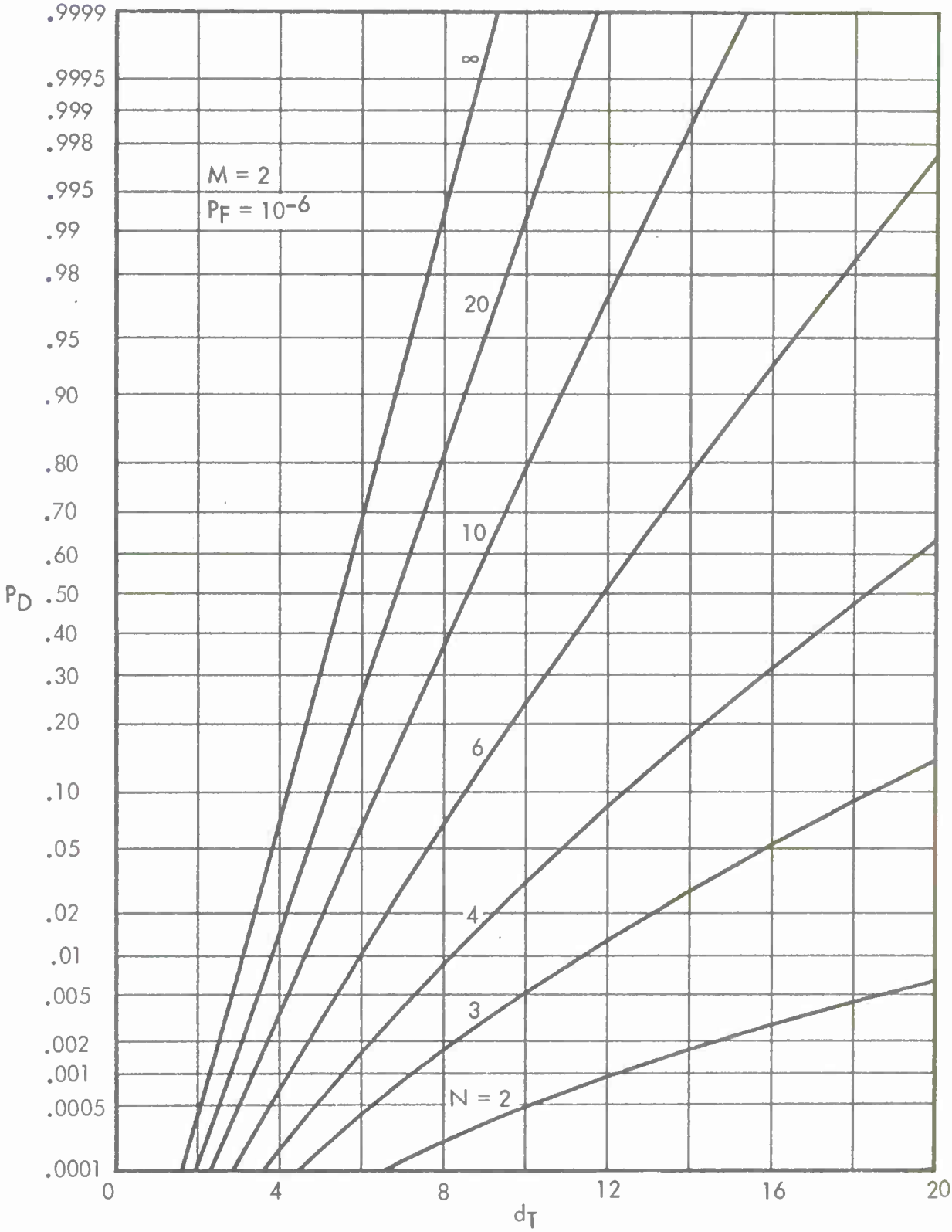


Figure 9. Detection Characteristics for UA Processor; M = 2, $P_F = 10^{-6}$

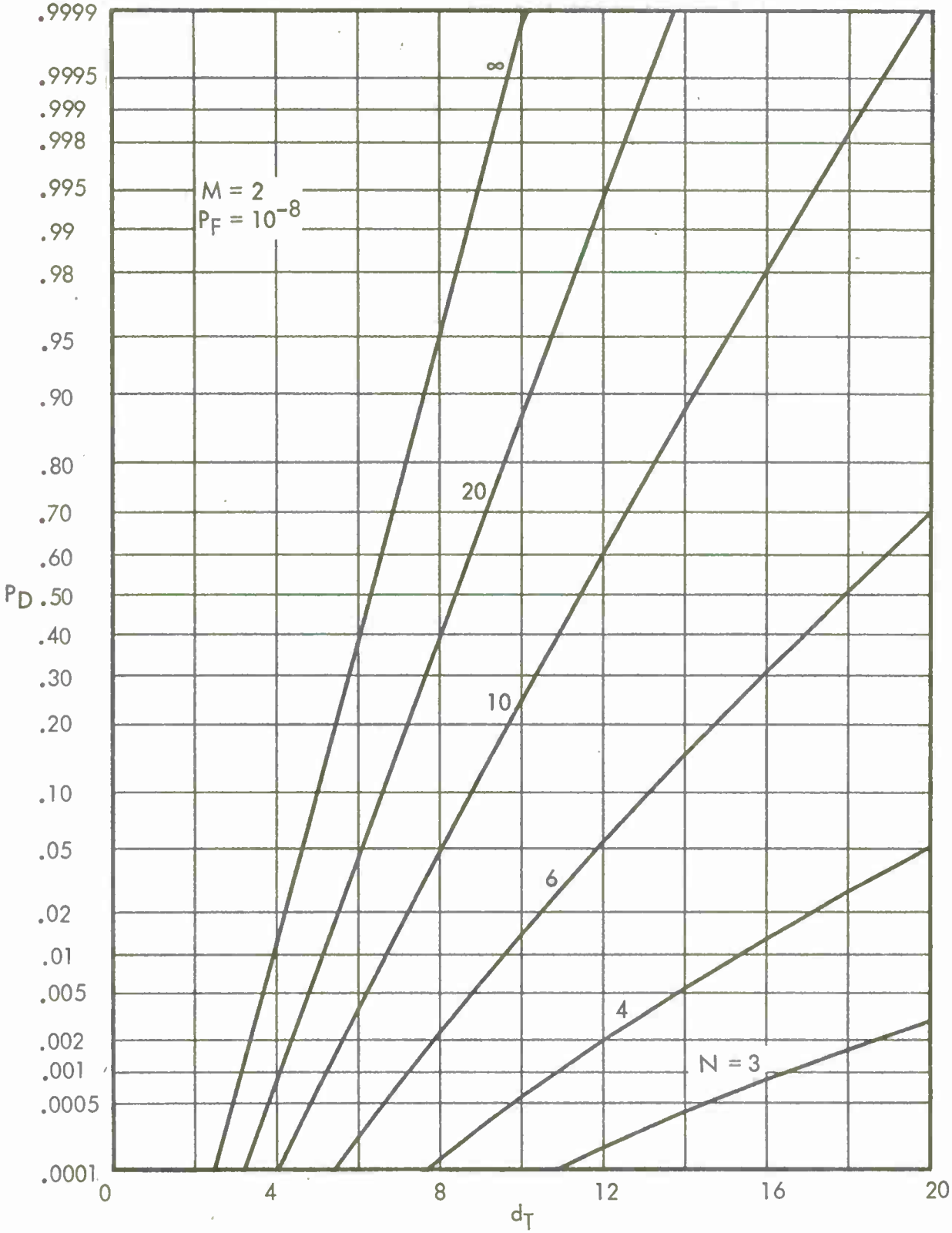


Figure 10. Detection Characteristics for UA Processor; M = 2, $P_F = 10^{-8}$

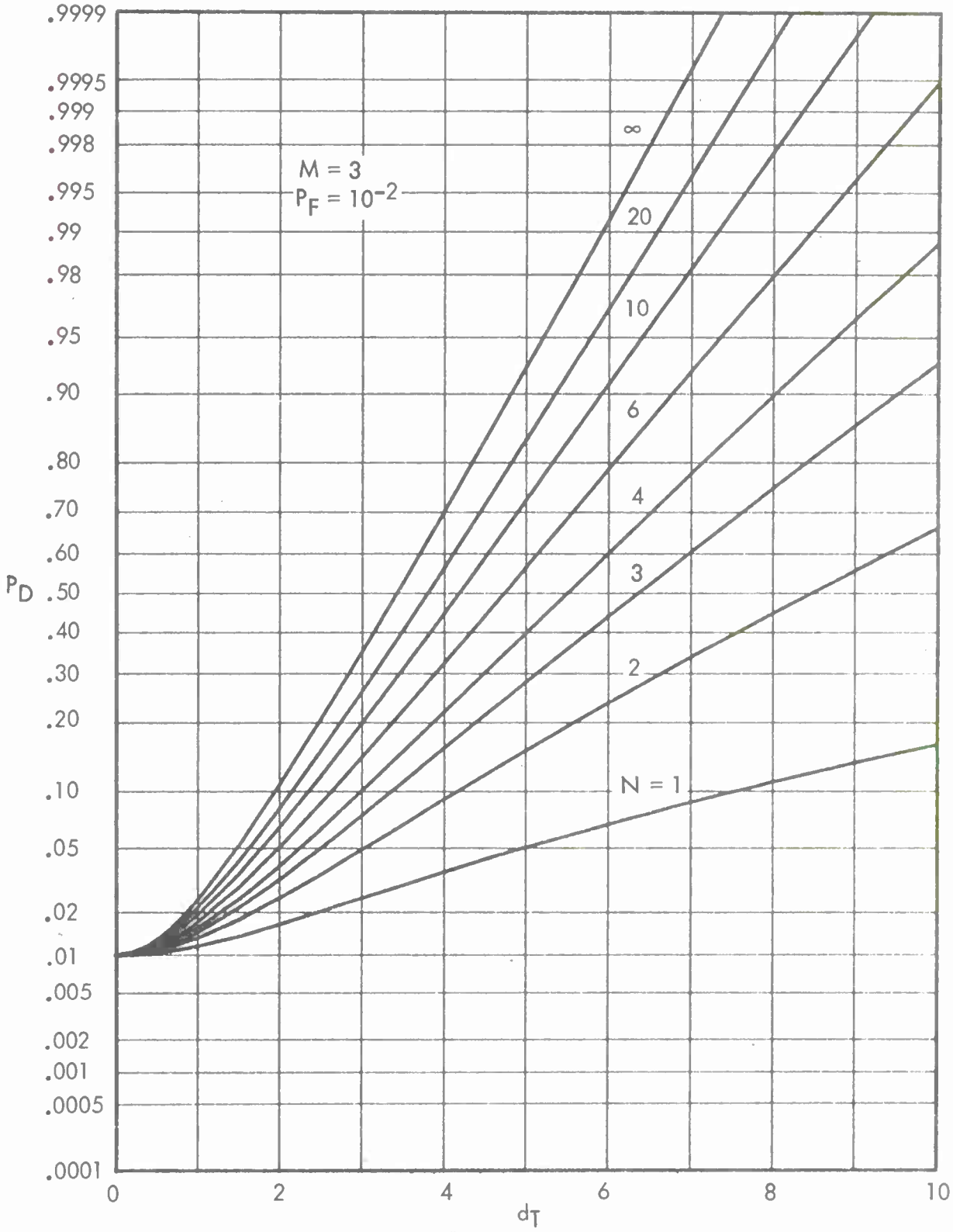


Figure 11. Detection Characteristics for UA Processor; M = 3, $P_F = 10^{-2}$

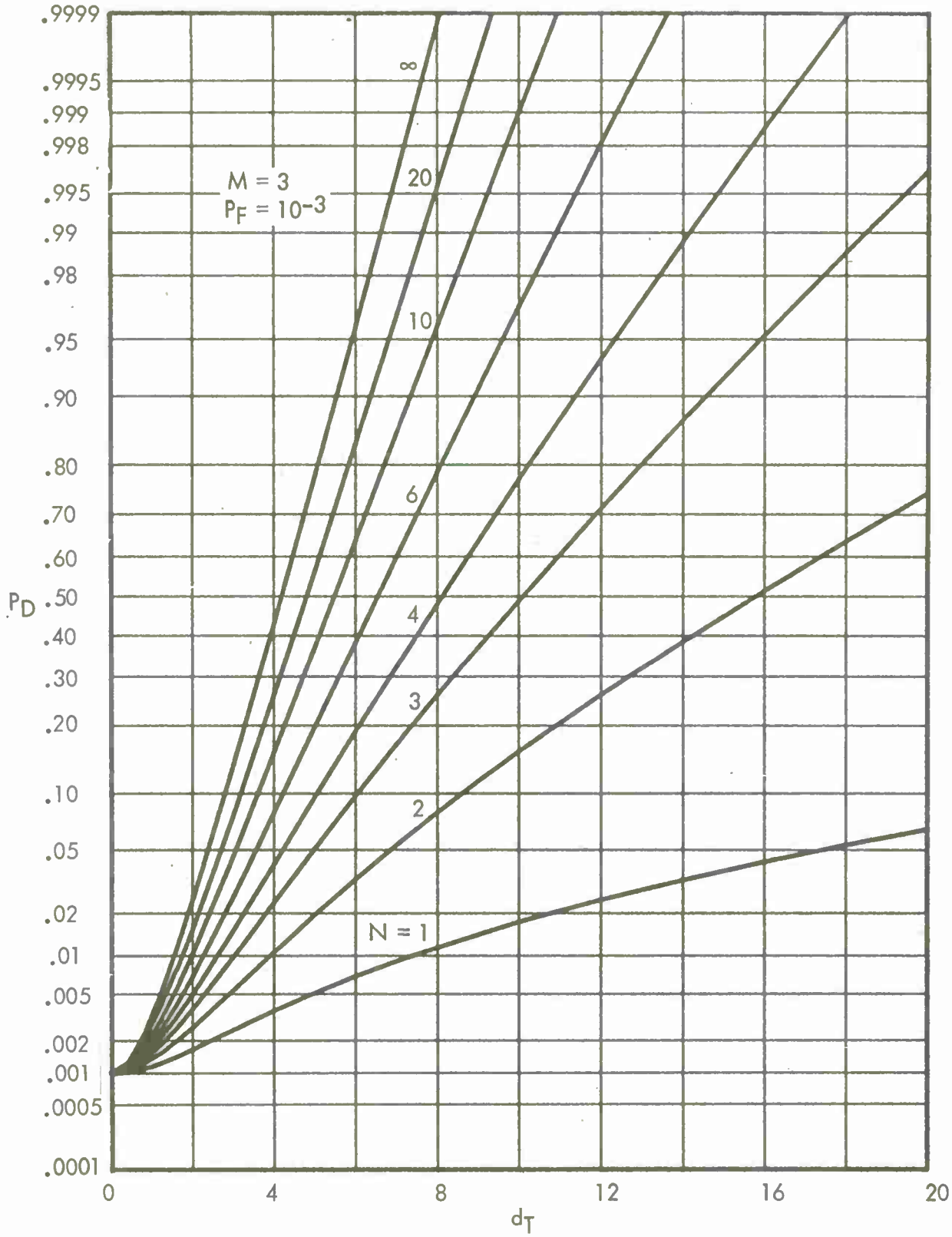


Figure 12. Detection Characteristics for UA Processor; M = 3, $P_F = 10^{-3}$

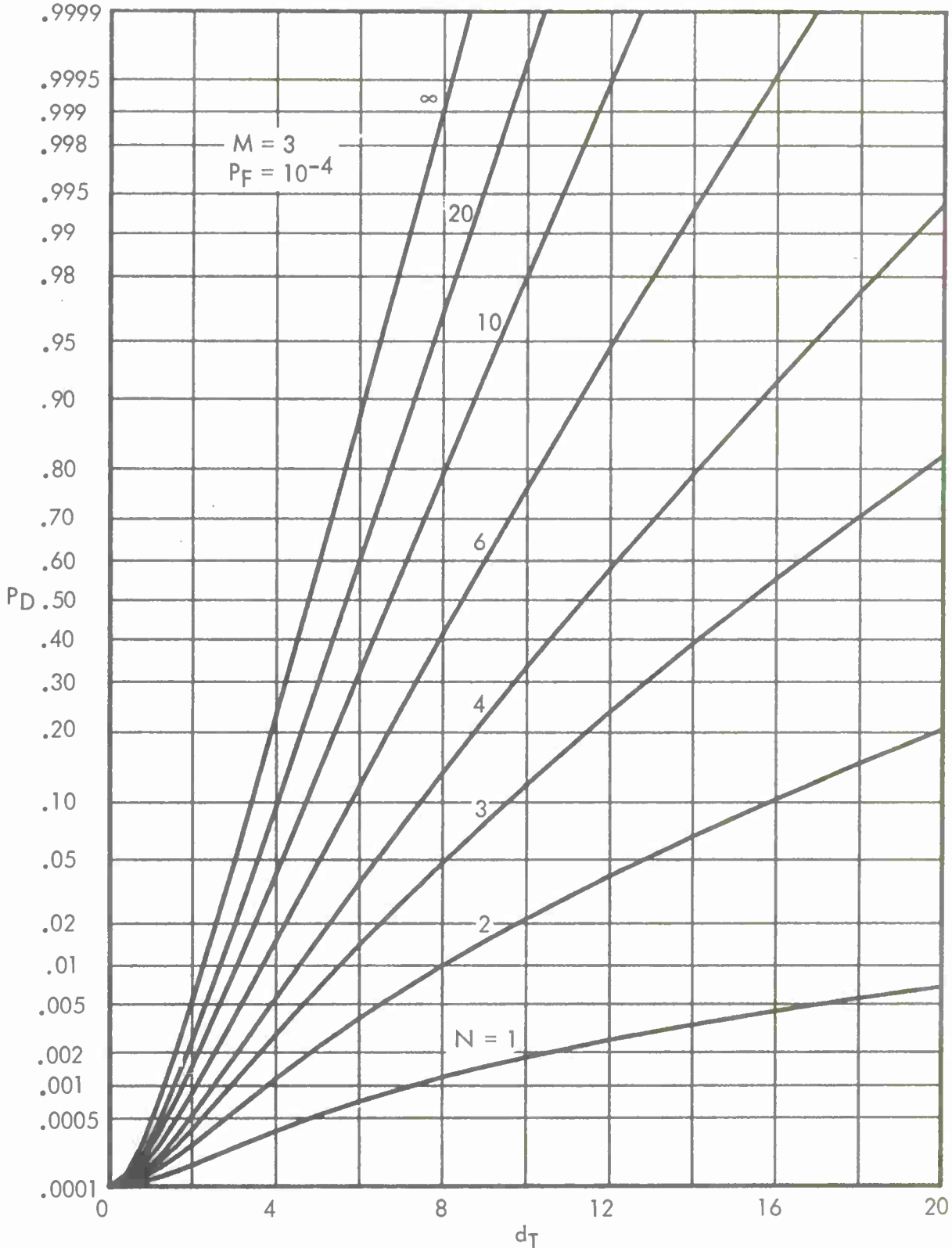


Figure 13. Detection Characteristics for UA Processor; M = 3, $P_F = 10^{-4}$

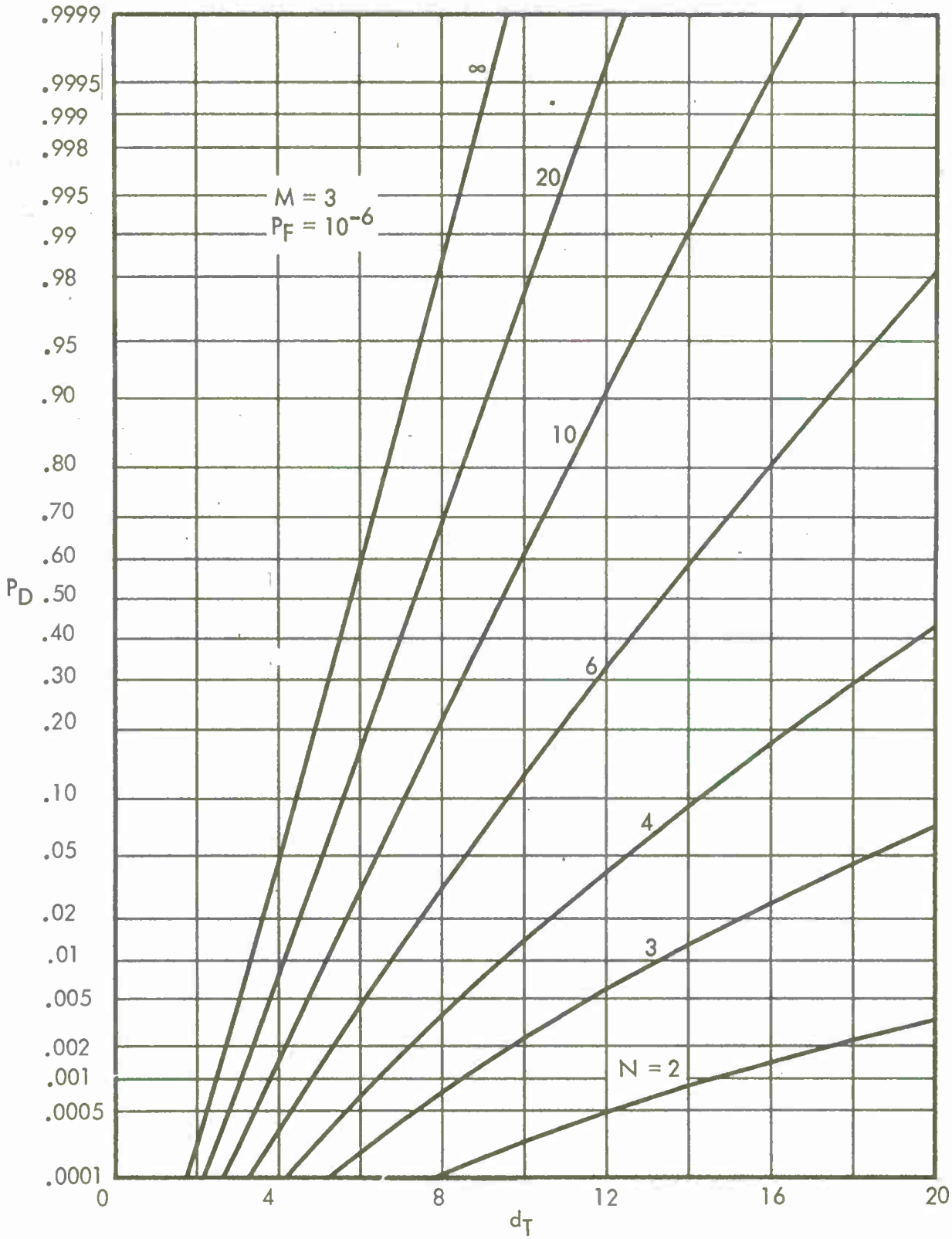


Figure 14. Detection Characteristics for UA Processor; M = 3, $P_F = 10^{-6}$

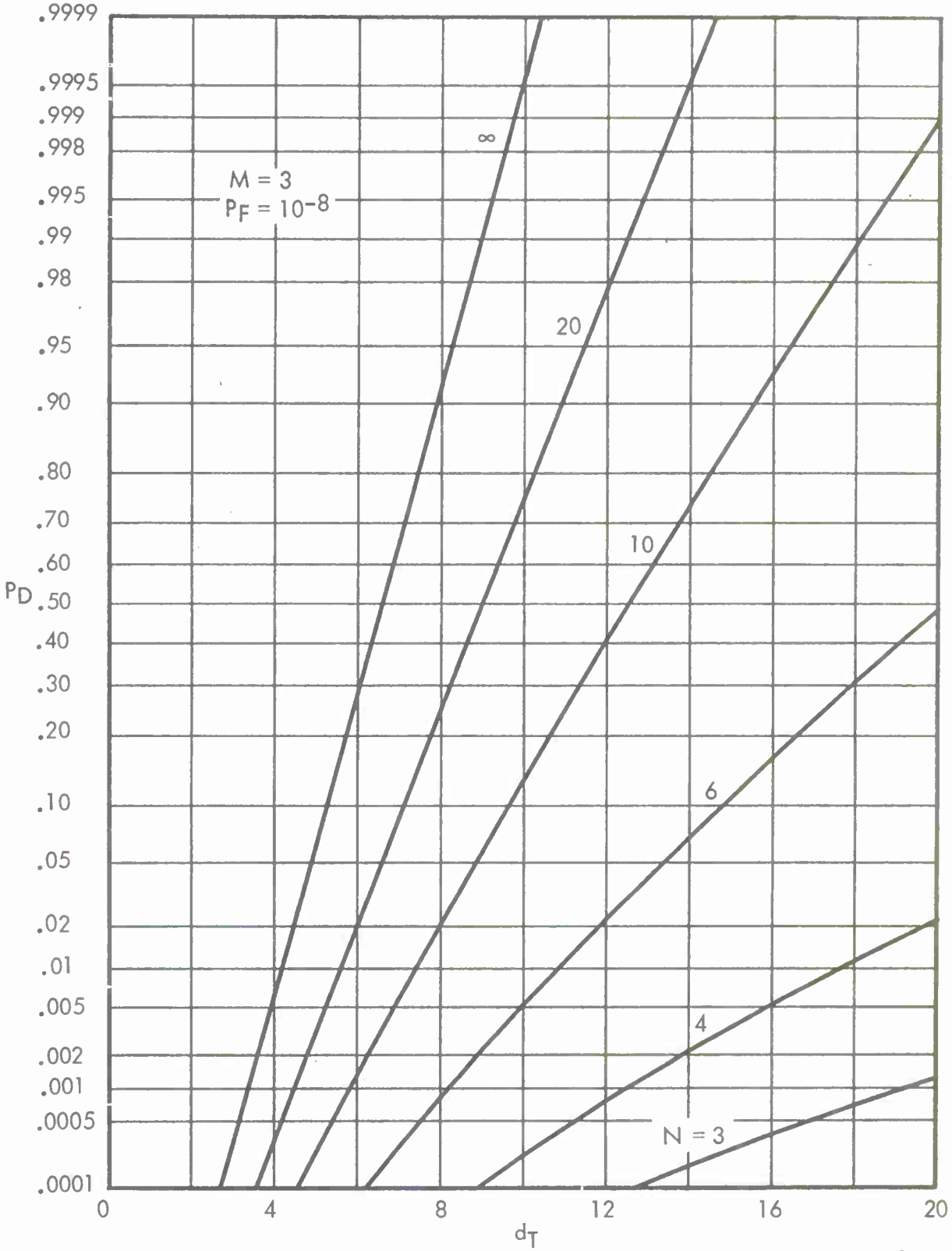


Figure 15. Detection Characteristics for UA Processor; M = 3, $P_F = 10^{-8}$

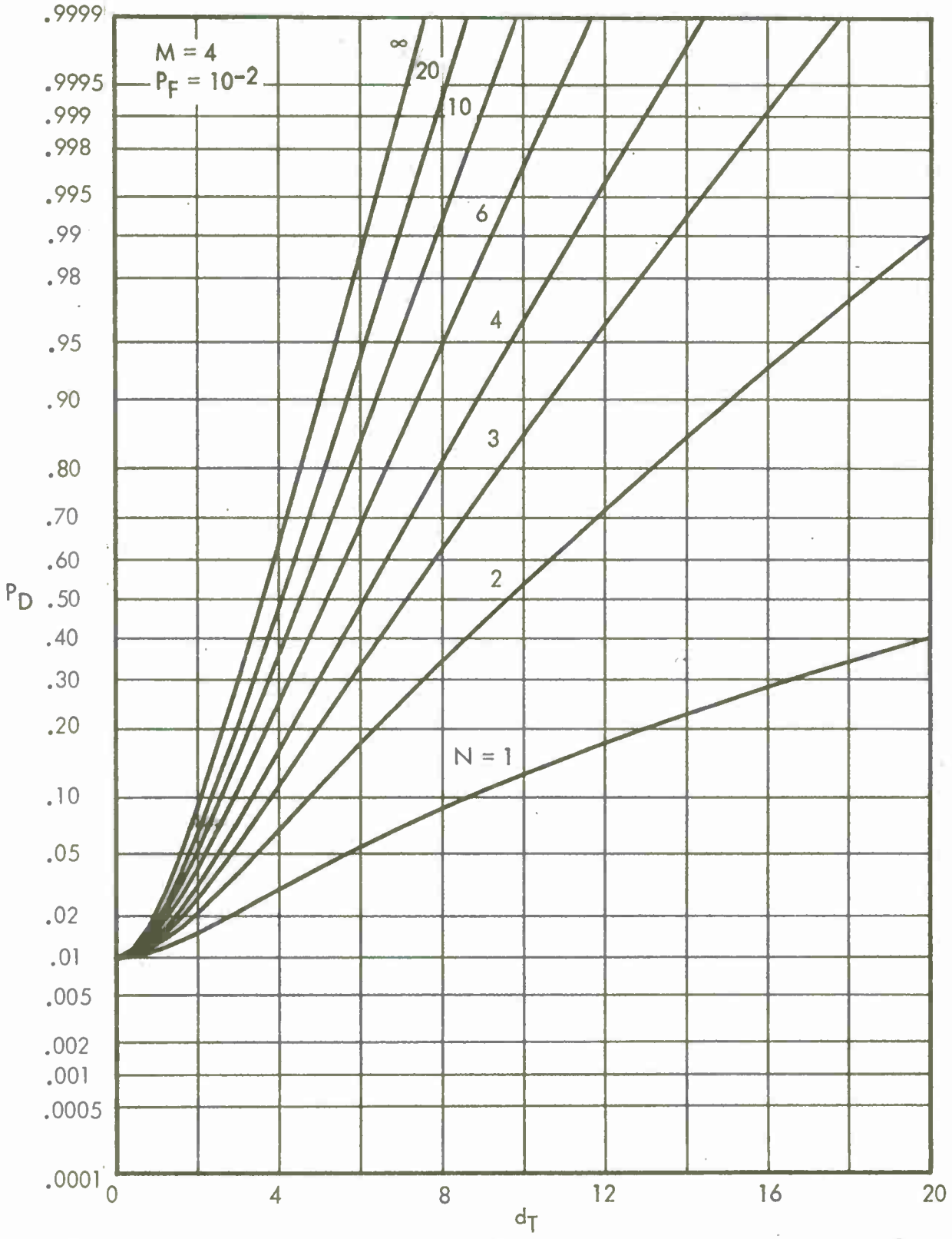


Figure 16. Detection Characteristics for UA Processor; M = 4, $P_F = 10^{-2}$

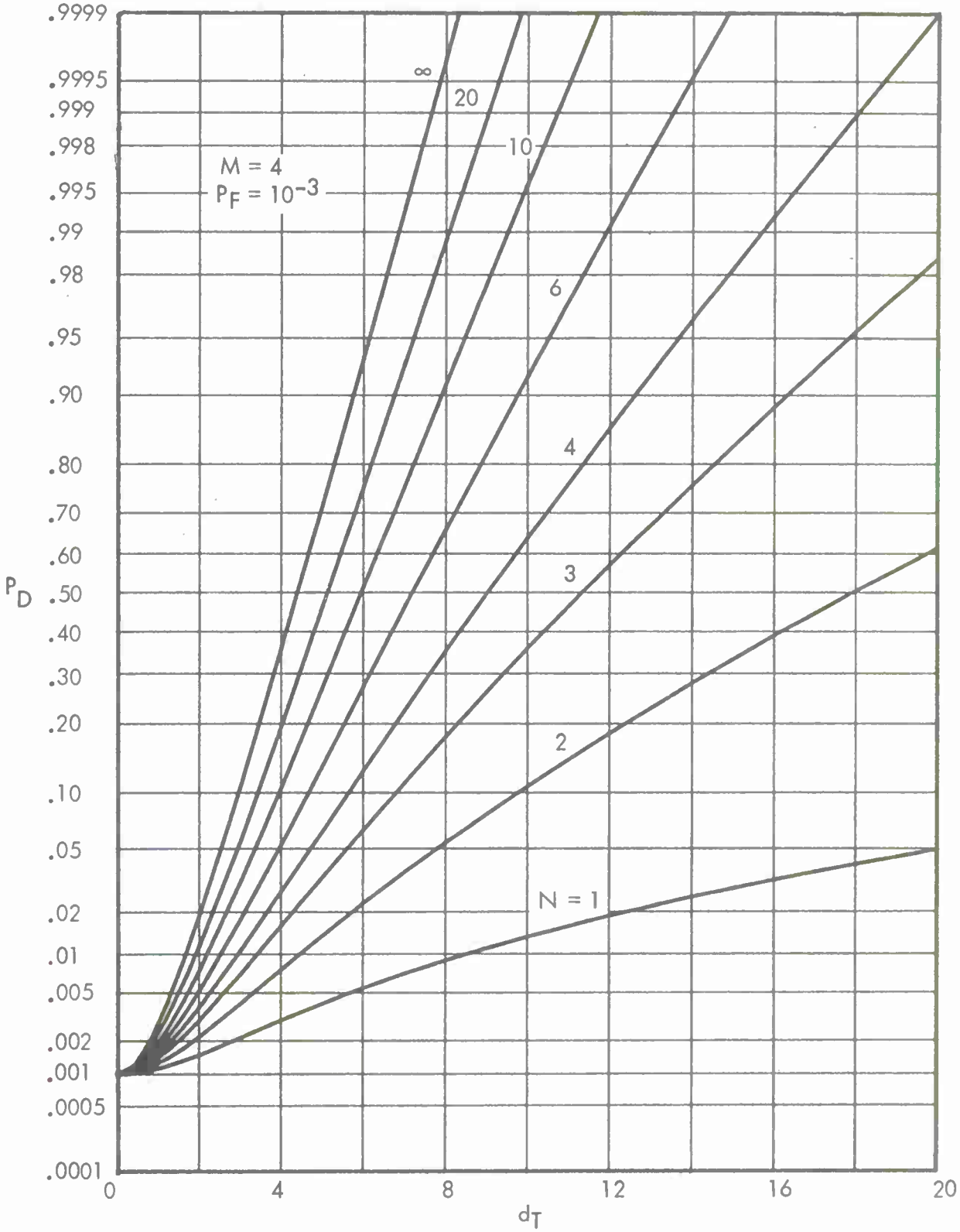


Figure 17. Detection Characteristics for UA Processor; M = 4, $P_F = 10^{-3}$

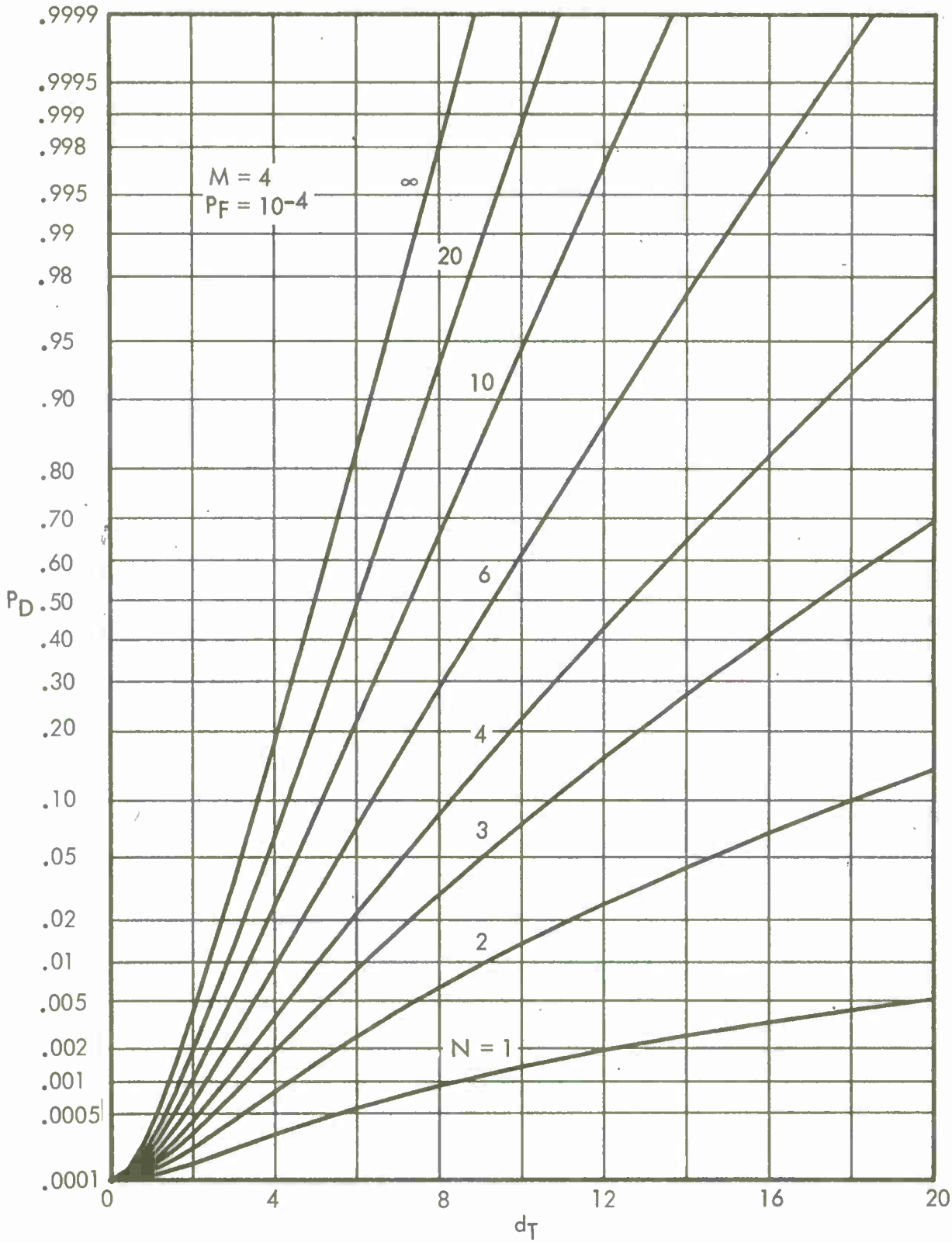


Figure 18. Detection Characteristics for UA Processor; M = 4, $P_F = 10^{-4}$

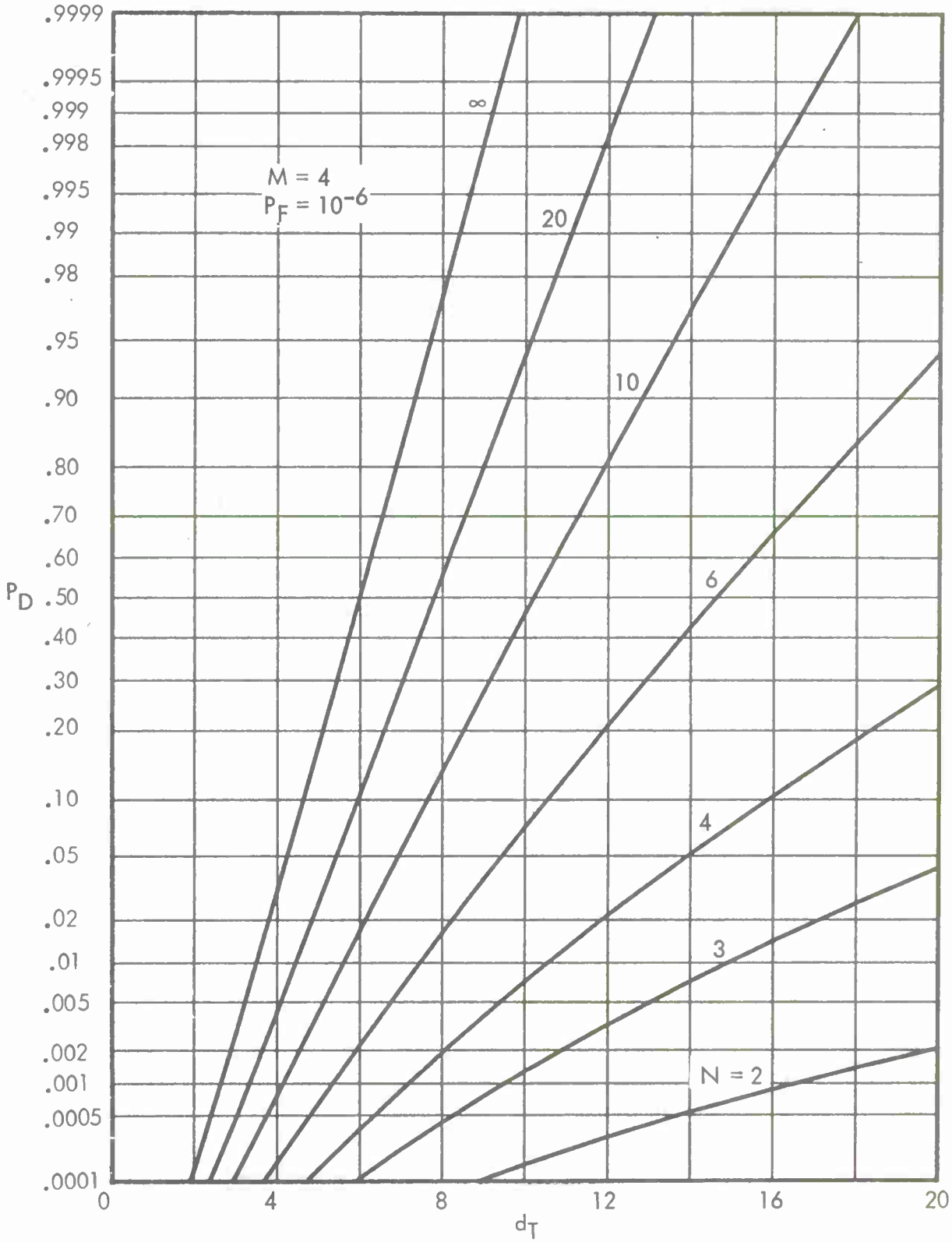


Figure 19. Detection Characteristics for UA Processor; M = 4, $P_F = 10^{-6}$

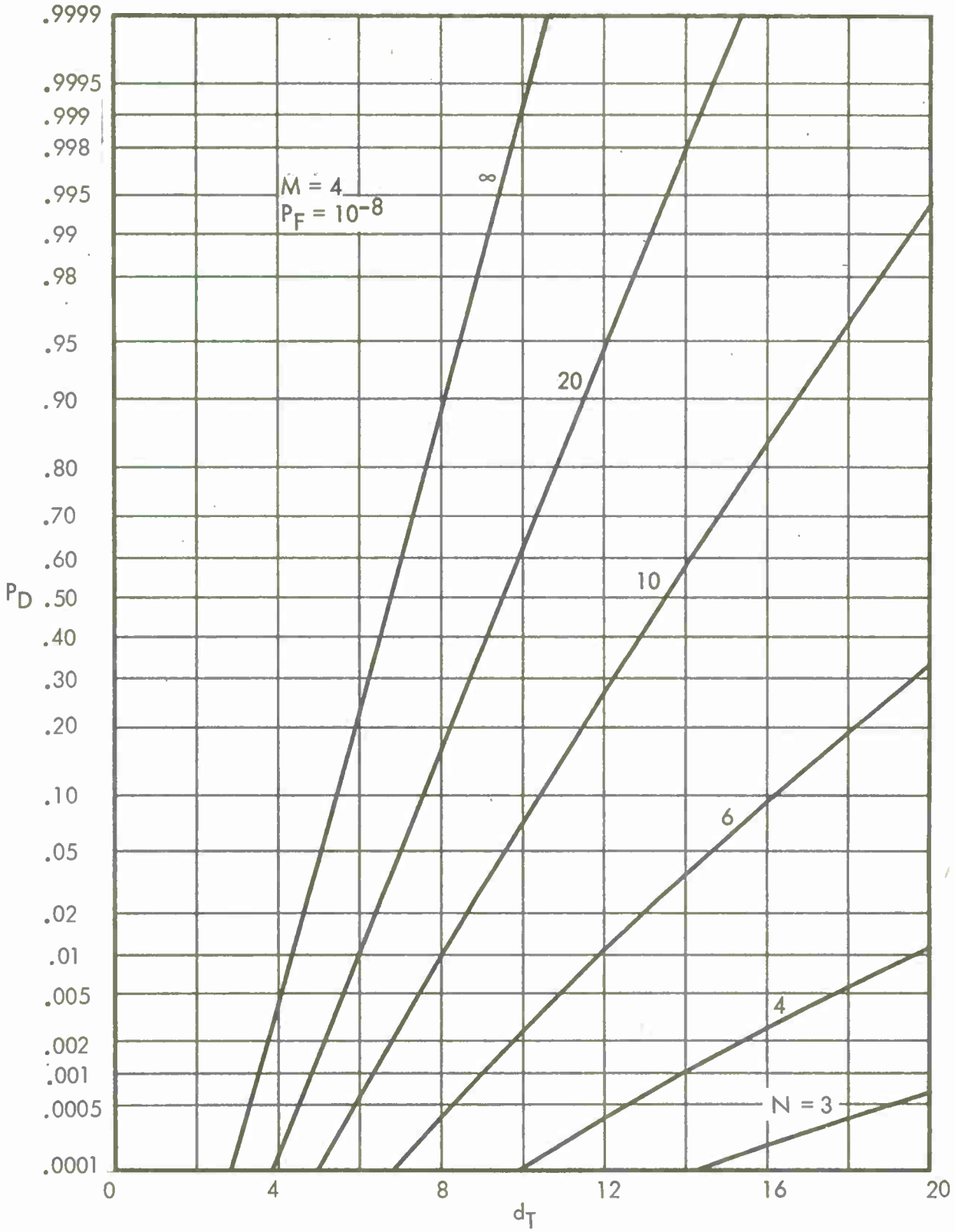


Figure 20. Detection Characteristics for UA Processor; M = 4, $P_F = 10^{-8}$

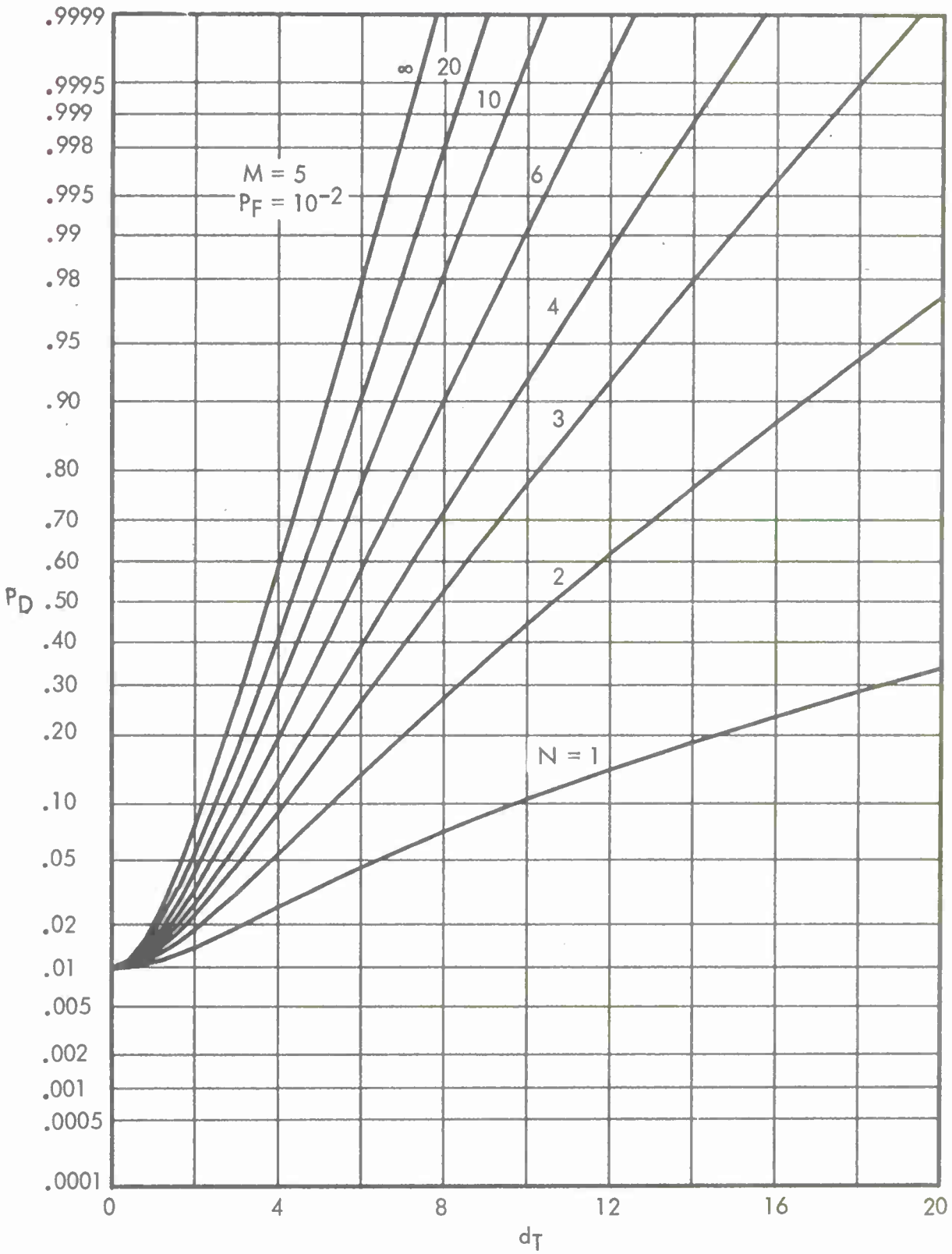


Figure 21. Detection Characteristics for UA Processor; M = 5, $P_F = 10^{-2}$

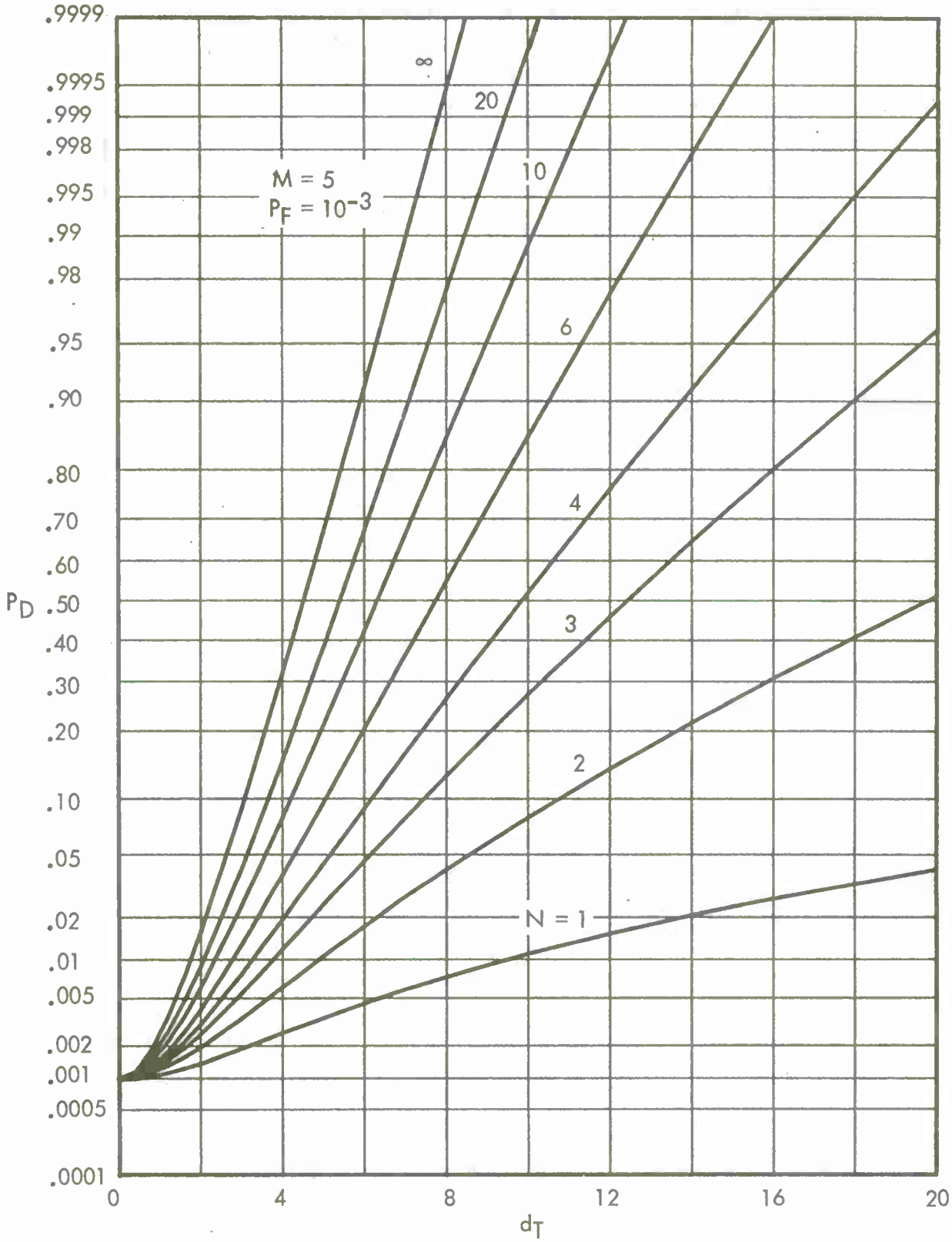


Figure 22. Detection Characteristics for UA Processor; M = 5, $P_F = 10^{-3}$

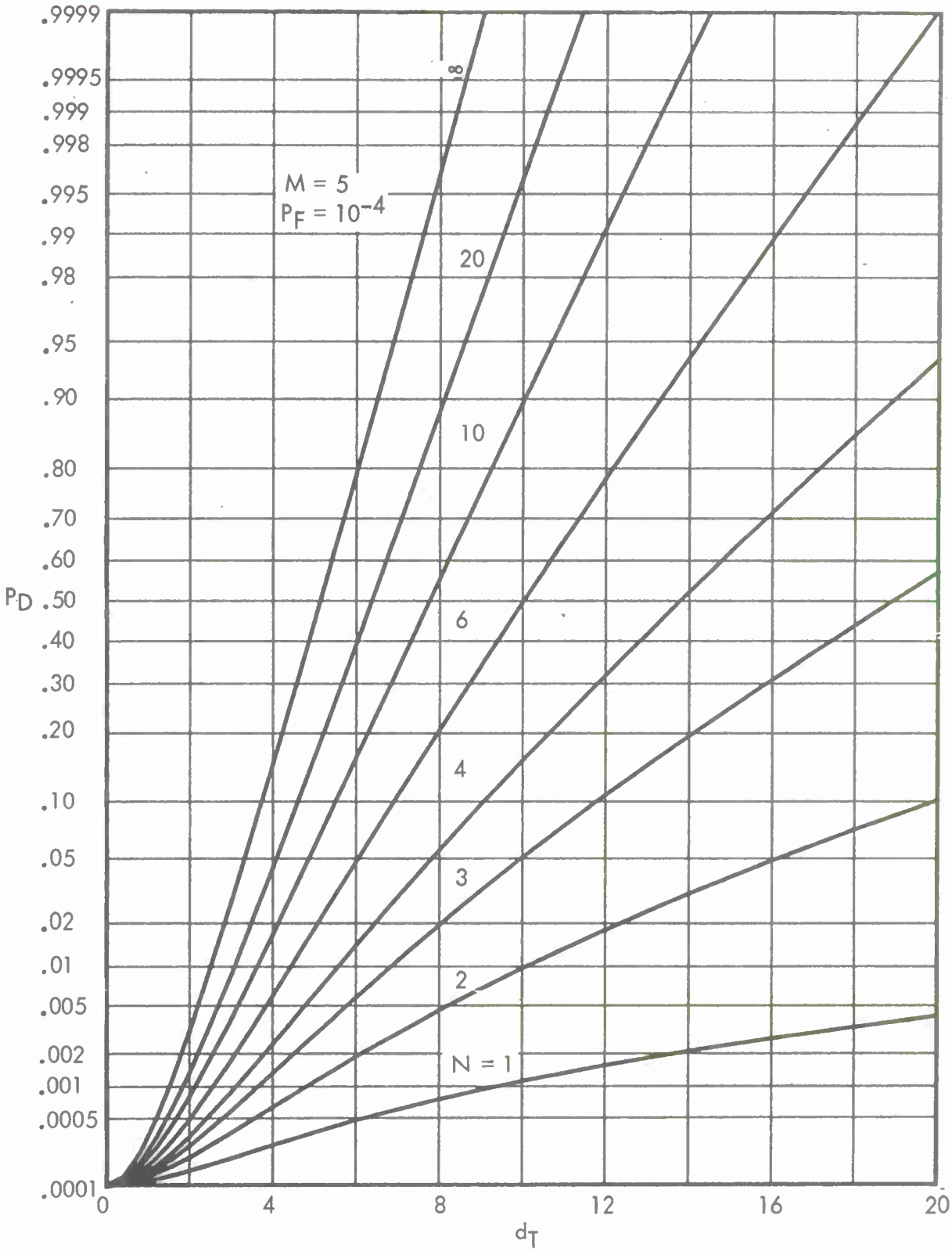


Figure 23. Detection Characteristics for UA Processor; M = 5, $P_F = 10^{-4}$

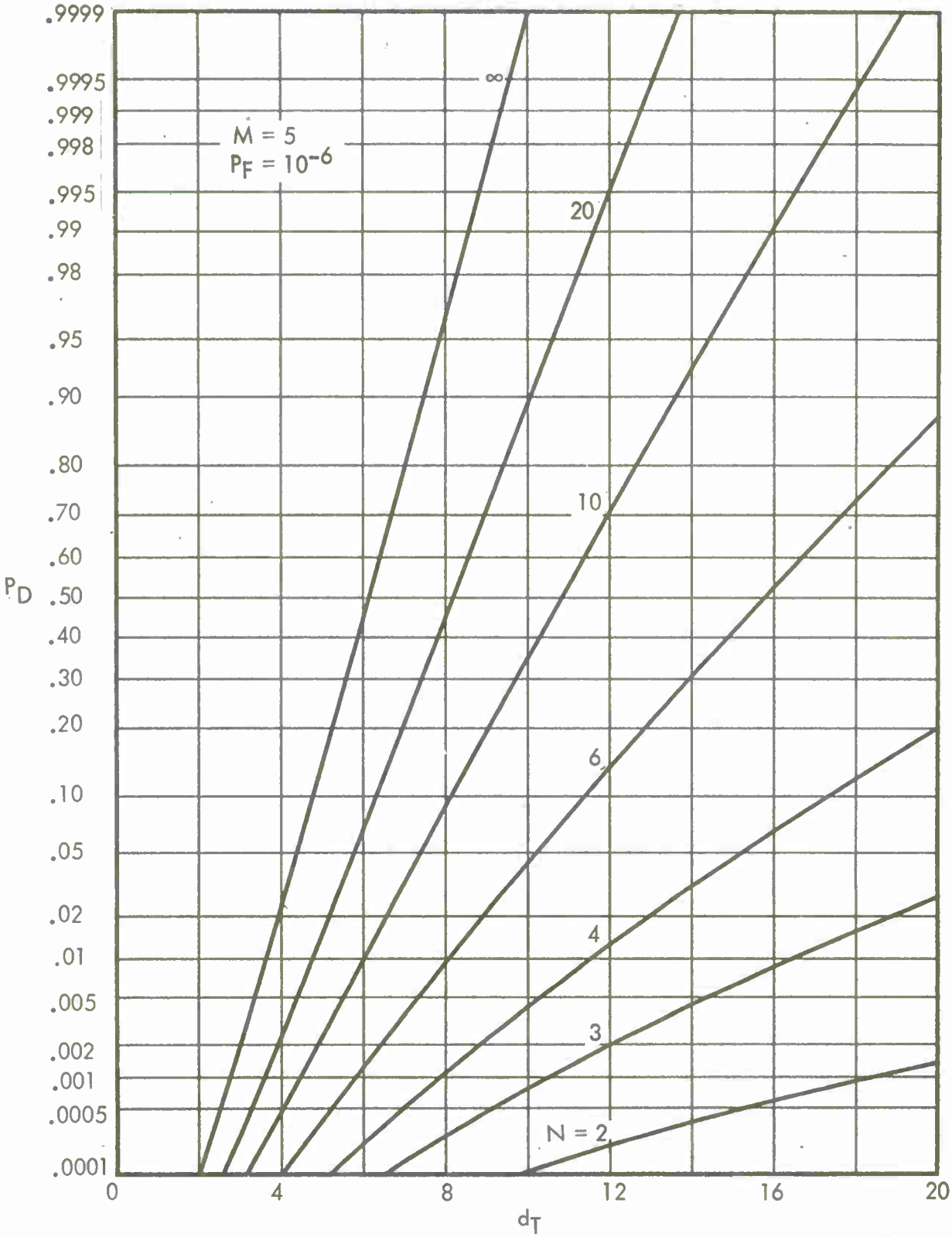


Figure 24. Detection Characteristics for UA Processor; M = 5, $P_F = 10^{-6}$

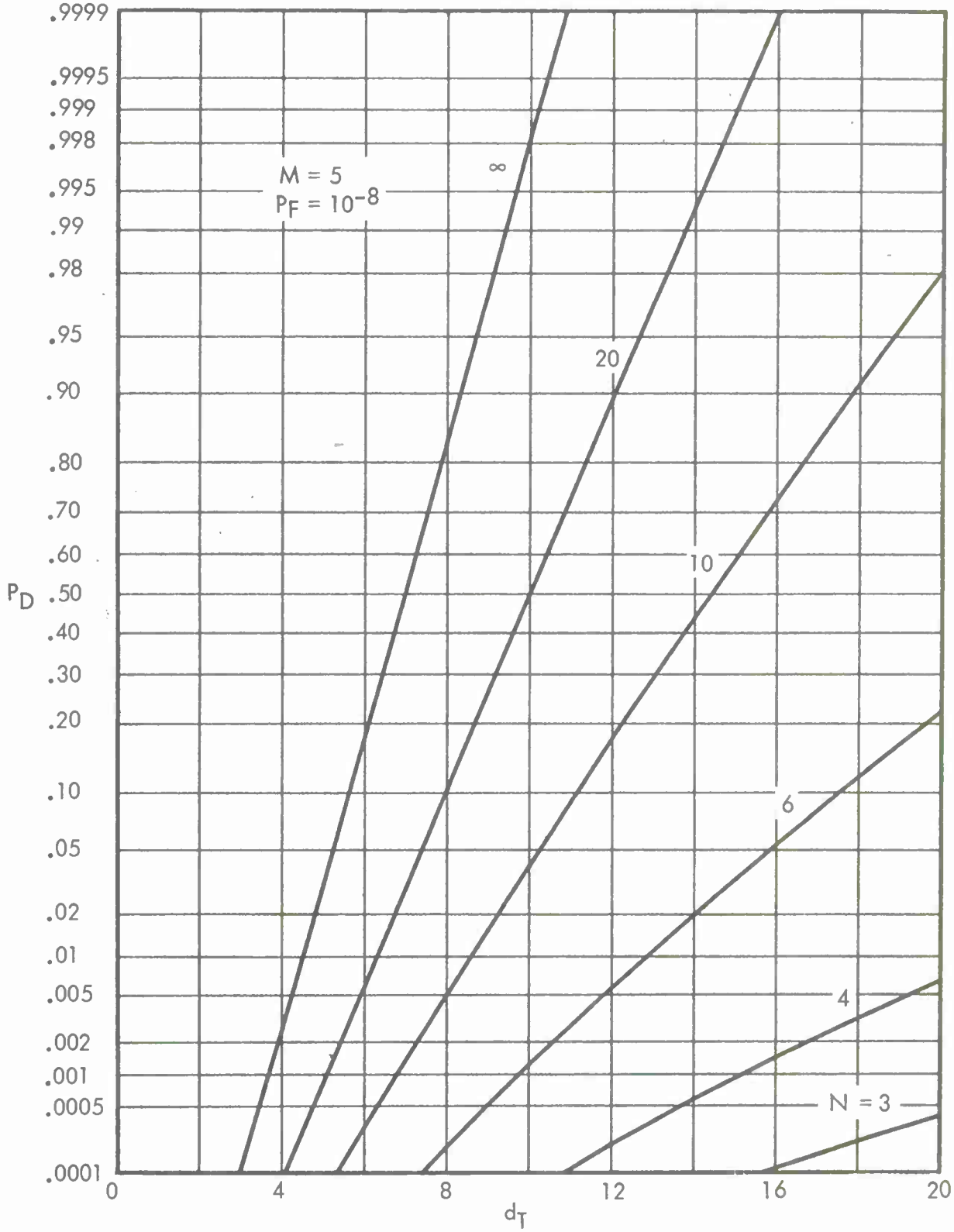


Figure 25. Detection Characteristics for UA Processor; M = 5, $P_F = 10^{-8}$

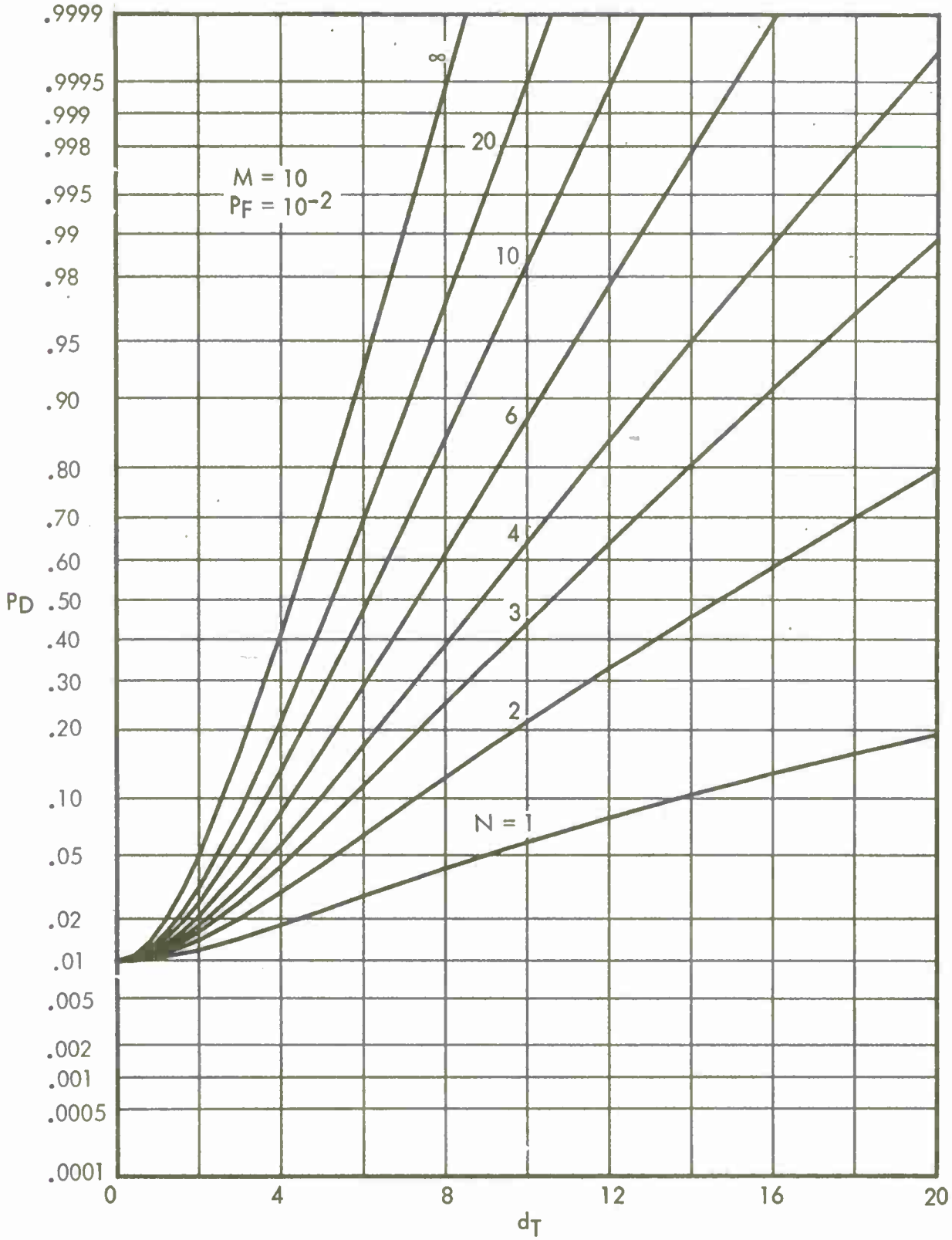


Figure 26. Detection Characteristics for UA Processor; M = 10, $P_F = 10^{-2}$

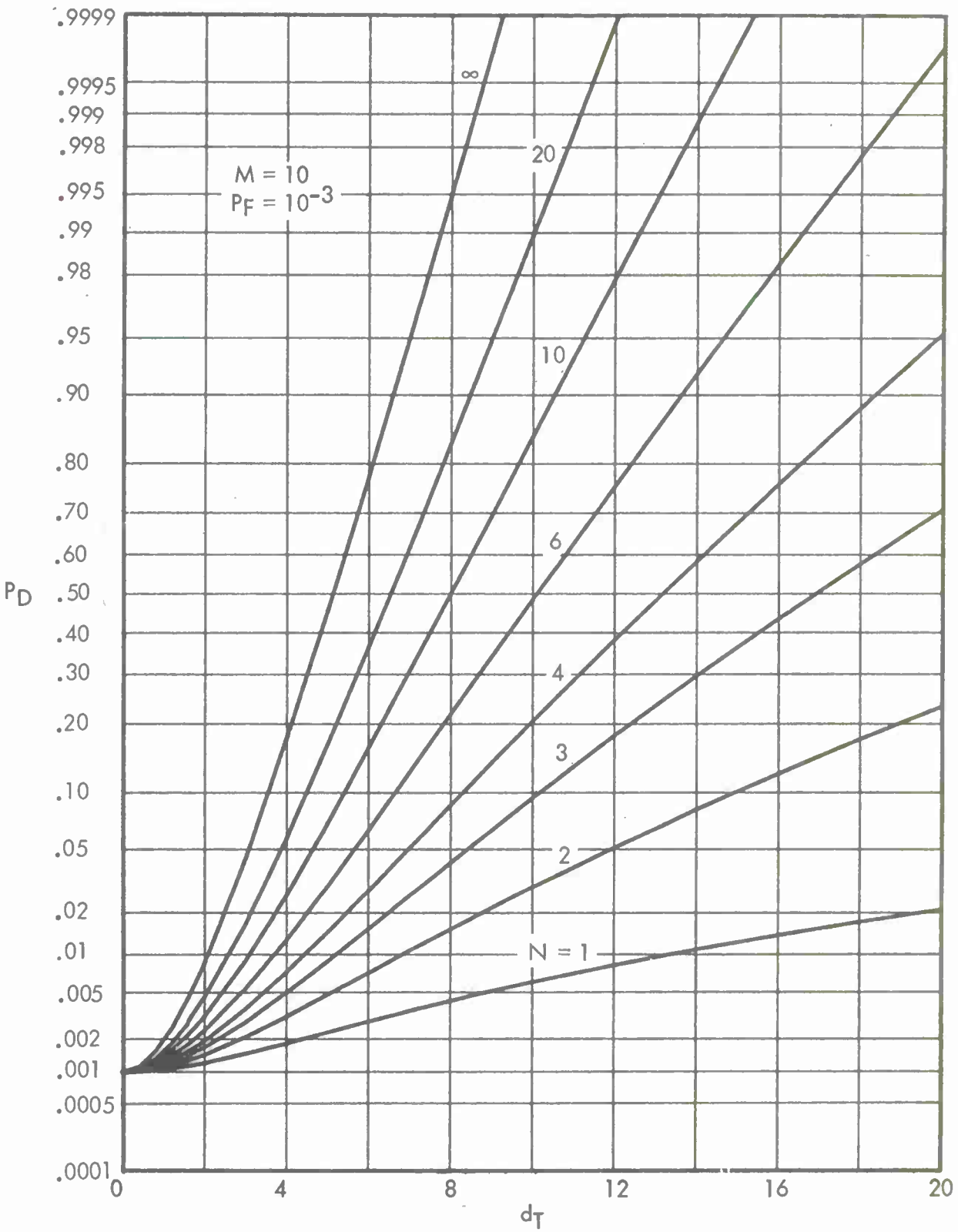


Figure 27. Detection Characteristics for UA Processor; M = 10, $P_F = 10^{-3}$

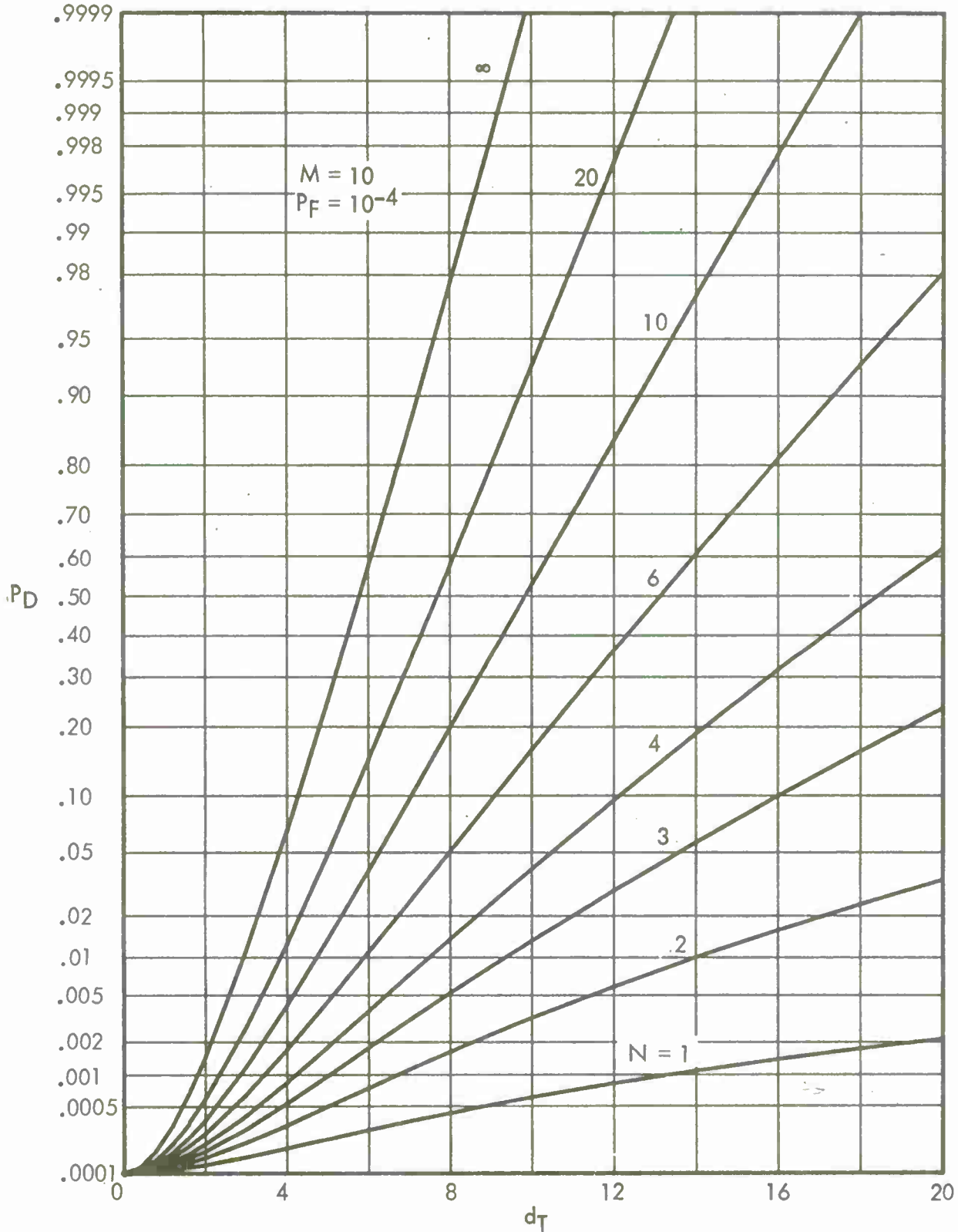


Figure 28. Detection Characteristics for UA Processor; M = 10, $P_F = 10^{-4}$

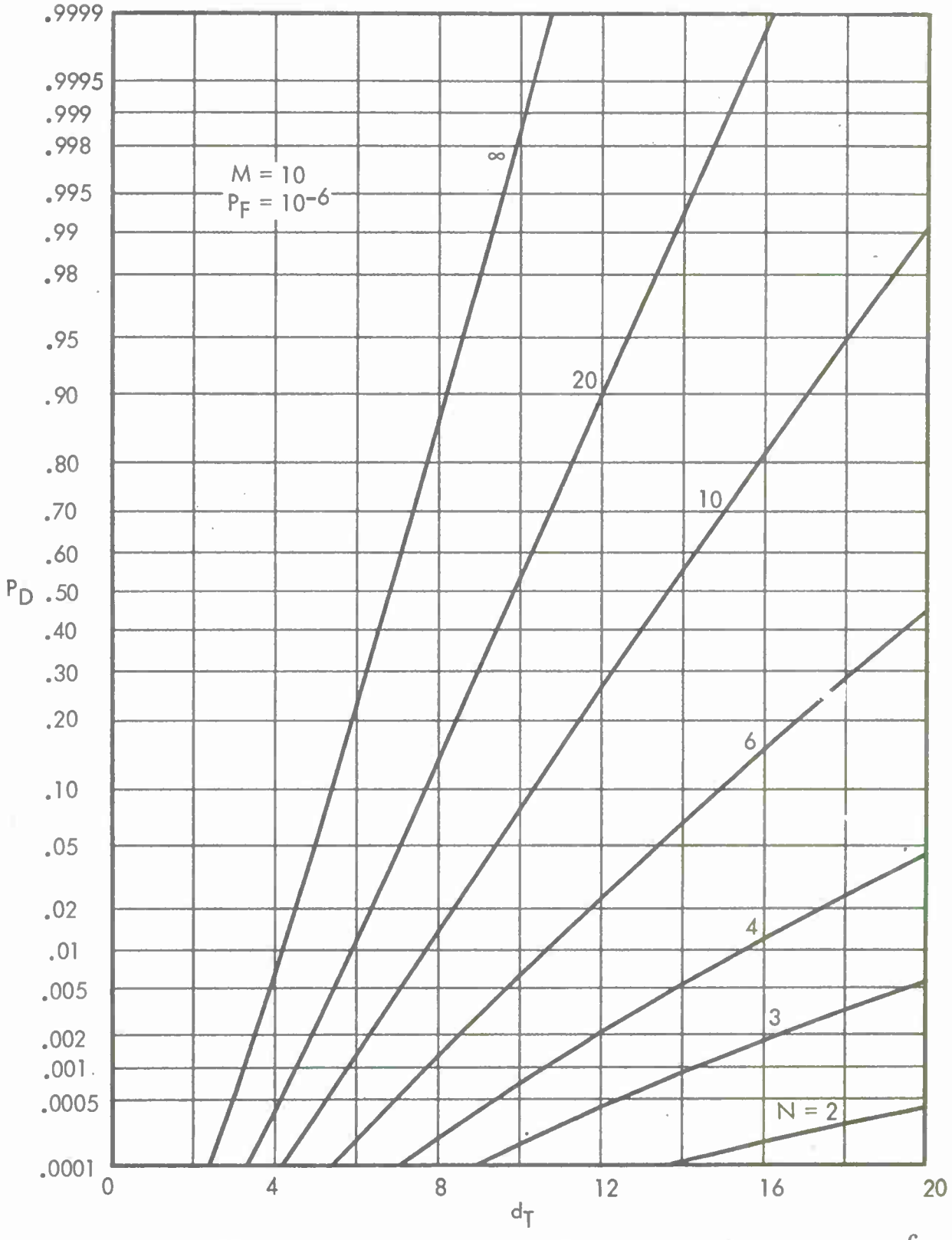


Figure 29. Detection Characteristics for UA Processor; M = 10, $P_F = 10^{-6}$

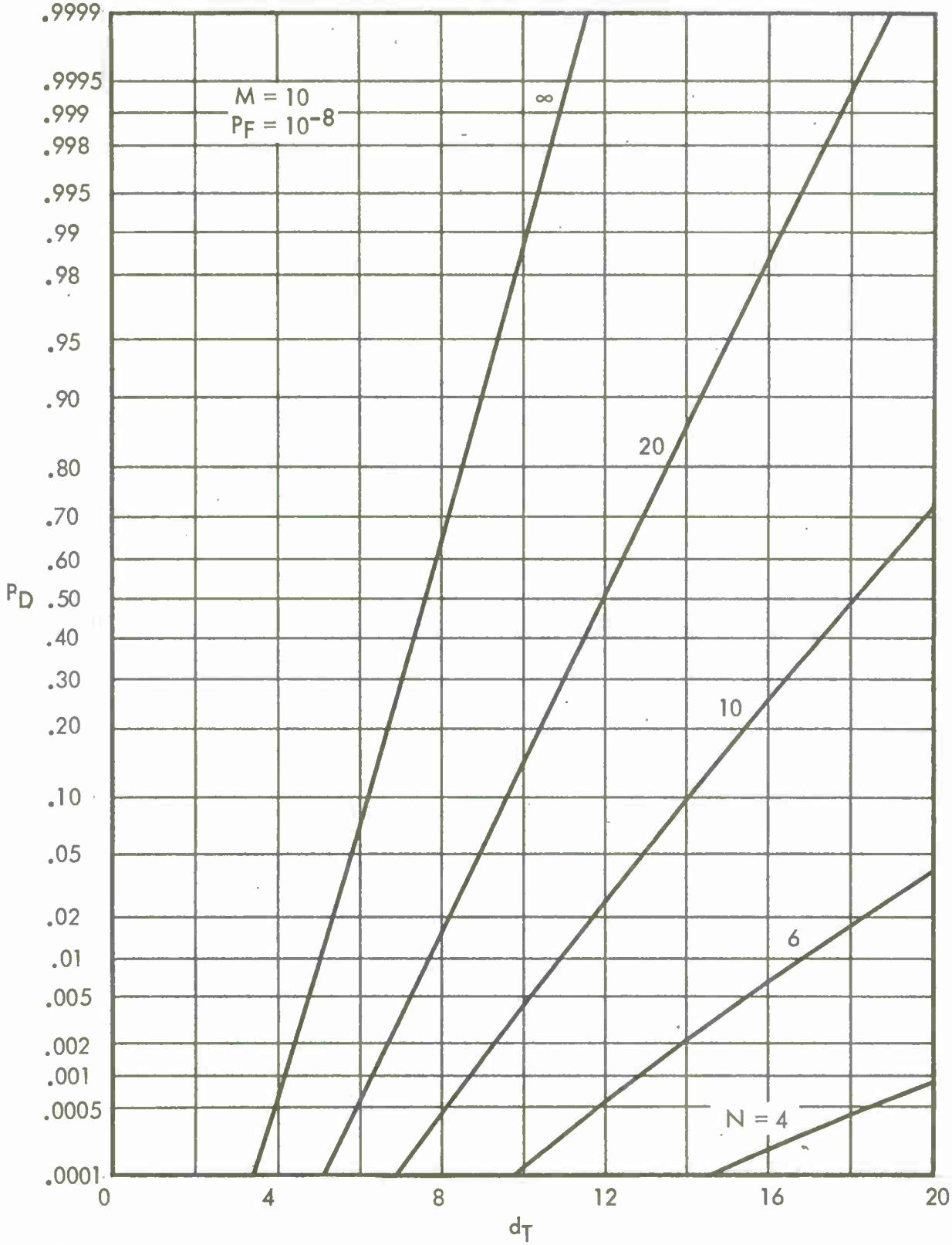


Figure 30. Detection Characteristics for UA Processor; M = 10, $P_F = 10^{-8}$

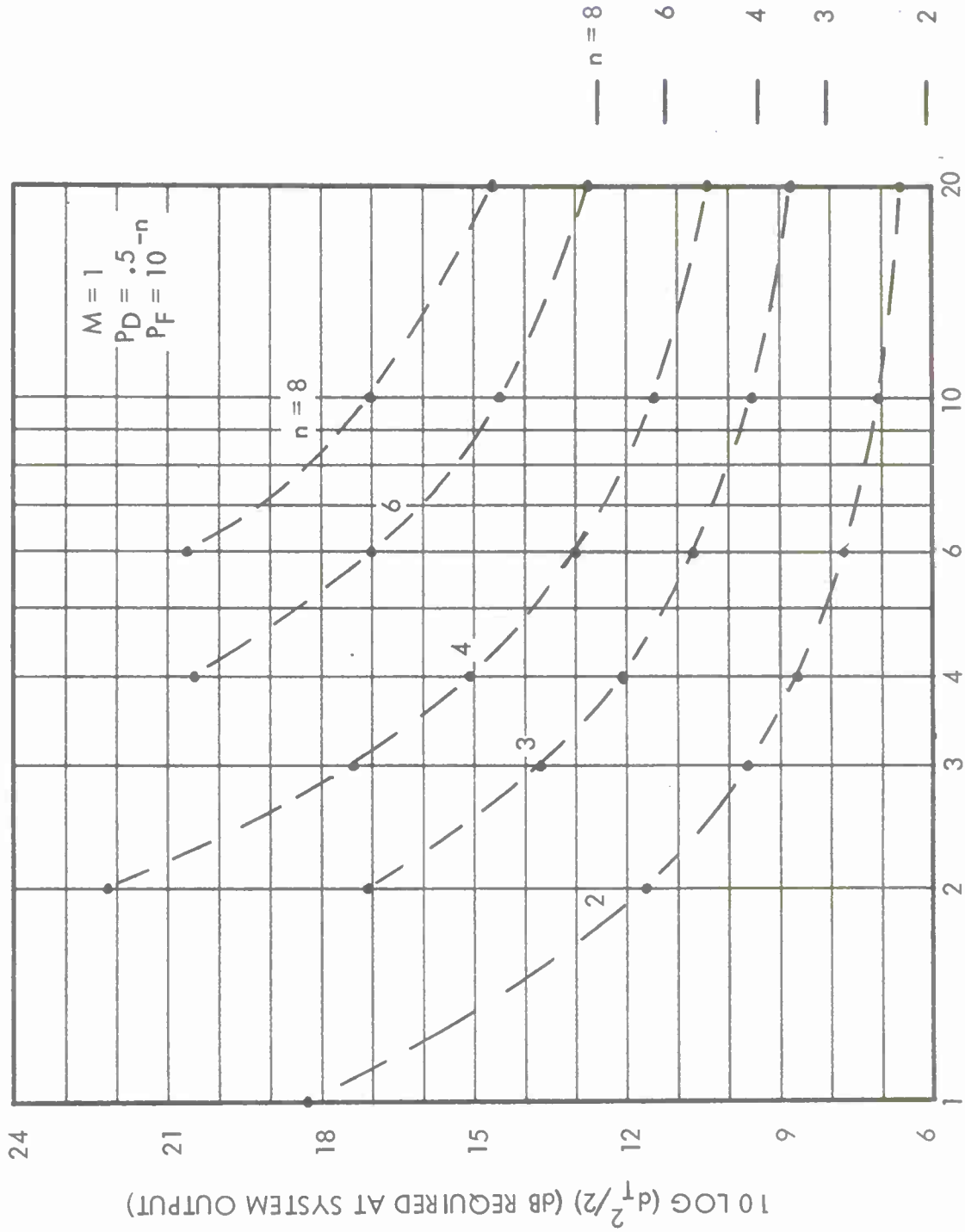


Figure 31. Required Signal-to-Noise Ratio for UA Processor; M = 1

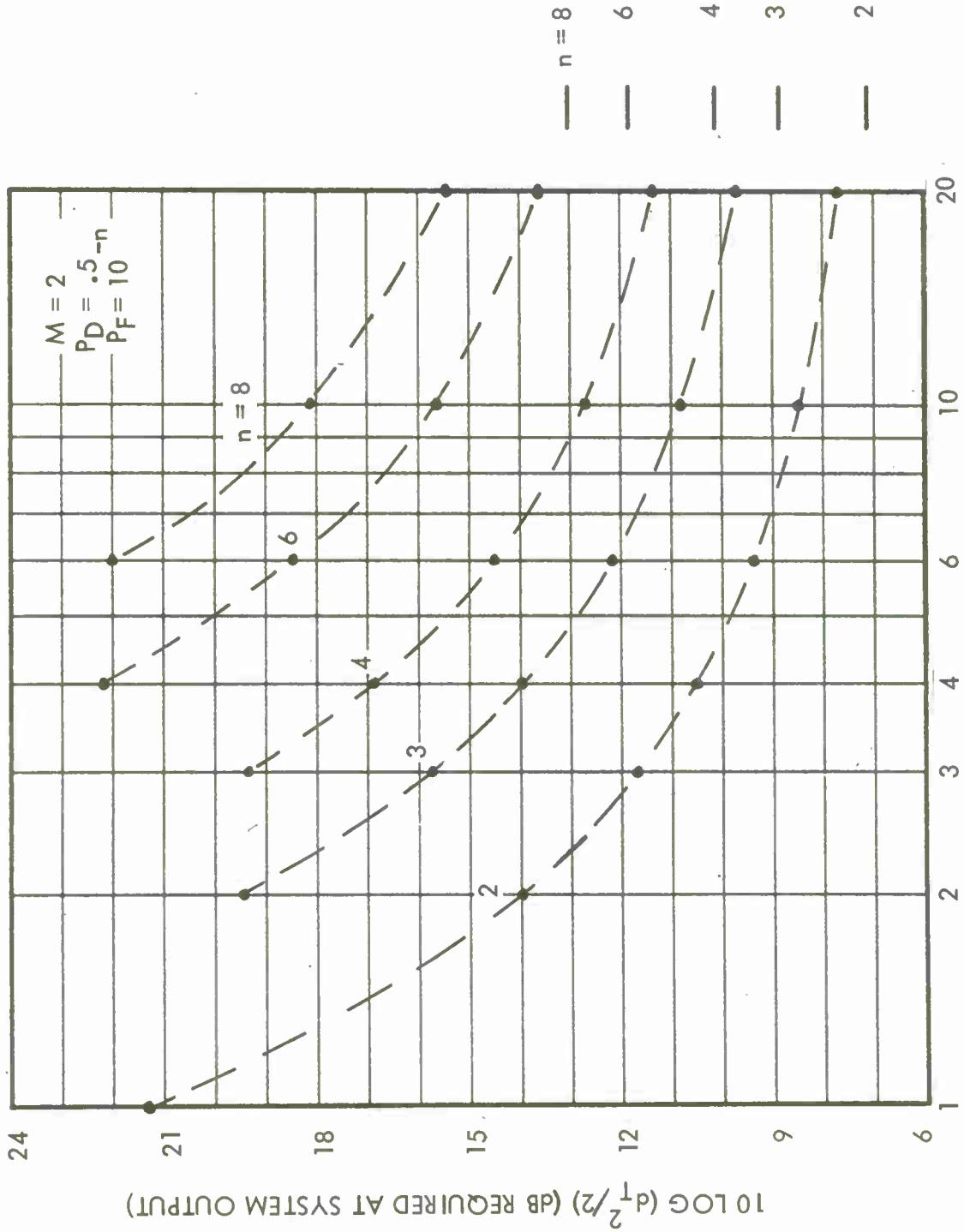


Figure 32. Required Signal-to-Noise Ratio for UA Processor; M = 2

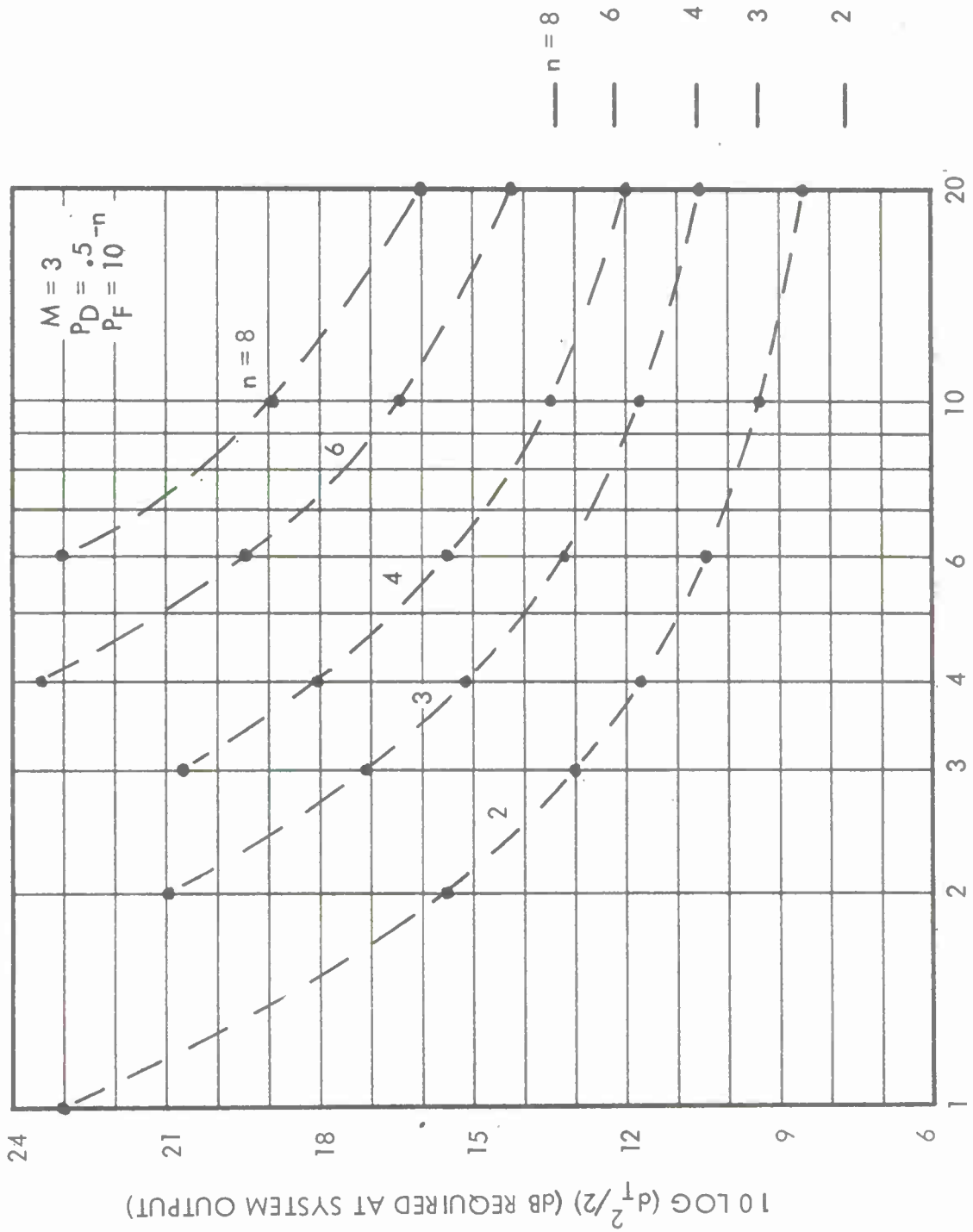


Figure 33. Required Signal-to-Noise Ratio for UA Processor; M = 3

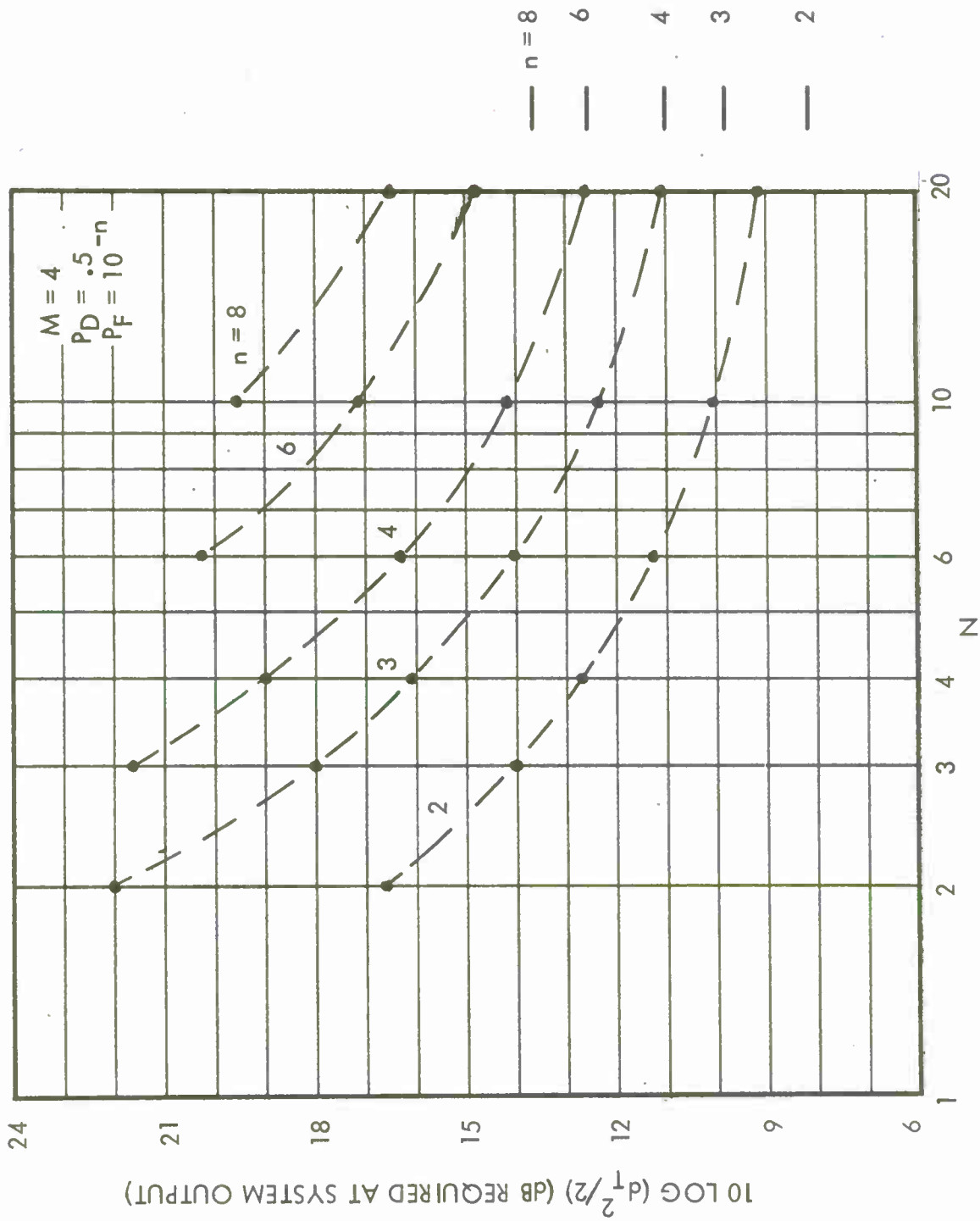


Figure 34. Required Signal-to-Noise Ratio for UA Processor; M = 4

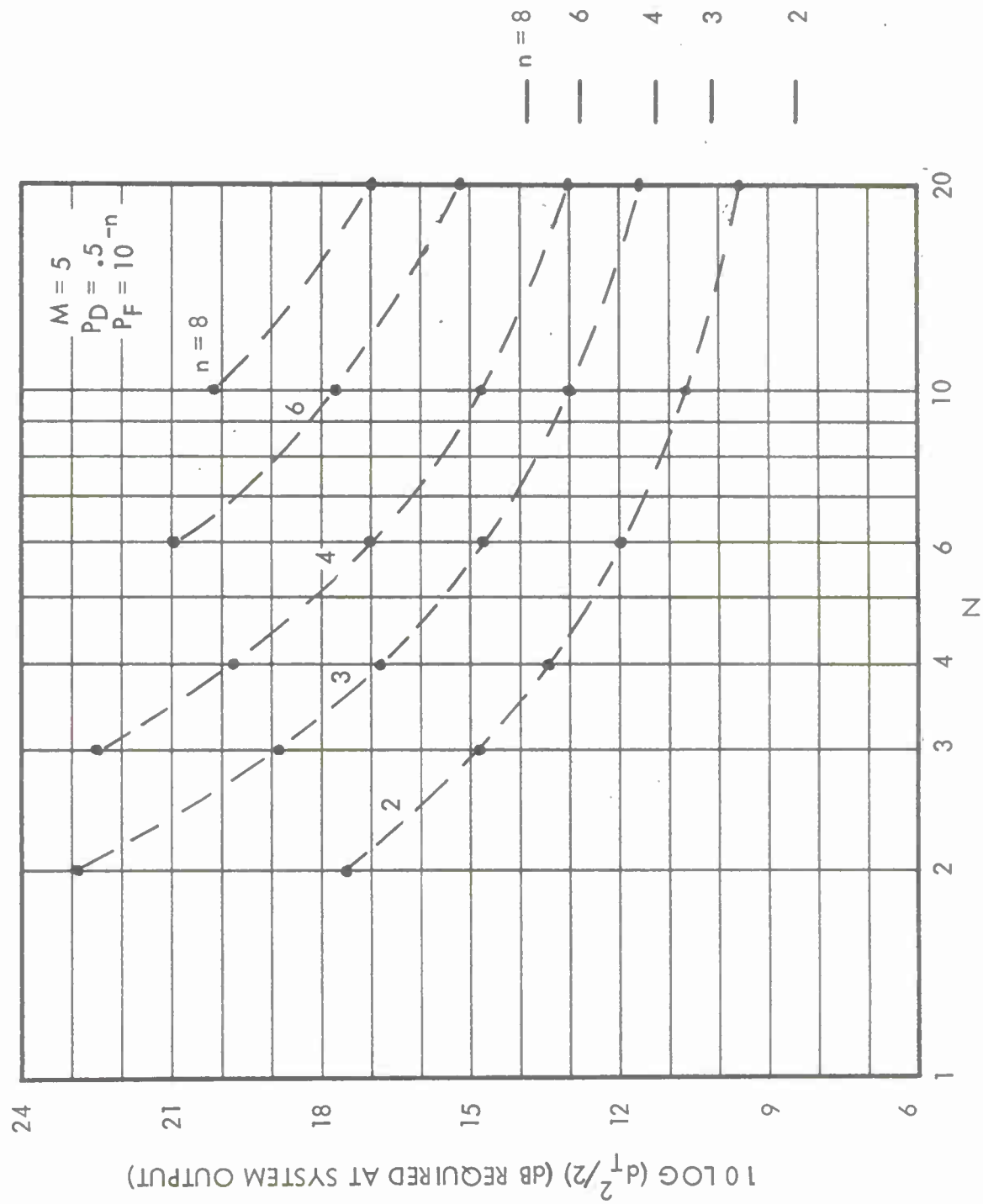


Figure 35. Required Signal-to-Noise Ratio for UA Processor; M = 5

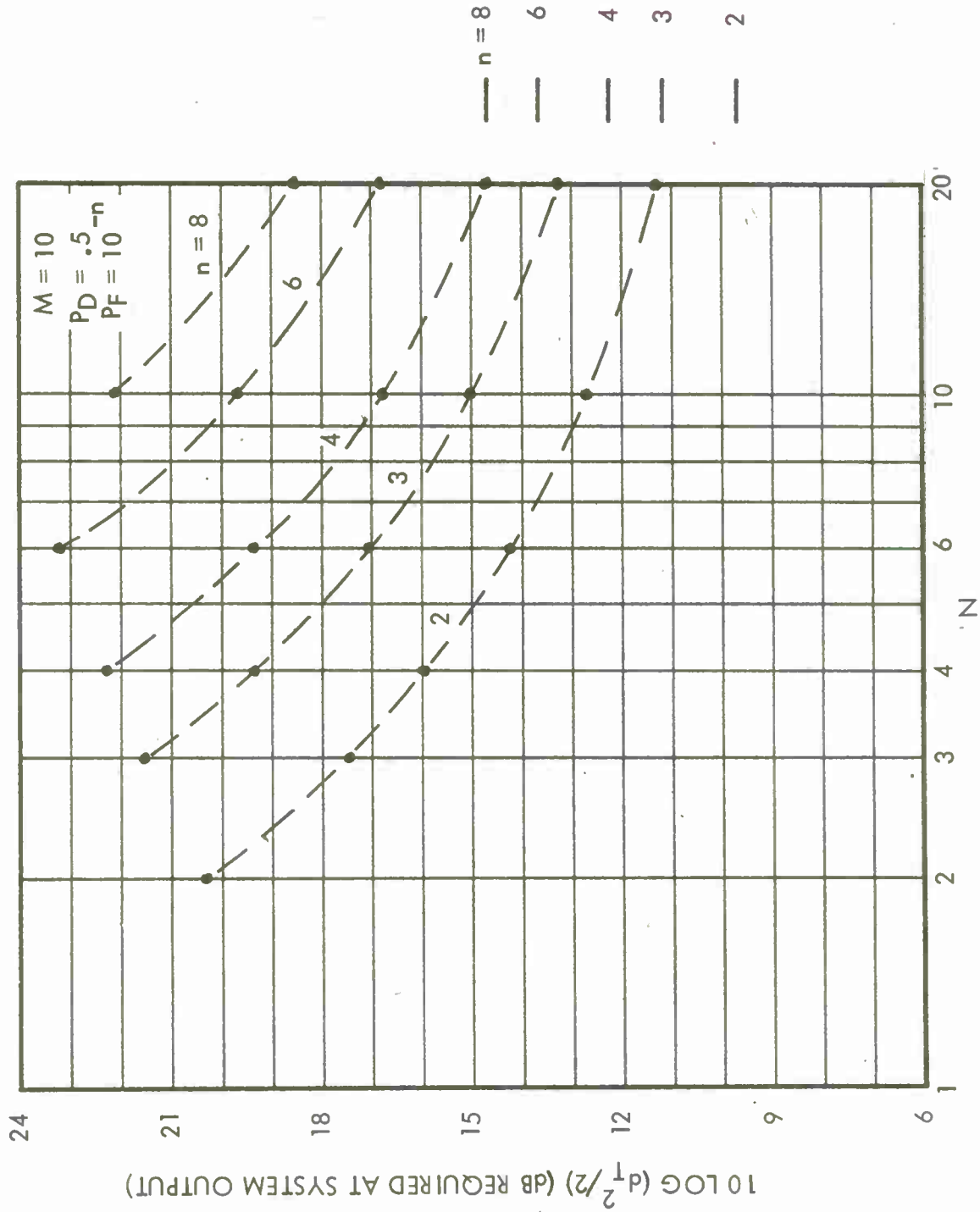


Figure 36. Required Signal-to-Noise Ratio for UA Processor; M = 10

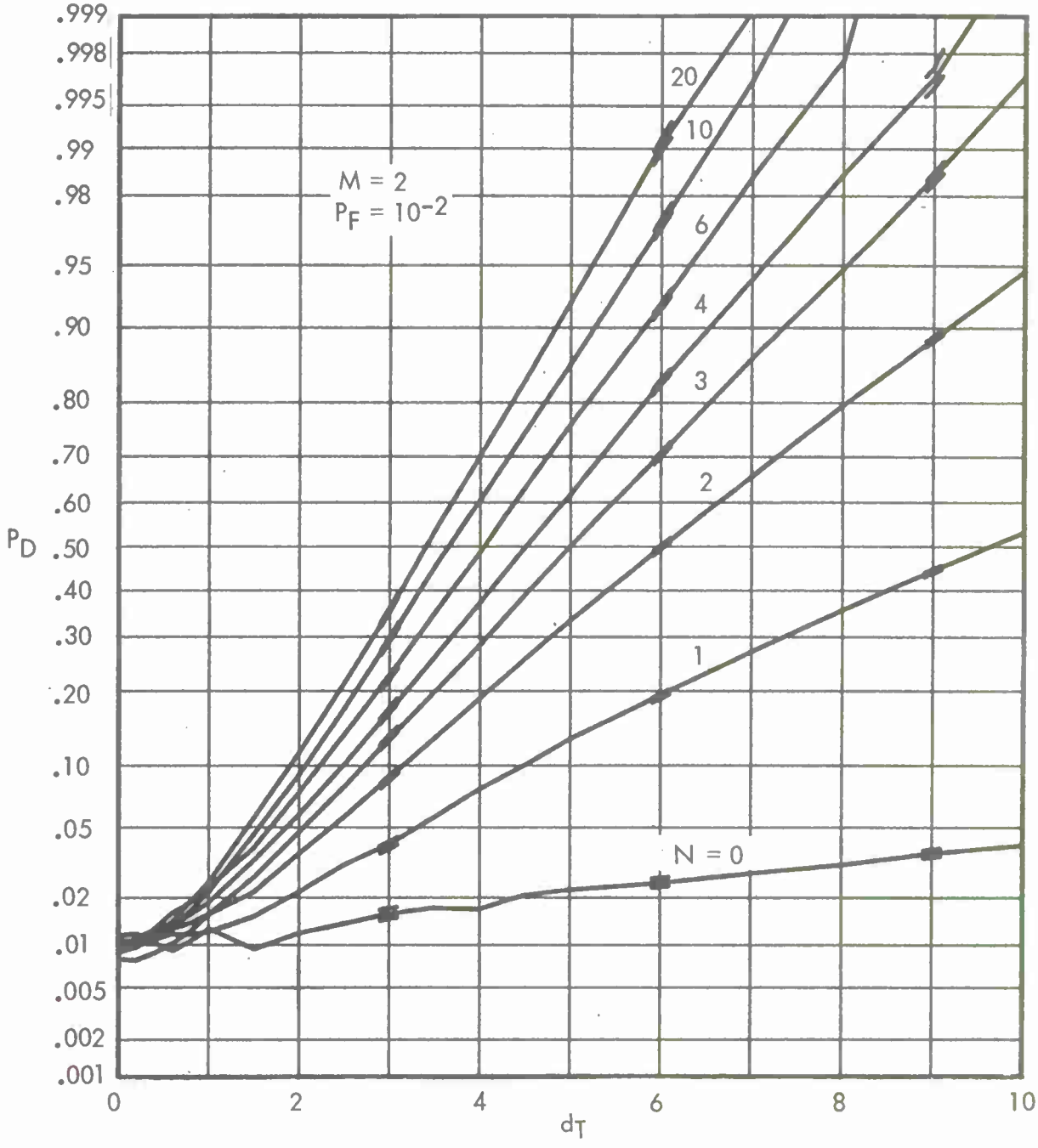


Figure 37. Detection Characteristics for EA Processor; M = 2, $P_F = 10^{-2}$

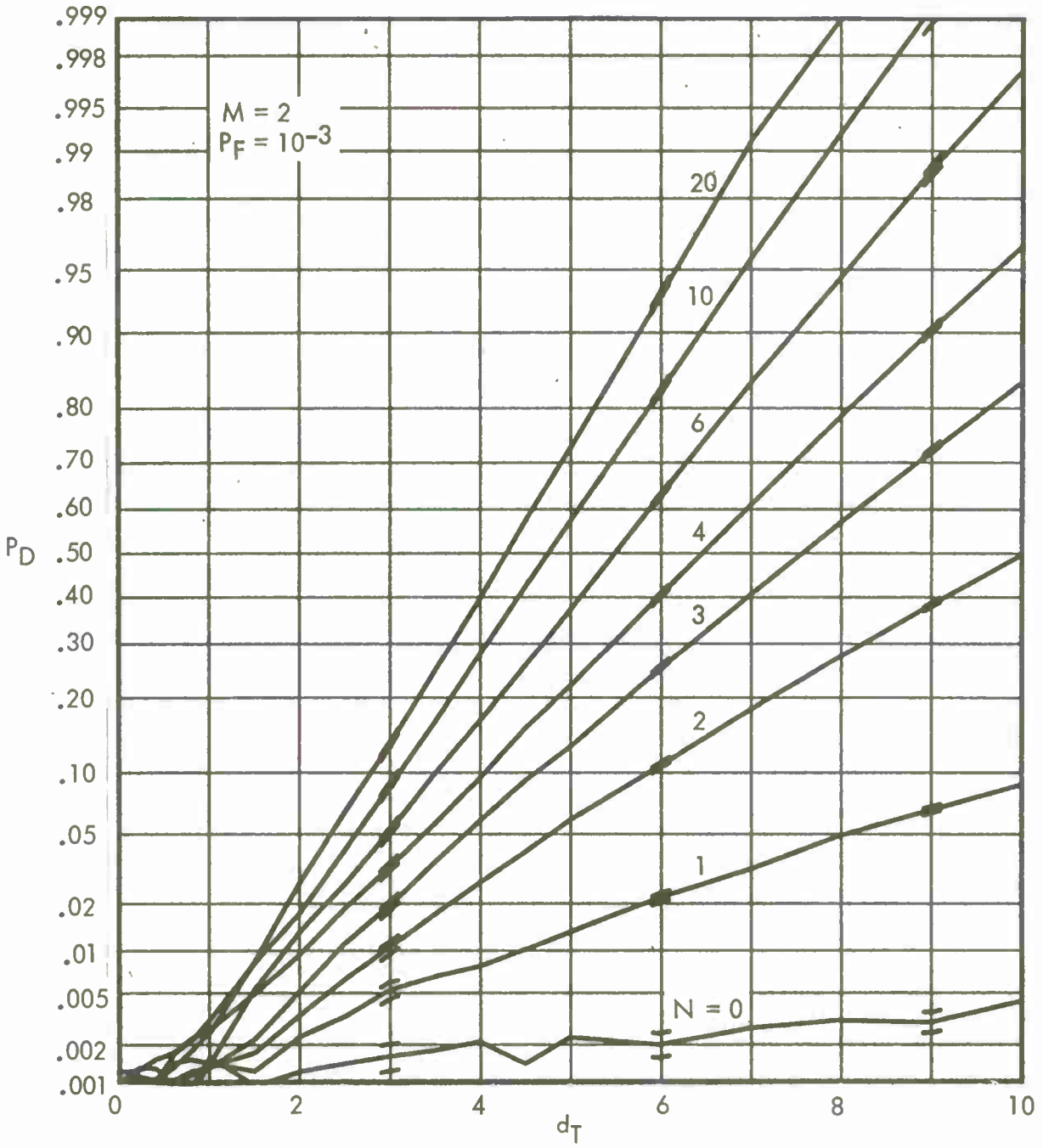


Figure 38. Detection Characteristics for EA Processor; M = 2, $P_F = 10^{-3}$

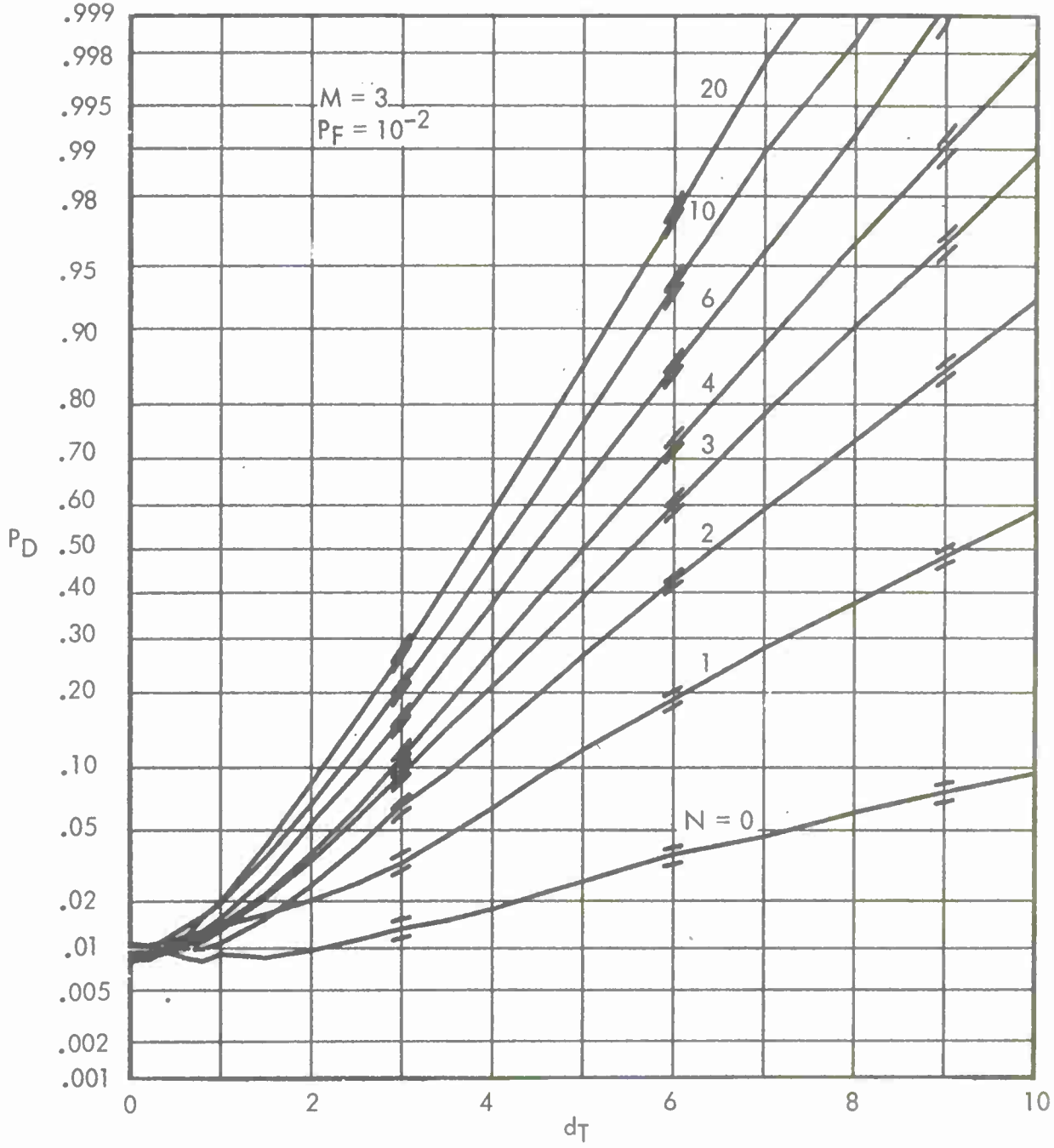


Figure 39. Detection Characteristics for EA Processor; M = 3, $P_F = 10^{-2}$

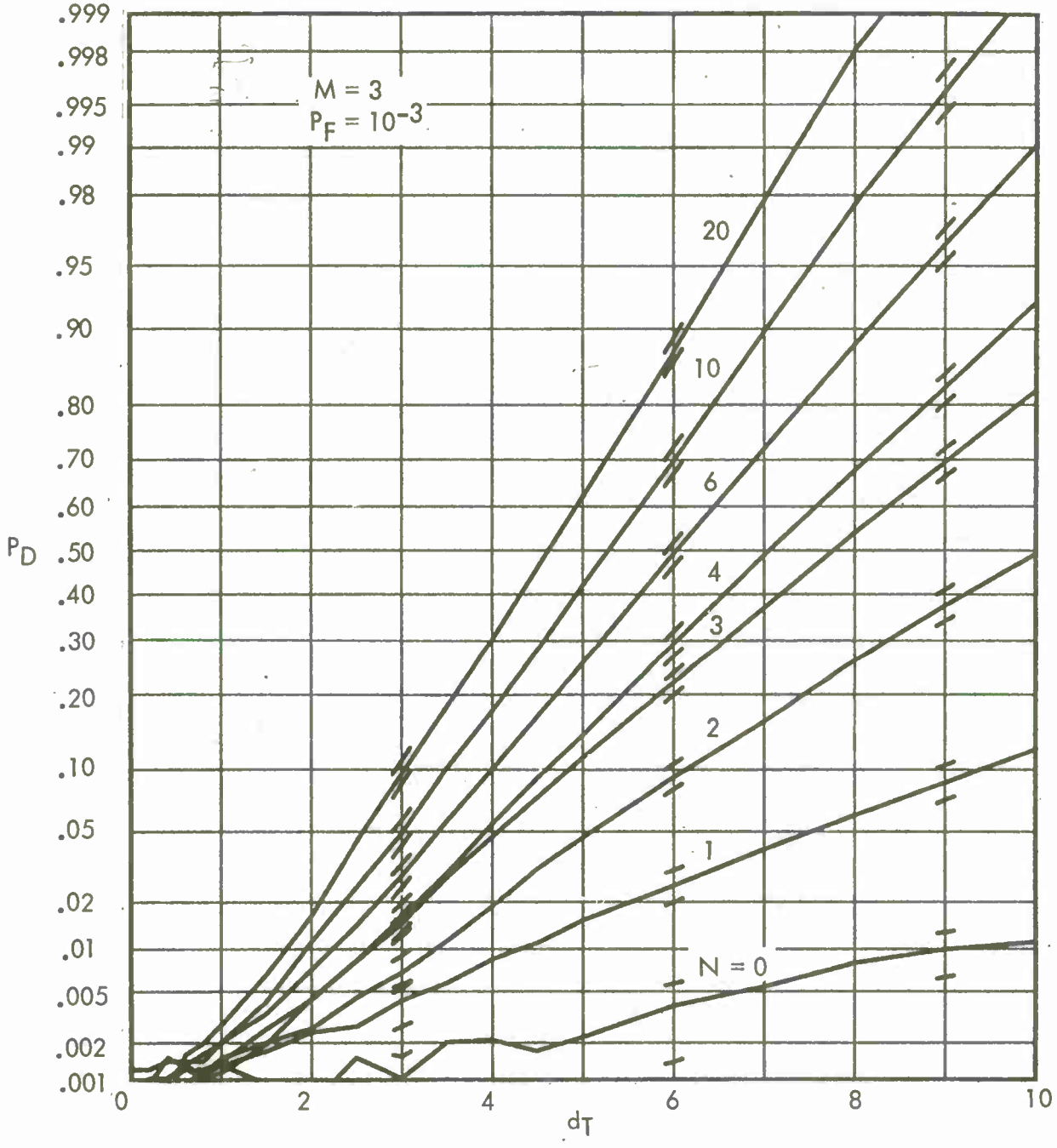


Figure 40. Detection Characteristics for EA Processor; M = 3, $P_F = 10^{-3}$

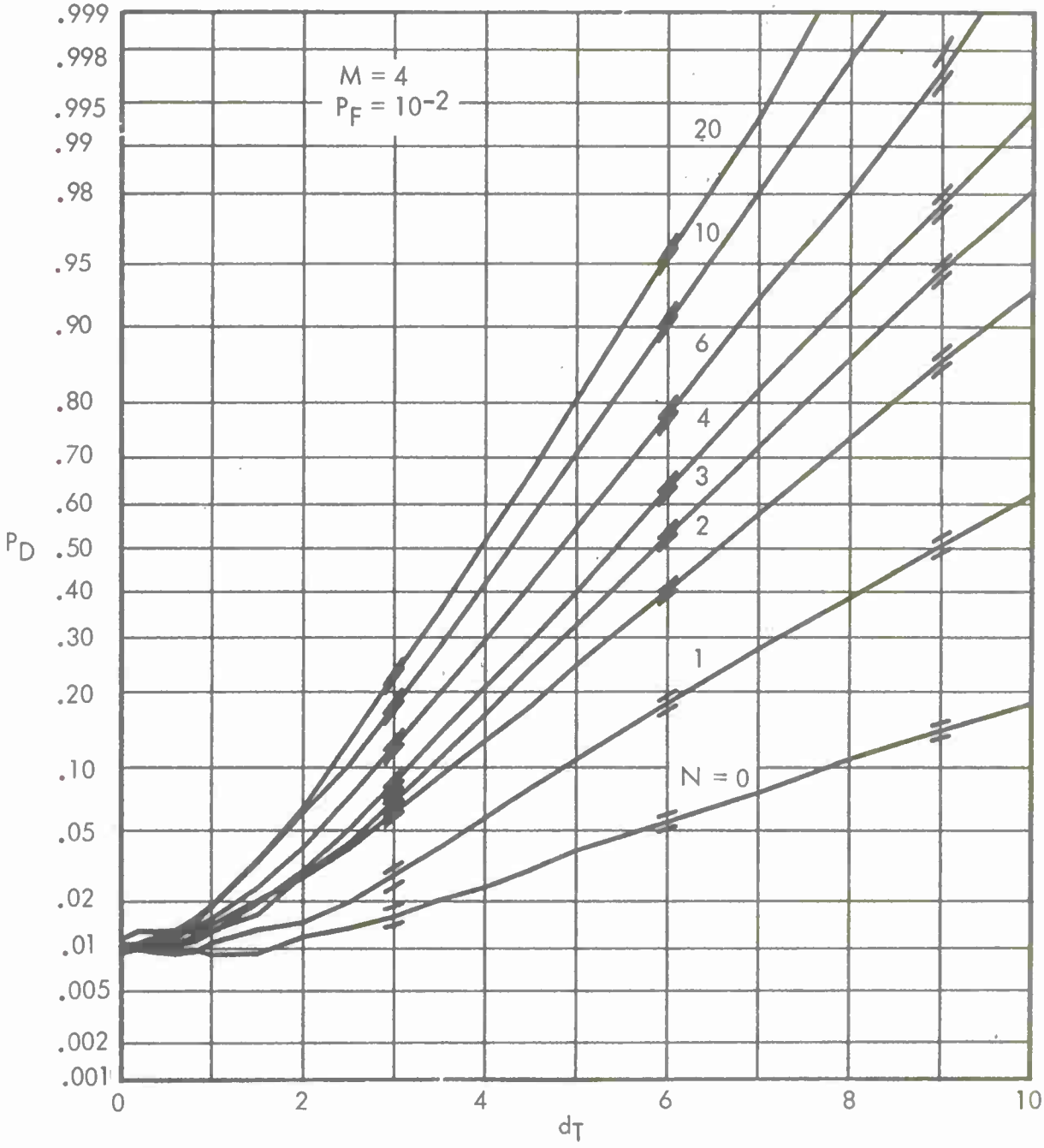


Figure 41. Detection Characteristics for EA Processor; M = 4, $P_F = 10^{-2}$

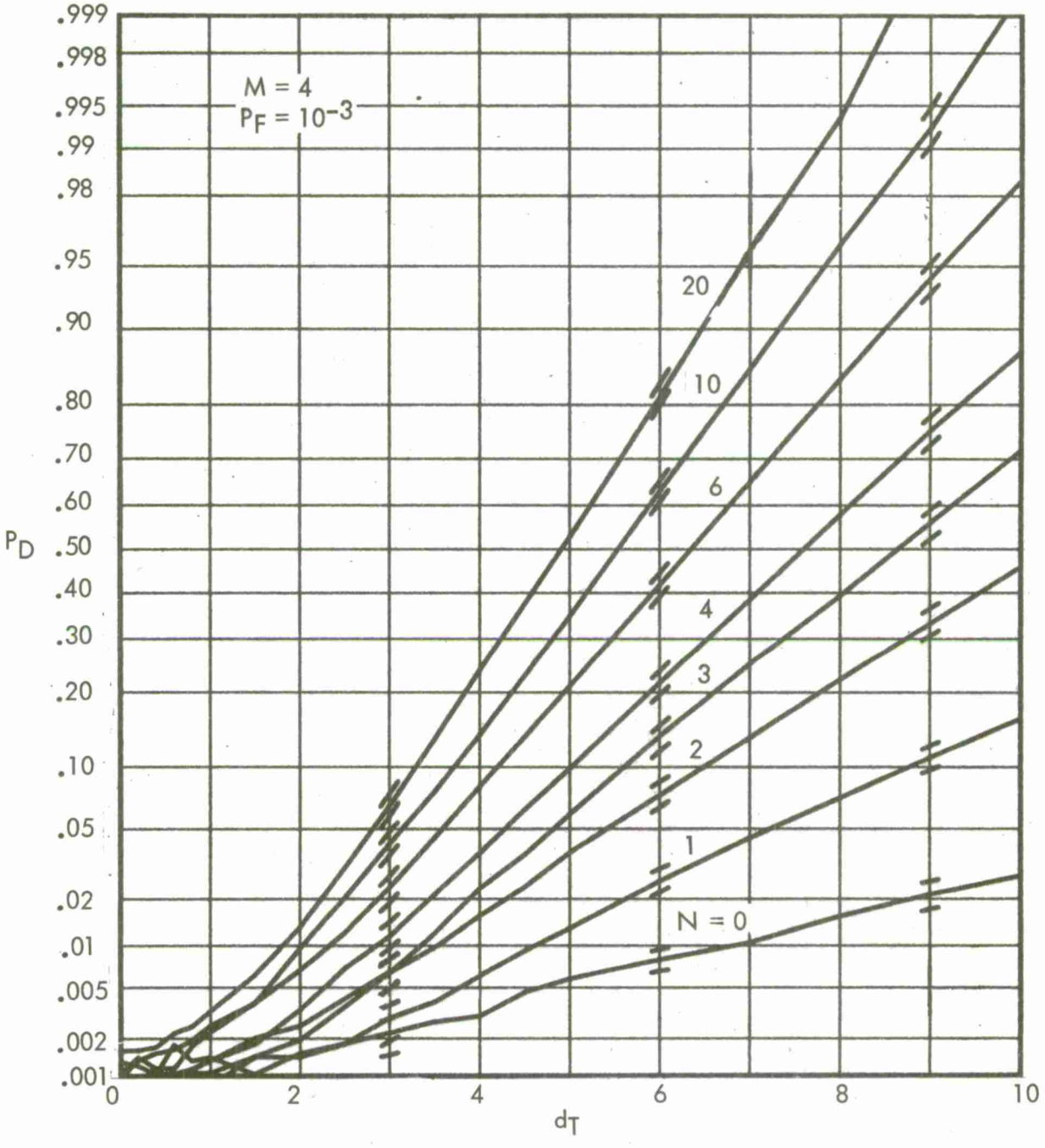


Figure 42. Detection Characteristics for EA Processor; M = 4, $P_F = 10^{-3}$

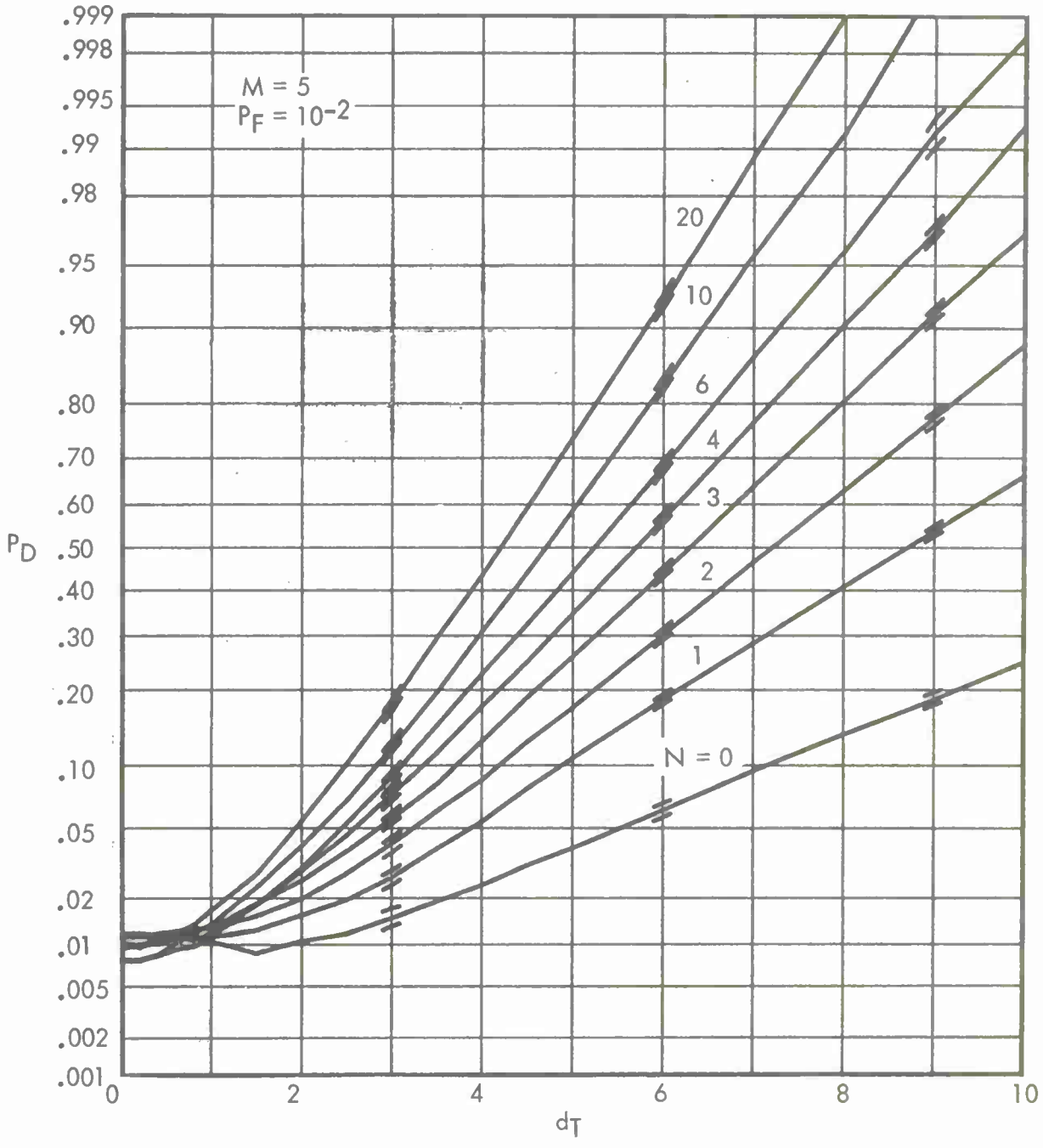


Figure 43. Detection Characteristics for EA Processor; M = 5, $P_F = 10^{-2}$

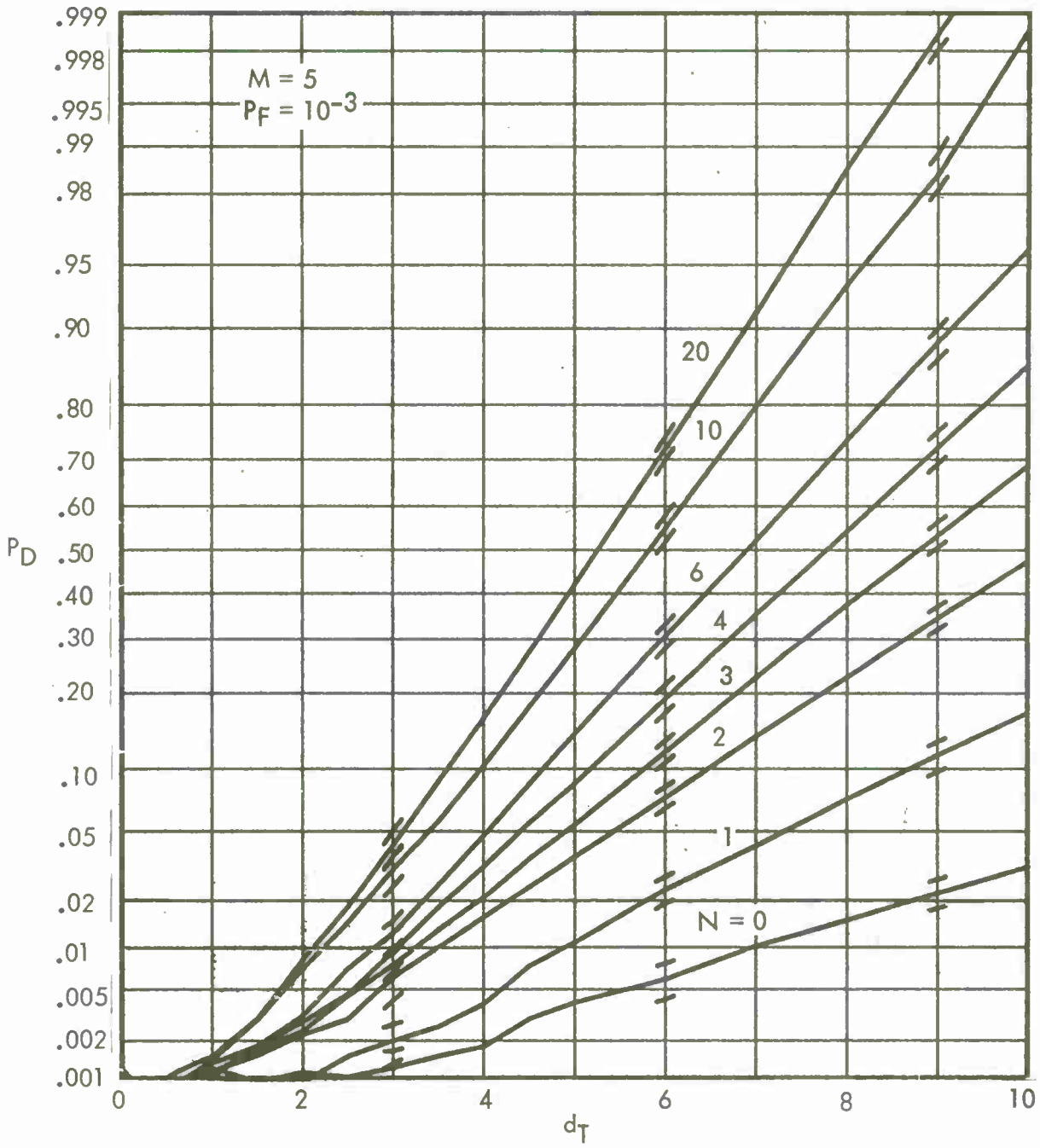


Figure 44. Detection Characteristics for EA Processor; M = 5, $P_F = 10^{-3}$

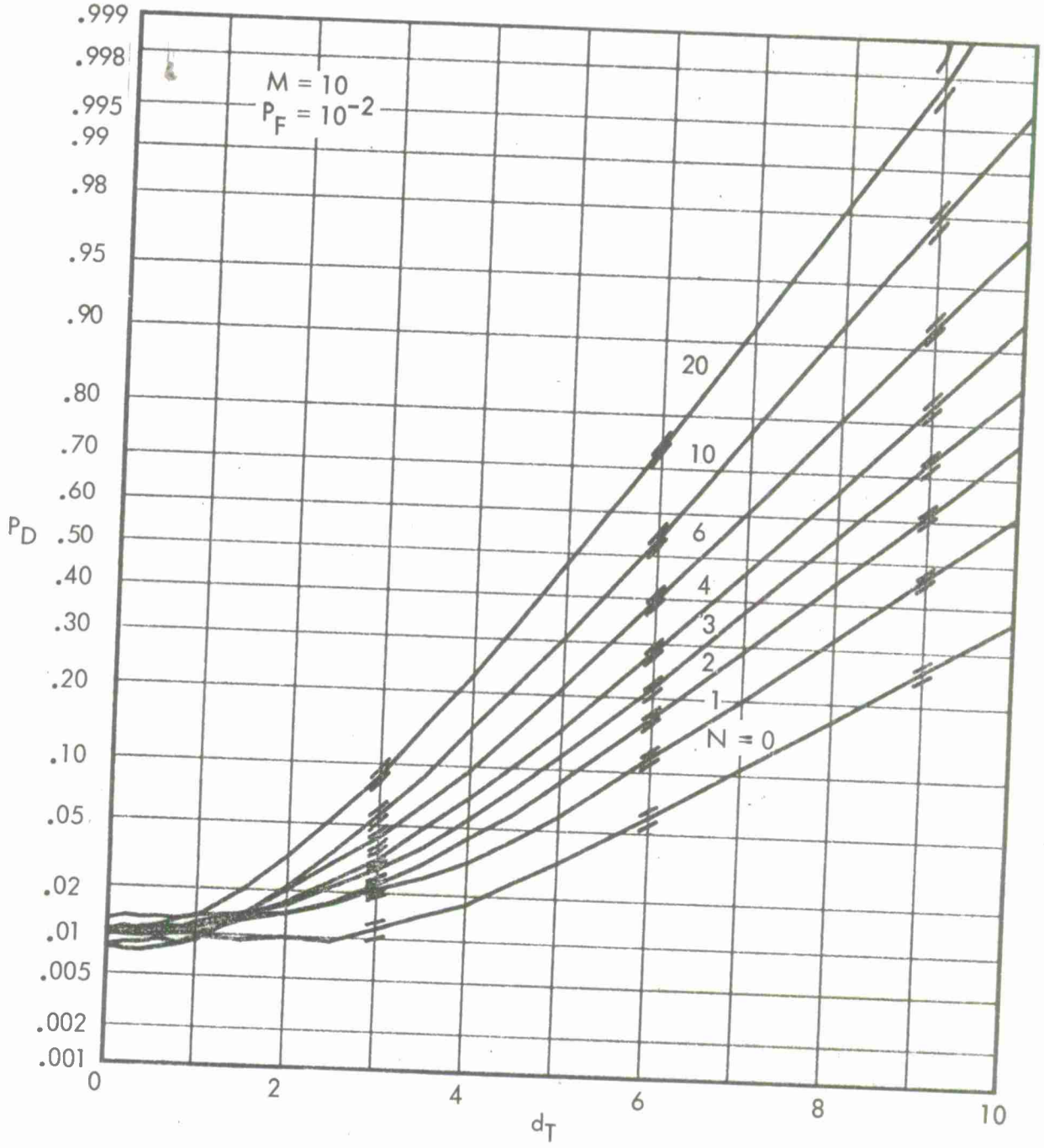


Figure 45. Detection Characteristics for EA Processor; M = 10, $P_F = 10^{-2}$

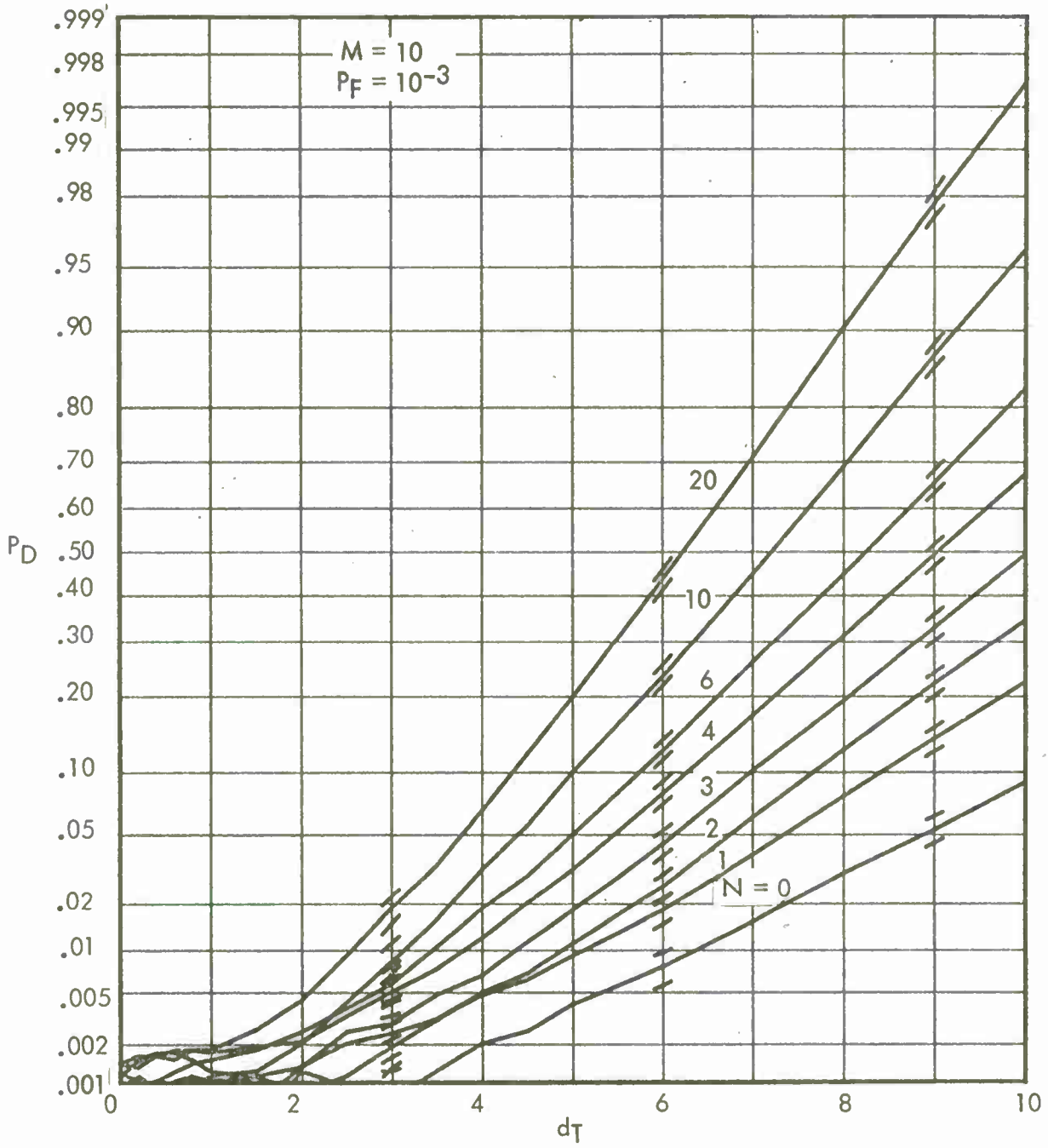


Figure 46. Detection Characteristics for EA Processor; M = 10, $P_F = 10^{-3}$

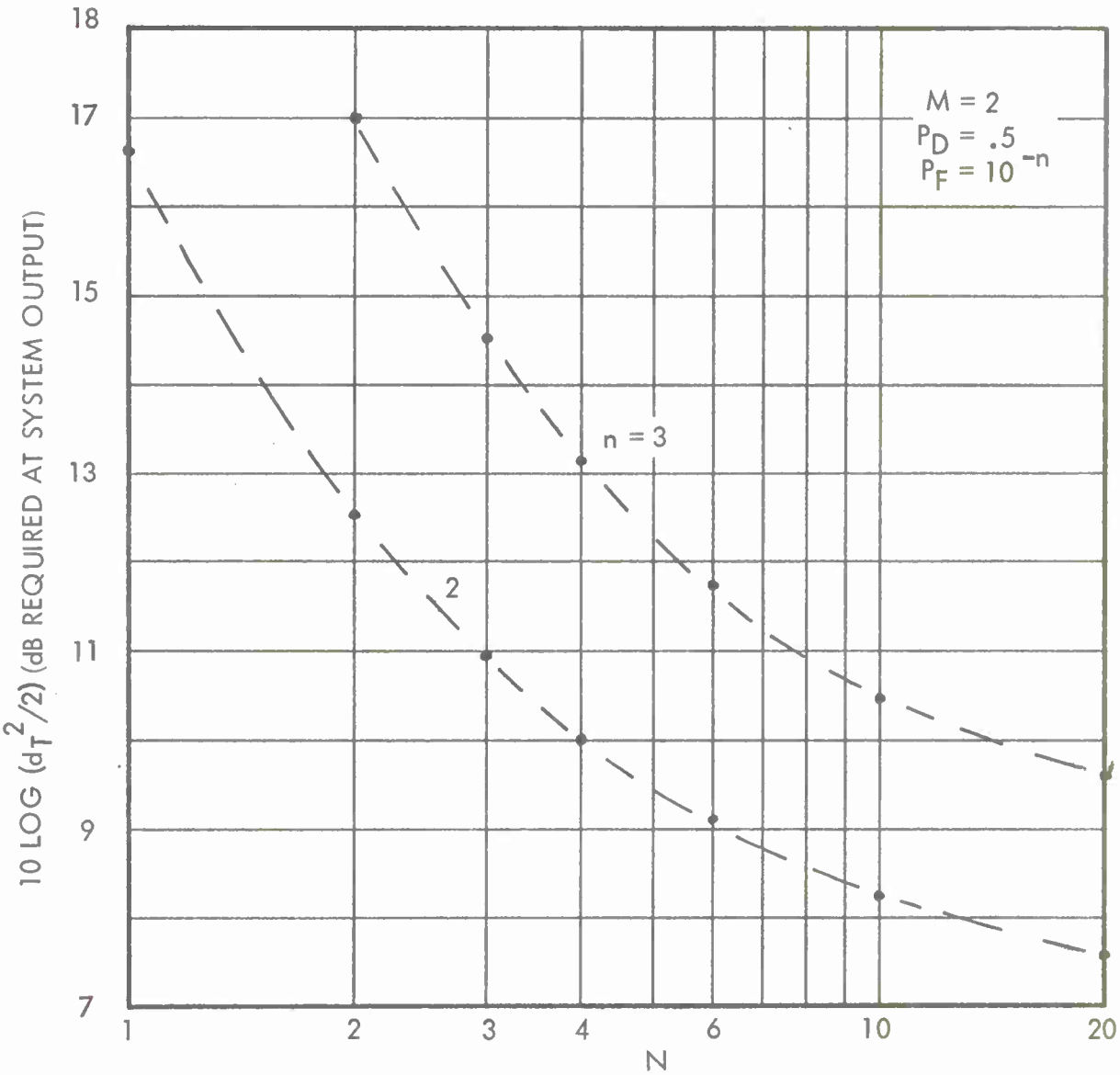


Figure 47. Required Signal-to-Noise Ratio for EA Processor; M = 2

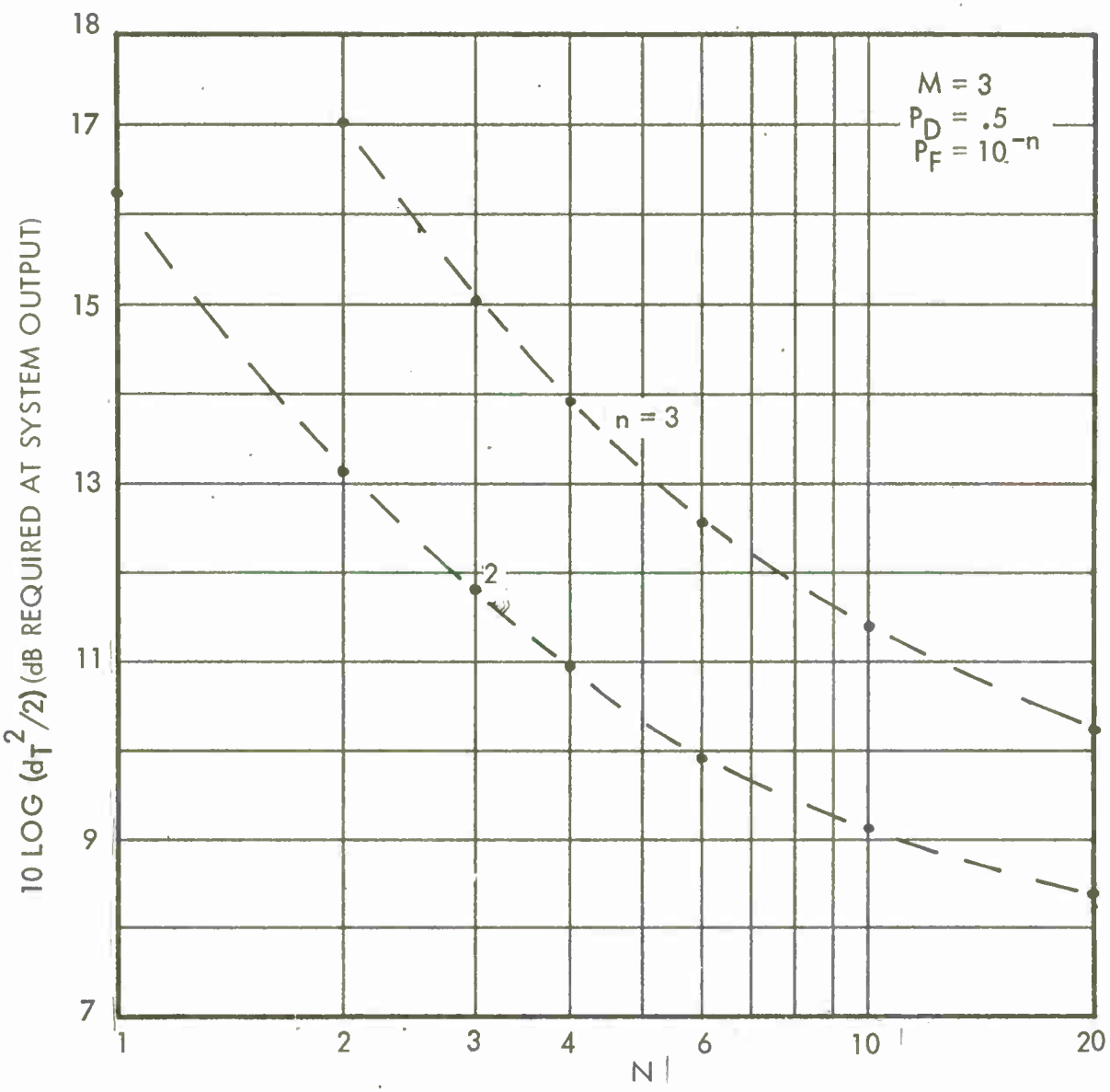


Figure 48. Required Signal-to-Noise Ratio for EA Processor; M = 3

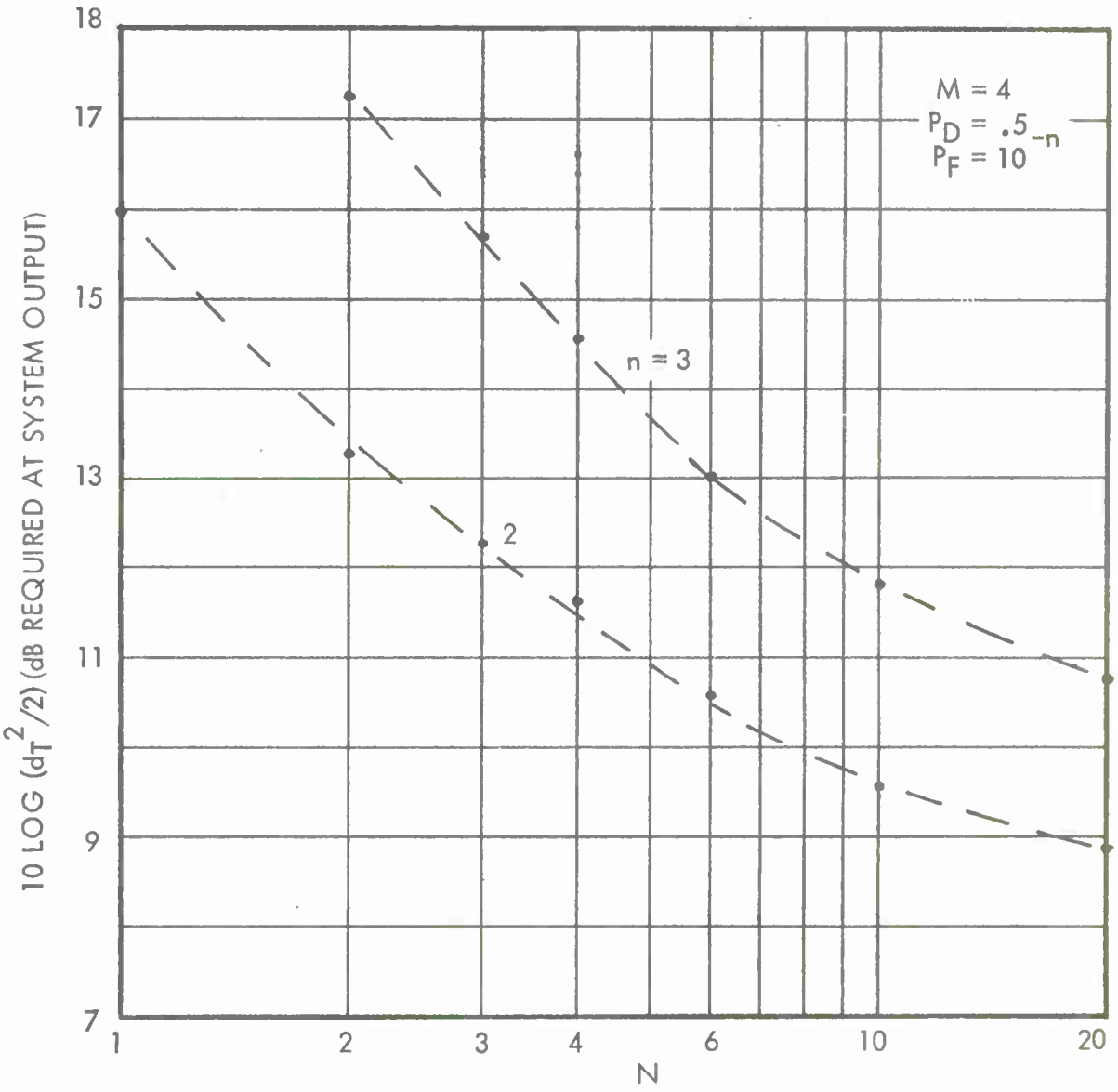


Figure 49. Required Signal-to-Noise Ratio for EA Processor; M = 4

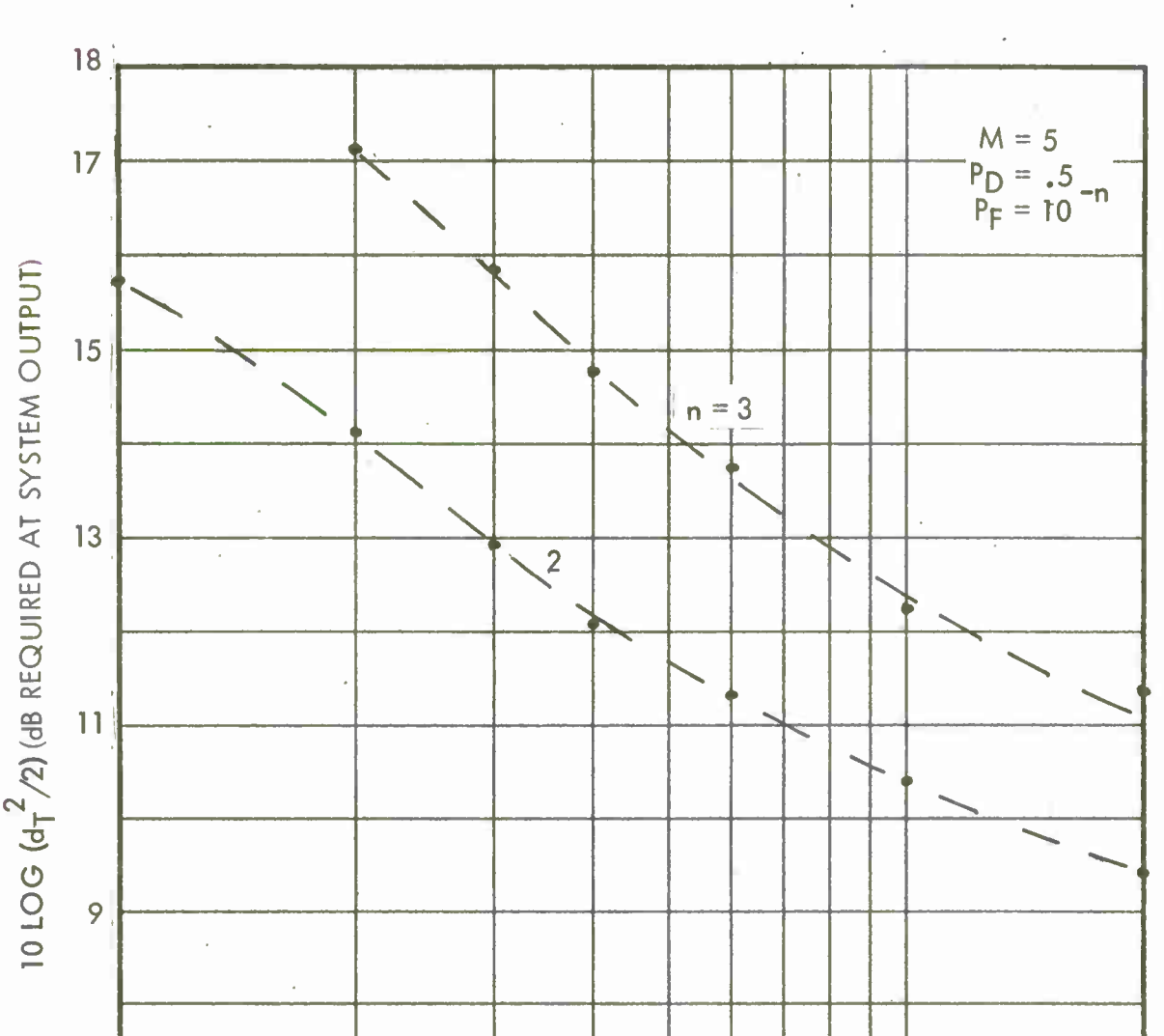


Figure 50. Required Signal-to-Noise Ratio for EA Processor; M = 5

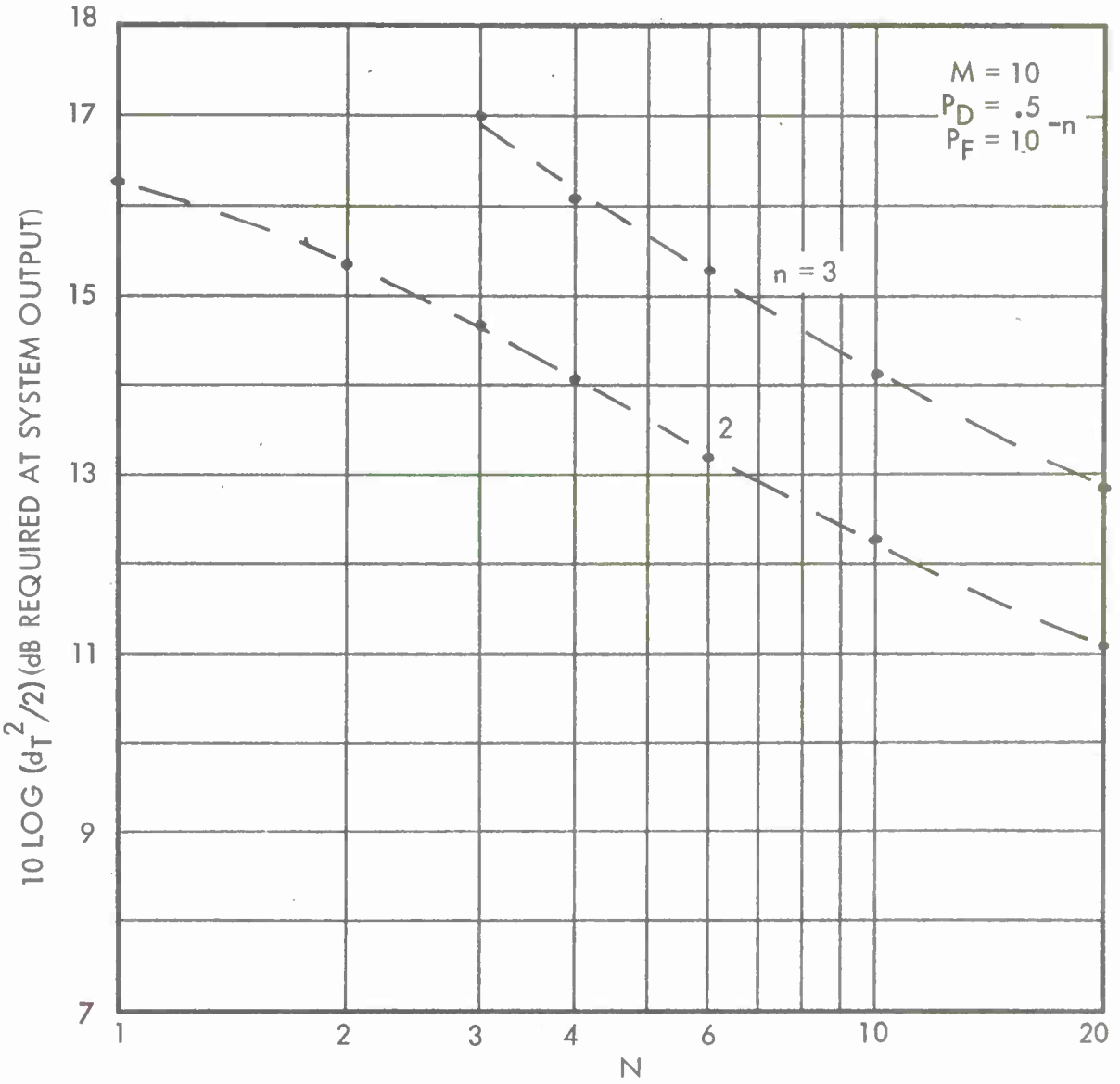


Figure 51. Required Signal-to-Noise Ratio for EA Processor; M = 10

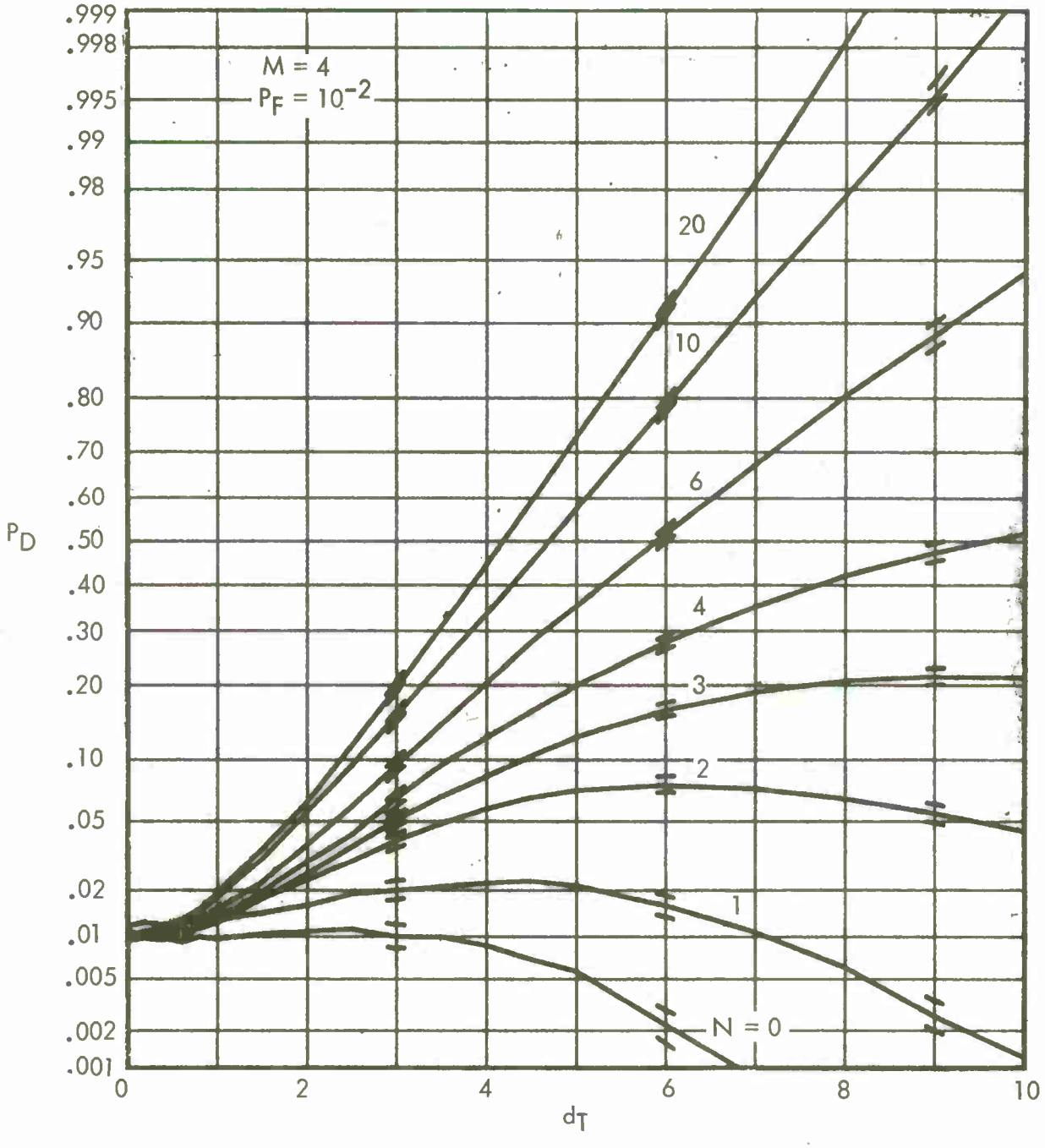


Figure 52. Detection Characteristics for EA Processor with Unequal Amplitudes; M = 4, $P_F = 10^{-2}$

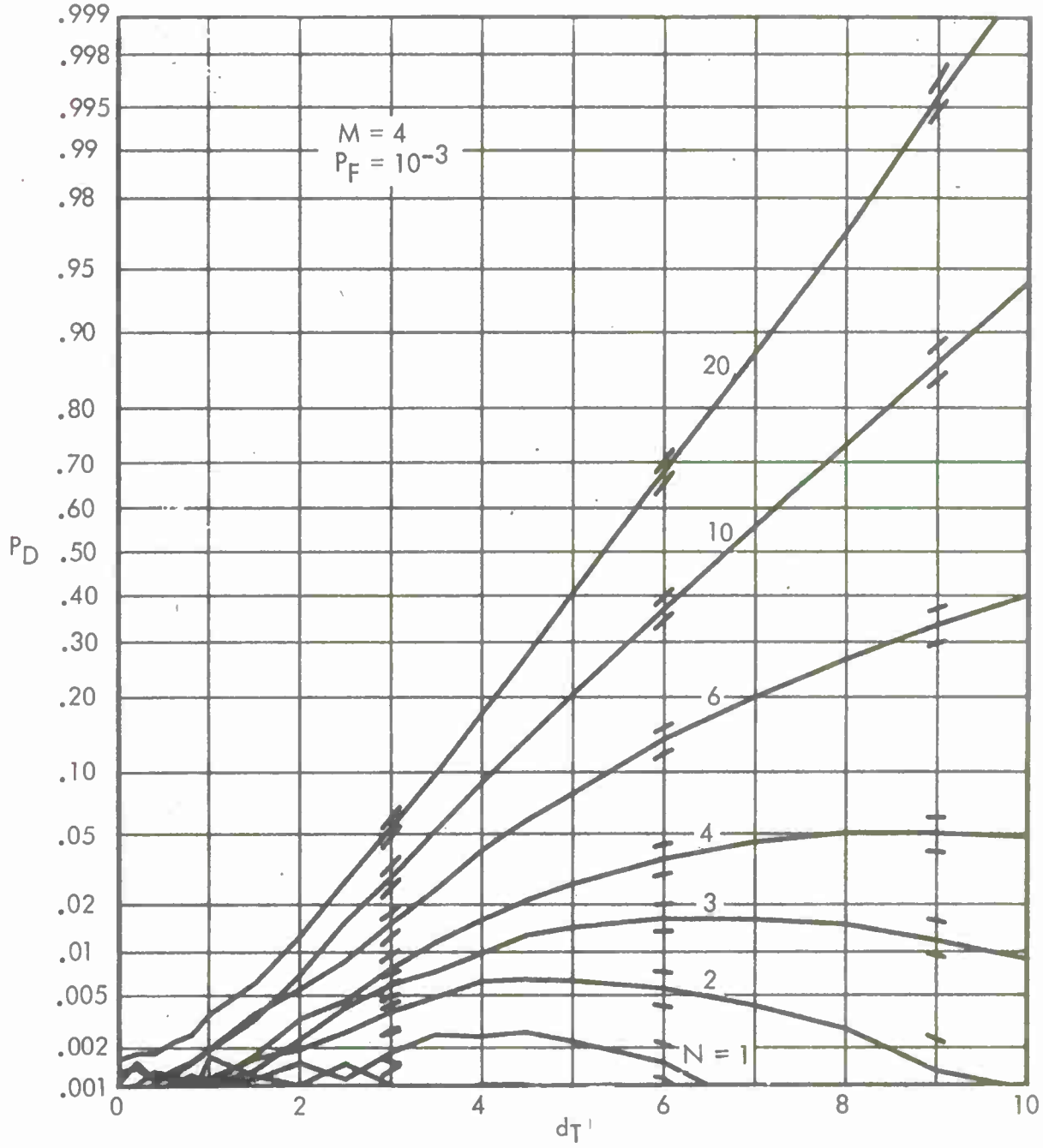


Figure 53. Detection Characteristics for EA Processor with Unequal Amplitudes; M = 4, $P_F = 10^{-3}$


REVERSE BLANK

# Appendix A

## PREDETECTION PROCESSING AND STATISTICS

Initial receiver processing consists of computing the complex quantities

$$\int dt\, F_k(t)\, V_k(t) = z_k\,, \quad 1 \le k \le M\,, \tag{A-1}$$

for the potential-signal-plus-noise branches, and

$$\int dt\, \tilde{F}_j(t)\, \tilde{V}_j(t) = \tilde{z}_j\,, \quad 1 \le j \le N\,, \tag{A-2}$$

for the noise-alone branches. (Integration is over the range of nonzero integrand.) In the above expressions, $\{V_k(t)\}$ and $\{\tilde{V}_j(t)\}$ are the complex envelopes of the received processes, and $\{F_k(t)\}$ and $\{\tilde{F}_j(t)\}$ are receiver filter complex envelopes that may or may not be optimum.* The complex random variables $\{z_k\}$ and $\{\tilde{z}_j\}$ are Gaussian because the input noises are stationary Gaussian processes.

Denoting ensemble averages on the noise by overbars, we can write

$$\overline{N_k(t)} = 0\,, \quad \overline{\tilde{N}_j(t)} = 0\,, \quad \text{all } k, j\,. \tag{A-3}$$

In (A-3), $\{N_k(t)\}$ and $\{\tilde{N}_j(t)\}$ are the complex envelopes of the received noise waveforms. Then the noise average

$$\bar{z}_k = \int dt\, F_k(t)\, \overline{V_k(t)} = \left\{ \begin{array}{c} \int dt\, F_k(t)\, S_k(t) \equiv A_{ko} \exp(i\psi_{ko}), \text{ for } H_1 \\ 0\,, \text{ for } H_o \end{array} \right\}, \quad 1 \le k \le M\,, \tag{A-4}$$

where $\{S_k(t)\}$ are the complex envelopes of the actual received signal waveforms. Similarly

$$\bar{\tilde{z}}_j = 0 \quad \text{for} \quad H_1 \text{ and } H_o\,, \quad 1 \le j \le N\,. \tag{A-5}$$

---

*For example, mismatch or misalignment in frequency and/or time are allowed.

Noting that

$$z_k - \bar{z}_k = \int dt\, F_k(t)\, N_k(t) , \quad 1 \le k \le M , \tag{A-6}$$

for $H_1$ and $H_o$, it is seen that

$$\overline{\left(z_k - \bar{z}_k\right)\left(z_\ell - \bar{z}_\ell\right)} = 0 \text{ for all } k, \ell , \tag{A-7}$$

since, for complex envelopes of stationary processes,

$$\overline{N_k(t)\, N_\ell(u)} = 0 \text{ for all } k, \ell . \tag{A-8}$$

Also, writing an element of the received noise crosscorrelation matrix as

$$\overline{N_k(t)\, N_\ell^*(u)} = R_{k\ell}(t - u) , \tag{A-9}$$

we obtain

$$\overline{\left(z_k - \bar{z}_k\right)\left(z_\ell - \bar{z}_\ell\right)^*} = \int\int dt\, du\, F_k(t)\, F_\ell^*(u)\, R_{k\ell}(t - u) \equiv 2\sigma_{k\ell}^2 . \tag{A-10}$$

Similarly, for the noise-alone branches,

$$\overline{\tilde{z}_j\, \tilde{z}_\ell} = 0 \tag{A-11}$$

and

$$\overline{\tilde{z}_j\, \tilde{z}_\ell^*} = \int\int dt\, du\, \tilde{F}_j(t)\, F_\ell^*(u)\, \tilde{R}_{j\ell}(t - u) \equiv 2\tilde{\sigma}_{j\ell}^2 . \tag{A-12}$$

In the present investigation, attention is restricted to the situation

$$\begin{aligned} \sigma_{k\ell}^2 &= \sigma_o^2\, \delta_{k\ell} , \\ \tilde{\sigma}_{j\ell}^2 &= \sigma_o^2\, \delta_{j\ell} . \end{aligned} \tag{A-13}$$

It is also assumed that

$$\overline{\left(z_k - \bar{z}_k\right)\tilde{z}_\ell^*} = 0, \quad \text{all } k, \ell , \tag{A-14}$$

which corresponds to uncorrelated noises in the potential-signal branches and noise-alone branches. An example of (A-13) and (A-14) is afforded by disjoint equal-gain filters and a fairly flat noise spectrum over the complete receiver filter bank.

## Appendix B

## PERFORMANCE EVALUATION OF UA PROCESSOR

Let

$$z_k = B_k \exp(i\theta_k), \quad 1 \le k \le M; \quad \tilde{z}_j = \tilde{B}_j \exp(i\tilde{\theta}_j), \quad 1 \le j \le N , \tag{B-1}$$

where $\{z_k\}$ and $\{\tilde{z}_j\}$ are the filter outputs defined previously (cf. appendix A). If we let vector

$$\mathbf{B} = \left[B_1 \cdots B_M \tilde{B}_1 \cdots \tilde{B}_N\right]^T , \tag{B-2}$$

then, if the Gaussian character of $\{z_k\}$ and $\{\tilde{z}_j\}$ and the statistics presented in appendix A are used, the PDF of $\mathbf{B}$ under hypothesis $H_1$ is

$$p(\mathbf{B}) = \prod_{k=1}^{M} \left\{ \int_{2\pi} d\theta_k \, \frac{B_k}{2\pi\sigma_o^2} \exp\left[ - \frac{B_k^2 - 2A_{ko} B_k \cos(\psi_{ko} - \theta_k) + A_{ko}^2}{2\sigma_o^2} \right] \right\}$$

$$\cdot \prod_{j=1}^{N} \left\{ \int_{2\pi} d\tilde{\theta}_j \, \frac{\tilde{B}_j}{2\pi\sigma_o^2} \exp\left[ - \frac{\tilde{B}_j^2}{2\sigma_o^2} \right] \right\} \tag{B-3}$$

$$= \prod_{k=1}^{M} \left\{ \frac{B_k}{\sigma_o^2} \exp\left[ - \frac{B_k^2 + A_{ko}^2}{2\sigma_o^2} \right] I_o\left( \frac{A_{ko} B_k}{\sigma_o^2} \right) \right\} \prod_{j=1}^{N} \left\{ \frac{\tilde{B}_j}{\sigma_o^2} \exp\left[ - \frac{\tilde{B}_j^2}{2\sigma_o^2} \right] \right\},$$

$$B_k > 0, \ \tilde{B}_j > 0 .$$

Here $A_{ko}$ is the <u>actual</u> amplitude of the complex sample of the signal output of the filter $F_k(t)$ ; that is,

$$A_{ko} = \left| \int dt \, F_k(t) \, S_k(t) \right| , \quad 1 \le k \le M , \tag{B-4}$$

where $S_k(t)$ is the actual received-signal complex envelope. The parameter $\sigma_o^2$ in the PDF (B-3) is proportional to the actual output noise variance of a typical filter (see (A-10) and (A-13)):

$$\sigma_o^2 = \frac{1}{2} \iint dt \, du \, F_1(t) \, F_1^*(u) \, R_{11}(t - u) . \tag{B-5}$$

The GLR test of interest is obtained from (19) and (B-1):

$$\frac{1}{M}\sum_{k=1}^{M} B_k^2 \gtrless r\,\frac{1}{N}\sum_{j=1}^{N} \tilde{B}_j^2 \,. \tag{B-6}$$

Let

$$U \equiv \sum_{k=1}^{M}\left(\frac{B_k}{\sigma_o}\right)^2, \quad V \equiv \sum_{j=1}^{N}\left(\frac{\tilde{B}_j}{\sigma_o}\right)^2, \quad \alpha \equiv r\,\frac{M}{N}, \quad d_k \equiv \frac{A_{ko}}{\sigma_o}. \tag{B-7}$$

Then test (B-6) can be written as

$$U \gtrless \alpha V \,. \tag{B-8}$$

The random variables U and V are statistically independent of each other; see (B-3). Therefore the characteristic function of U is (reference 6, 6.631 4)

$$f_U(\xi) = \overline{\exp(i\xi U)} = \prod_{k=1}^{M}\left\{\int_0^\infty dx\, \exp(i\xi x^2)\; x\, \exp\left[-\frac{x^2 + d_k^2}{2}\right] I_o(d_k x)\right\} \tag{B-9}$$

$$= (1 - i2\xi)^{-M} \exp\left(\frac{i d_T^2\, \xi}{1 - i2\xi}\right),$$

where

$$\frac{1}{2}\, d_T^2 \equiv \sum_{k=1}^{M} \frac{1}{2}\, d_k^2 = \sum_{k=1}^{M} \frac{\left|\int dt\, F_k(t)\, S_k(t)\right|^2 / 2}{\frac{1}{2}\iint dt\, du\, F_1(t)\, F_1^*(u)\, R_{11}(t-u)} \,. \tag{B-10}$$

From (B-9), the PDF of U can be determined to be

$$p_U(x) = \frac{1}{2}\exp\left(-\frac{x + d_T^2}{2}\right)\left(\frac{x}{d_T^2}\right)^{\frac{M-1}{2}} I_{M-1}\left(d_T x^{1/2}\right), \quad x > 0 \,. \tag{B-11}$$

In a similar manner, the PDF of V can be shown to be

$$p_V(y) = \frac{1}{2}\exp\left(-\frac{y}{2}\right)\frac{(y/2)^{N-1}}{(N-1)!}, \quad y > 0 \,. \tag{B-12}$$

From (B-8), (B-11), and (B-12), there is obtained for the probability of detection

$$P_D = \text{Prob}\,(U > \alpha V) = \int_0^\infty dx\; p_U(x) \int_0^{x/\alpha} dy\; p_V(y)\;. \tag{B-13}$$

Consider the inner integral in (B-13):

$$\begin{aligned}\int_0^{x/\alpha} dy\; p_V(y) &= 1 - \int_{x/\alpha}^\infty dy\; \frac{1}{2} \exp\left(-\frac{y}{2}\right) \frac{(y/2)^{N-1}}{(N-1)!} \\ &= 1 - \exp\left(-\frac{x}{2\alpha}\right) \sum_{k=0}^{N-1} \frac{1}{k!} \left(\frac{x}{2\alpha}\right)^k\;.\end{aligned} \tag{B-14}$$

Substitution of (B-11) and (B-14) in (B-13) and a change of variable, $x = t^2$, yields

$$P_D = 1 - \frac{\exp\left(-d_T^2/2\right)}{d_T^{M-1}} \sum_{k=0}^{N-1} \frac{1}{k!} \left(\frac{1}{2\alpha}\right)^k \int_0^\infty dt\; t^{M+2k} \exp\left[-\frac{t^2}{2}\left(1+\frac{1}{\alpha}\right)\right] I_{M-1}(d_T t). \tag{B-15}$$

Recall the identity

$$I_{M-1}(d_T\, t) = \frac{1}{i^{M-1}}\, J_{M-1}(i d_T\, t)\;; \tag{B-16}$$

then the integral in (B-15) can be evaluated from reference 6, 6.631 1 as

$$\begin{aligned}&\int_0^\infty dt\; \frac{t^{M+2k}}{i^{M-1}} \exp\left[-\frac{t^2}{2}\left(1+\frac{1}{\alpha}\right)\right] J_{M-1}(i d_T t) \\ &= \frac{d_T^{M-1}\, \Gamma(M+k)}{2^M \left(\frac{\alpha+1}{2\alpha}\right)^{M+k} (N-1)!}\; {}_1F_1\left(M+k;\, M;\, \frac{d_T^2}{2}\,\frac{\alpha}{\alpha+1}\right) \\ &= 2^k \left(\frac{\alpha}{\alpha+1}\right)^{M+k} d_T^{M-1}\, \frac{(M+k-1)!}{(M-1)!} \exp\left(\frac{d_T^2}{2}\,\frac{\alpha}{\alpha+1}\right) {}_1F_1\left(-k;\, M;\, -\frac{d_T^2}{2}\,\frac{\alpha}{\alpha+1}\right),\end{aligned} \tag{B-17}$$

where ${}_1F_1(a;b;x)$ denotes the confluent hypergeometric function. One form for the probability of detection for the UA processor is thus

$$P_D = 1 - \exp\left(-\frac{d_T^2}{2}\,\frac{1}{\alpha+1}\right)\left(\frac{\alpha}{\alpha+1}\right)^M \sum_{k=0}^{N-1}\binom{M-1+k}{k}\frac{1}{(\alpha+1)^k}\,{}_1F_1\left(-k; M; -\frac{d_T^2}{2}\,\frac{\alpha}{\alpha+1}\right), \quad \text{(B-18)}$$

where (from (B-7))

$$\alpha = r\,\frac{M}{N}\,. \quad \text{(B-19)}$$

The probability of false alarm is obtained when $d_T = 0$ in (B-18):

$$P_F = 1 - \left(\frac{\alpha}{\alpha+1}\right)^M \sum_{k=0}^{N-1}\binom{M-1+k}{k}\frac{1}{(\alpha+1)^k}\,. \quad \text{(B-20)}$$

An alternative form for $P_D$ can be obtained by first noting that (reference 7, 13.6.9)

$$\binom{M-1+k}{k}\,{}_1F_1(-k; M; x) = L_k^{(M-1)}(x)\,, \quad \text{(B-21)}$$

where the generalized Laguerre polynomials $\left(L_k^{(M-1)}(x)\right)$ satisfy the recurrence relations

$$L_o^{(M-1)}(x) = 1, \qquad L_1^{(M-1)}(x) = M - x\,,$$

$$L_k^{(M-1)}(x) = \frac{2k-2+M-x}{k}\,L_{k-1}^{(M-1)}(x) - \frac{k-2+M}{k}\,L_{k-2}^{(M-1)}(x), \quad k \geq 2\,. \quad \text{(B-22)}$$

Substitution of (B-21) in (B-18) gives

$$P_D = 1 - \exp\left(-\frac{d_T^2}{2}\,\frac{1}{\alpha+1}\right)\left(\frac{\alpha}{\alpha+1}\right)^M \sum_{k=0}^{N-1}\frac{1}{(\alpha+1)^k}\,L_k^{(M-1)}\left(-\frac{d_T^2}{2}\,\frac{\alpha}{\alpha+1}\right) \quad \text{(B-23)}$$

$$\equiv 1 - \exp\left(-\frac{d_T^2}{2}\,\frac{1}{\alpha+1}\right)\left(\frac{\alpha}{\alpha+1}\right)^M \sum_{k=0}^{N-1} G_k\left(-\frac{d_T^2}{2}\,\frac{\alpha}{\alpha+1}, \alpha, M\right).$$

(For M = 1, the upper line of (B-23) agrees with reference 2, eq. (14).) It is seen that (B-23) is a series of positive terms that satisfy the recursion relations:

$$G_o(x,\alpha,M) = 1, \quad G_1(x,\alpha,M) = \frac{M-x}{\alpha+1},$$

$$G_k(x,\alpha,M) = \frac{2k-2+M-x}{k(\alpha+1)} G_{k-1}(x,\alpha,M) - \frac{k-2+M}{k(\alpha+1)^2} G_{k-2}(x,\alpha,M), \quad k \geq 2 . \tag{B-24}$$

We consider now an alternative expression for the probability of detection for the UA processor:

$$P_D = \text{Prob}(U > \alpha V) = \int_0^\infty dy\, p_V(y) \int_{\alpha y}^\infty dx\, p_U(x) . \tag{B-25}$$

Using (B-11), we can write the inner integral in (B-25) as

$$\begin{aligned}
\int_{\alpha y}^\infty dx\, p_U(x) &= \int_{\alpha y}^\infty dx\, \frac{1}{2} \exp\left(-\frac{x+d_T^2}{2}\right)\left(\frac{x}{d_T^2}\right)^{\frac{M-1}{2}} I_{M-1}\left(d_T x^{1/2}\right) \\
&= \int_{(\alpha y)^{1/2}}^\infty dt\, t \exp\left(-\frac{t^2+d_T^2}{2}\right)\left(\frac{t}{d_T}\right)^{M-1} I_{M-1}(d_T t) \\
&= Q_M\left(d_T, (\alpha y)^{1/2}\right) \\
&= Q\left(d_T, (\alpha y)^{1/2}\right) + \exp\left(-\frac{\alpha y + d_T^2}{2}\right)\sum_{k=1}^{M-1}\left(\frac{\alpha y}{d_T^2}\right)^{k/2} I_k\left(d_T (\alpha y)^{1/2}\right),
\end{aligned} \tag{B-26}$$

where $Q_M(a,b)$ is the generalization of the Q-function (reference 3). Then $P_D$, (B-25), becomes, with the help of (B-12),

$$\begin{aligned}
P_D = \int_0^\infty dy\, \frac{1}{2} \exp\left(-\frac{y}{2}\right) \frac{(y/2)^{N-1}}{(N-1)!} \Bigg[ & Q\left(d_T, (\alpha y)^{1/2}\right) \\
& + \exp\left(-\frac{\alpha y + d_T^2}{2}\right) \sum_{k=1}^{M-1} \left(\frac{\alpha y}{d_T^2}\right)^{k/2} I_k\left(d_T (\alpha y)^{1/2}\right)\Bigg] ,
\end{aligned} \tag{B-27}$$

which by a change of variable, $y = t^2$, can be written in the form

$$P_D = \int_0^\infty dt\, t \exp\left(-\frac{t^2}{2}\right) \frac{t^{2(N-1)}}{2^{N-1}(N-1)!} \left[Q(d_T, \alpha^{1/2} t) + \exp\left(-\frac{\alpha t^2 + d_T^2}{2}\right) \sum_{k=1}^{M-1} \left(\frac{\alpha^{1/2}}{d_T} t\right)^k I_k(d_T \alpha^{1/2} t)\right] \tag{B-28}$$

$$\equiv I_1 + I_2 .$$

Now consider the term $I_1$, which is defined as

$$I_1 = \int_0^\infty dt \exp(-t^2/2) \frac{t^{2N-1}}{2^{N-1}(N-1)!} Q(d_T, \alpha^{1/2} t)$$

$$= \int_0^\infty dt \exp(-t^2/2) \frac{t^{2N-1}}{2^{N-1}(N-1)!} \int_{\alpha^{1/2} t}^\infty dx\, x \exp\left(-\frac{x^2 + d_T^2}{2}\right) I_o(d_T x) . \tag{B-29}$$

By interchanging the order of integration in (B-29) and then making a change of variable, $v = t^2/2$, we obtain

$$I_1 = \int_0^\infty dx\, x \exp\left(-\frac{x^2 + d_T^2}{2}\right) I_o(d_T x) \int_0^{x/\alpha^{1/2}} dt \exp(-t^2/2) \frac{t^{2N-1}}{2^{N-1}(N-1)!}$$

$$= 1 - \sum_{k=0}^{N-1} \frac{1}{k!} \int_0^\infty dx \frac{x^{2k+1}}{(2\alpha)^k} \exp\left(-\frac{x^2 + d_T^2}{2}\right) I_o(d_T x) \exp\left(-\frac{x^2}{2\alpha}\right), \tag{B-30}$$

which can be evaluated as (reference 6, 6.631 1)

$$I_1 = 1 - \frac{\alpha}{\alpha+1} \exp\left(-\frac{d_T^2}{2}\right) \sum_{k=0}^{N-1} \frac{1}{(\alpha+1)^k} \, {}_1F_1\left(k+1;\, 1;\, \frac{d_T^2}{2}\,\frac{\alpha}{\alpha+1}\right)$$

$$= 1 - \frac{\alpha}{\alpha+1} \exp\left(-\frac{d_T^2}{2}\,\frac{1}{\alpha+1}\right) \sum_{k=0}^{N-1} \frac{1}{(\alpha+1)^k} \, {}_1F_1\left(-k;\, 1;\, -\frac{d_T^2}{2}\,\frac{\alpha}{\alpha+1}\right) \qquad \text{(B-31)}$$

$$= 1 - \frac{\alpha}{\alpha+1} \exp\left(-\frac{d_T^2}{2}\,\frac{1}{\alpha+1}\right) \sum_{k=0}^{N-1} \frac{1}{(\alpha+1)^k} \, L_k\left(-\frac{d_T^2}{2}\,\frac{\alpha}{\alpha+1}\right),$$

with

$$L_n^{(0)}(x) \equiv L_n(x) \qquad \text{(B-32)}$$

The remaining term $I_2$ in (B-28) can be developed as (reference 6, 6.631 1)

$$I_2 = \exp\left(-\frac{d_T^2}{2}\right) \frac{1}{2^{N-1}(N-1)!} \sum_{k=1}^{M-1} \left(\frac{\alpha}{d_T^2}\right)^{k/2} \int_0^\infty dt\, t^{2N-1+k} \exp\left(-\frac{t^2}{2}(1+\alpha)\right) I_k(d_T \alpha^{1/2} t)$$

$$= \frac{1}{(1+\alpha)^N} \exp\left(-\frac{d_T^2}{2}\,\frac{1}{1+\alpha}\right) \sum_{k=1}^{M-1} \binom{N-1+k}{k} \left(\frac{\alpha}{1+\alpha}\right)^k \, {}_1F_1\left(1-N;\, k+1;\, -\frac{d_T^2}{2}\,\frac{\alpha}{1+\alpha}\right). \qquad \text{(B-33)}$$

Substituting (B-31) and (B-33) in (B-28) yields

$$P_D = 1 - \frac{\alpha}{1+\alpha} \exp\left(-\frac{d_T^2}{2}\,\frac{1}{1+\alpha}\right) \sum_{k=0}^{N-1} \frac{1}{(1+\alpha)^k} \, {}_1F_1\left(-k;\, 1;\, -\frac{d_T^2}{2}\,\frac{\alpha}{1+\alpha}\right) \qquad \text{(B-34)}$$

$$+ \frac{1}{(1+\alpha)^N} \exp\left(-\frac{d_T^2}{2}\,\frac{1}{1+\alpha}\right) \sum_{k=1}^{M-1} \binom{N-1+k}{k} \left(\frac{\alpha}{1+\alpha}\right)^k \, {}_1F_1\left(1-N;\, k+1;\, -\frac{d_T^2}{2}\,\frac{\alpha}{1+\alpha}\right).$$

We have, therefore, the alternative forms (B-18), (B-23), and (B-34) for $P_D$, where $\alpha = rM/N$.

For $d_T = 0$, using $\alpha = rM/N$, (B-34) yields

$$P_F = \frac{1}{(1 + rM/N)^N} \sum_{k=0}^{M-1} \binom{N-1+k}{k} \left(\frac{rM/N}{1 + rM/N}\right)^k . \tag{B-35}$$

Note that

$$(1 + rM/N)^N \sim \exp(rM) \quad \text{as} \quad N \to \infty , \tag{B-36}$$

and

$$\binom{N-1+k}{k} \left(\frac{rM}{N}\right)^k = \frac{N(N+1) \ldots (N-1+k)}{k!} \left(\frac{rM}{N}\right)^k \sim \frac{(rM)^k}{k!} \text{ as } N \to \infty . \tag{B-37}$$

Therefore, from (B-35),

$$P_F \sim \exp(-rM) \sum_{k=0}^{M-1} \frac{1}{k!} (rM)^k \text{ as } N \to \infty. \tag{B-38}$$

This agrees with reference 3, (2.17), p. 175. Also as $N \to \infty$, (B-6) becomes

$$\frac{1}{M} \sum_{k=1}^{M} B_k^2 \gtrless r \overline{\tilde{B}_1^2} = r\, 2\sigma_o^2 ; \tag{B-39}$$

that is, the UA test for $N \to \infty$ is

$$\frac{1}{M} \sum_{k=1}^{M} \left(\frac{B_k}{\sigma_o}\right)^2 \gtrless 2r \tag{B-40}$$

or, using (B-7),

$$U \gtrless 2Mr . \tag{B-41}$$

Now, use of (B-25) and (B-26) shows that

$$P_D \sim Q_M\left(d_T, (2Mr)^{1/2}\right) \text{ as } N \to \infty. \tag{B-42}$$

This is in agreement with reference 3, (2.19), p. 176.

A table of required threshold values r in (B-6) is presented in table B-1. This table was determined from (B-35) and (B-38).

Table B-1. Threshold Values r for UA Processor

| N \ $P_F$ | $10^{-2}$ | $10^{-3}$ | $10^{-4}$ | $10^{-6}$ | $10^{-8}$ | |
|---|---|---|---|---|---|---|
| 1 | 99. | 999. | 9999. | 999999. | 99999999. | |
| 2 | 18. | 61.2455532 | 198. | 1998. | 19998. | |
| 3 | 10.9247665 | 27. | 61.6330407 | 297. | 1389.47665 | |
| 4 | 8.64911064 | 18.4936530 | 36. | 122.491106 | 396. | |
| 6 | 6.92660814 | 12.9736660 | 21.8495330 | 54. | 123.266081 | (a) M = 1 |
| 10 | 5.84893192 | 9.95262315 | 15.1188643 | 29.8107171 | 53.0957344 | |
| 20 | 5.17850824 | 8.25075089 | 11.6978638 | 19.9052463 | 30.2377286 | |
| ∞ | 4.60517019 | 6.90775528 | 9.21034037 | 13.8155106 | 18.4206807 | |

| N \ $P_F$ | $10^{-2}$ | $10^{-3}$ | $10^{-4}$ | $10^{-6}$ | $10^{-8}$ | |
|---|---|---|---|---|---|---|
| 1 | 99.2493719 | 999.249937 | 9999.24999 | 999999.250 | 99999999.25 | |
| 2 | 15.9770249 | 53.4358291 | 171.870780 | 1730.71738 | 17319.1747 | |
| 3 | 9.14830103 | 21.9235414 | 49.4186582 | 236.233970 | 1103.33419 | |
| 4 | 7.00607662 | 14.3915845 | 27.4928357 | 92.1698584 | 296.668412 | |
| 6 | 5.41195143 | 9.63272610 | 15.7925977 | 38.0476483 | 85.9572018 | (b) M = 2 |
| 10 | 4.43069016 | 7.09603407 | 10.4147233 | 19.7920962 | 34.6109950 | |
| 20 | 3.82829355 | 5.69813414 | 7.75922632 | 12.6065444 | 18.6643142 | |
| ∞ | 3.31917603 | 4.61670674 | 5.87818562 | 8.34421042 | 10.7678926 | |

| N \ $P_F$ | $10^{-2}$ | $10^{-3}$ | $10^{-4}$ | $10^{-6}$ | $10^{-8}$ | |
|---|---|---|---|---|---|---|
| 1 | 99.3325889 | 999.333259 | 9999.33333 | 999999.333 | 99999999.3 | |
| 2 | 15.2068649 | 50.5250219 | 162.187065 | 1631.88194 | 16328.8205 | |
| 3 | 8.46612534 | 20.0296547 | 44.9092656 | 213.942069 | 998.499699 | |
| 4 | 6.37068073 | 12.8580261 | 24.3565038 | 81.1059802 | 260.530367 | |
| 6 | 4.82057350 | 8.37881423 | 13.5601910 | 32.2606939 | 72.5053353 | (c) M = 3 |
| 10 | 3.87142682 | 6.01860847 | 8.67889223 | 16.1732390 | 27.9997019 | |
| 20 | 3.29101239 | 4.73056833 | 6.30305962 | 9.97677756 | 14.5488339 | |
| ∞ | 2.80198231 | 3.74295742 | 4.64272354 | 6.37638938 | 8.06043792 | |

Table B-1 (Cont'd). Threshold Values r for UA Processor

| N \ $P_F$ | $10^{-2}$ | $10^{-3}$ | $10^{-4}$ | $10^{-6}$ | $10^{-8}$ |
|---|---|---|---|---|---|
| 1 | 99.3742148 | 999.374922 | 9999.37499 | 999999.375 | 99999999.4 |
| 2 | 14.7988888 | 48.9961888 | 157.112691 | 1580.13871 | 15810.3883 |
| 3 | 8.10165137 | 19.0303331 | 42.5408682 | 202.267363 | 943.627975 |
| 4 | 6.02887011 | 12.0455412 | 22.7056389 | 75.3107695 | 241.628275 |
| 6 | 4.49936528 | 7.71035231 | 12.3807118 | 29.2278151 | 65.4777610 |
| 10 | 3.56441205 | 5.43999319 | 7.75725282 | 14.2739056 | 24.5490000 |
| 20 | 2.99298087 | 4.20703658 | 5.52574668 | 8.59348159 | 12.4009667 |
| ∞ | 2.51127938 | 3.26556019 | 3.97845350 | 5.33761427 | 6.64618478 |

(d) M = 4

| N \ $P_F$ | $10^{-2}$ | $10^{-3}$ | $10^{-4}$ | $10^{-6}$ | $10^{-8}$ |
|---|---|---|---|---|---|
| 1 | 99.3991960 | 999.399920 | 9999.39999 | 999999.400 | 99999999.4 |
| 2 | 14.5459008 | 48.0525891 | 153.984789 | 1548.25988 | 15491.0000 |
| 3 | 7.87411853 | 18.4109248 | 41.0768153 | 195.062504 | 909.776375 |
| 4 | 5.81429386 | 11.5400561 | 21.6825553 | 71.7299629 | 229.958941 |
| 6 | 4.29605440 | 7.29202903 | 11.6467066 | 27.3500642 | 61.1356414 |
| 10 | 3.36818639 | 5.07524621 | 7.18053924 | 13.0944804 | 22.4142485 |
| 20 | 2.80054511 | 3.87438608 | 5.03629308 | 7.73123567 | 11.0695697 |
| ∞ | 2.32092512 | 2.95882985 | 3.55640140 | 4.68630468 | 5.76639616 |

(e) M = 5

| N \ $P_F$ | $10^{-2}$ | $10^{-3}$ | $10^{-4}$ | $10^{-6}$ | $10^{-8}$ |
|---|---|---|---|---|---|
| 1 | 99.4491708 | 999.449917 | 9999.44999 | 999999.450 | 99999999.45 |
| 2 | 14.0196087 | 46.1002576 | 147.522750 | 1482.43958 | 14831.5970 |
| 3 | 7.39583189 | 17.1201102 | 38.0358331 | 180.127861 | 839.636486 |
| 4 | 5.35909494 | 10.4796828 | 19.5469671 | 64.2836270 | 205.719307 |
| 6 | 3.85843310 | 6.40480557 | 10.1014505 | 23.4241458 | 52.0825303 |
| 10 | 2.93773528 | 4.28996645 | 5.95161262 | 10.6085787 | 17.9392886 |
| 20 | 2.36887612 | 3.14498953 | 3.97720089 | 5.89378598 | 8.25675959 |
| ∞ | 1.87831174 | 2.26573733 | 2.61929866 | 3.27103405 | 3.87990075 |

(f) M = 10

## Appendix C

## DERIVATION OF $P_F$ FOR EA PROCESSOR WITH M = 2 AND ARBITRARY N

For the EA processor with M = 2 and arbitrary N, GLR test (24) takes the form

$$\left(\sum_{k=1}^{2} B_k\right)^2 \gtrless \gamma \left(\sum_{k=1}^{2} B_k^2 + \sum_{j=1}^{N} \tilde{B}_j^2\right) ; \qquad \text{(C-1)}$$

here, as in (B-1), we have let $B_k = |z_k|$ and $\tilde{B}_j = |\tilde{z}_j|$. The threshold $\gamma$ need never deviate outside the range $[0, 2]$; the lower limit on the range follows because the left side of (C-1) can never be negative. The upper limit holds true since the left side of (C-1) can never be larger than $2 \sum_{k=1}^{2} B_k^2$ (by Schwarz's inequality).

For signal-absent, the PDF of all envelope samples in (C-1) is Rayleigh:

$$p(B) = B \exp(-B^2/2), \quad B > 0 . \qquad \text{(C-2)}$$

Since a common absolute scaling of envelopes obviously does not affect the decision made in (C-1), a convenient scaling has been selected in (C-2), with no loss of generality. This is a manifestation of the CFAR capability of test (C-1).

Let us assume temporarily that $N \geq 1$ and let

$$v = \frac{1}{2} \sum_{j=1}^{N} \tilde{B}_j^2 . \qquad \text{(C-3)}$$

Then the PDF of random variable v is

$$p(v) = \frac{v^{N-1} \exp(-v)}{(N-1)!} , \quad v > 0 . \qquad \text{(C-4)}$$

Now let

$$B_1 = (2r)^{1/2} \cos\theta , \quad B_2 = (2r)^{1/2} \sin\theta , \quad 0 < r < \infty , \quad 0 < \theta < \pi/2 , \qquad \text{(C-5)}$$

in (C-1), and employ (C-3); there follows for test (C-1)

$$\sin(2\theta) \gtrless \gamma \frac{v}{r} + \gamma - 1 . \tag{C-6}$$

The joint PDF for random variables $r$ and $\theta$ is obtained according to

$$\begin{aligned} p(r,\theta) &= p(B_1 = \sqrt{2r}\cos\theta,\ B_2 = \sqrt{2r}\sin\theta) \times \left|\text{Jacobian}\right| \\ &= r\exp(-r)\sin(2\theta), \quad 0 < r < \infty, \quad 0 < \theta < \pi/2 . \end{aligned} \tag{C-7}$$

Therefore the variables $r$ and $\theta$ are independent with PDFs

$$\begin{aligned} p(r) &= r\exp(-r), \quad 0 < r < \infty , \\ p(\theta) &= \sin(2\theta) , \quad 0 < \theta < \pi/2 . \end{aligned} \tag{C-8}$$

Now define the random variable

$$q = v/r . \tag{C-9}$$

The PDF for $q$ (which is independent of $\theta$) is given by

$$\begin{aligned} p(q) &= \int_{-\infty}^{\infty} dr\,|r|\,p_r(r)\,p_v(qr) \\ &= \int_0^{\infty} dr\ r\ r\exp(-r)\frac{(qr)^{N-1}\exp(-qr)}{(N-1)!} \\ &= N(N+1)\frac{q^{N-1}}{(1+q)^{N+2}} , \quad q > 0 . \end{aligned} \tag{C-10}$$

Furthermore, test (C-6) can now be expressed as

$$\sin(2\theta) \gtrless \gamma q + \gamma - 1 . \tag{C-11}$$

At this point it is convenient to define random variable $u = \sin(2\theta)$. Then the probability of false alarm is given by

$$\begin{aligned} P_F &= \text{Prob}\,(u > \gamma q + \gamma - 1) \\ &= \int_{-\infty}^{\infty} dq\,p_q(q) \int_{\gamma q+\gamma-1}^{\infty} du\,p_u(u) . \end{aligned} \tag{C-12}$$

Now the inner integral in (C-12) can be evaluated as follows:

$$\int_U^\infty du\, p_u(u) = \text{Prob}\,(u > U) = \text{Prob}\left(\sin(2\theta) > U\right)$$

$$= 2 \int_{\frac{1}{2}\arcsin(U)}^{\pi/4} d\theta\, \sin(2\theta) = \begin{cases} 1\,, & U < 0 \\ (1 - U^2)^{1/2}, & 0 < U < 1 \\ 0\,, & 1 < U \end{cases} . \qquad \text{(C-13)}$$

Consequently (C-12) becomes

$$P_F = \int_{-\infty}^{\frac{1-\gamma}{\gamma}} dq\, p_q(q)\; 1 + \int_{\frac{1-\gamma}{\gamma}}^{\frac{2-\gamma}{\gamma}} dq\, p_q(q) \left[1 - (\gamma q + \gamma - 1)^2\right]^{1/2} . \qquad \text{(C-14)}$$

At this point, we must separate the derivation into two parts: one for $0 \le \gamma \le 1$ and another for $1 \le \gamma \le 2$. We consider the latter case first. For $1 \le \gamma \le 2$, (C-14) becomes, by use of (C-10),

$$P_F = \int_0^{\frac{2-\gamma}{\gamma}} dq\, N(N+1)\, \frac{q^{N-1}}{(1+q)^{N+2}} \left[1 - (\gamma q + \gamma - 1)^2\right]^{1/2}$$

$$= N(N+1)\gamma \int_0^{\frac{2-\gamma}{\gamma}} dq\, \frac{q^{N-1}}{(1+q)^{N+2}}\, (1+q)^{1/2} \left(\frac{2-\gamma}{\gamma} - q\right)^{1/2} . \qquad \text{(C-15)}$$

Next let $q = \frac{2-\gamma}{\gamma}\, x$ in (C-15); then (reference 7, 15.3.1, 15.1.8)

$$P_F = N(N+1)\,\gamma \left(\frac{2-\gamma}{\gamma}\right)^{N+\frac{1}{2}} \int_0^1 dx\, x^{N-1} (1-x)^{\frac{1}{2}} \left(1 + \frac{2-\gamma}{\gamma}\, x\right)^{-N-\frac{3}{2}}$$

$$= N(N+1)\,\gamma \left(\frac{2-\gamma}{\gamma}\right)^{N+\frac{1}{2}} \frac{\Gamma(N)\,\Gamma\left(\frac{3}{2}\right)}{\Gamma\left(N+\frac{3}{2}\right)}\, F\left(N+\frac{3}{2},\, N;\, N+\frac{3}{2};\, -\frac{2-\gamma}{\gamma}\right) \qquad \text{(C-16)}$$

$$= \frac{\Gamma\left(\frac{3}{2}\right)\Gamma(N+2)}{\Gamma\left(N+\frac{3}{2}\right)}\, (2\gamma)^{\frac{1}{2}} \left(1 - \frac{\gamma}{2}\right)^{N+\frac{1}{2}}, \quad 1 \le \gamma \le 2 .$$

Equation (C-16) is a general relation for $P_F$ for $\gamma$ in the range $[1,2]$. Although (C-16) was derived for $N \geq 1$, it may be shown, by a separate derivation, to apply to $N = 0$ as well. (For $N = 0$, the allowed range for $\gamma$ does not include $(0,1)$, but is restricted to $[1,2]$.)

For the complementary range of $\gamma$, namely $[0,1]$, we return to (C-14) and employ (C-10) to obtain

$$P_F = I_1 + I_2 , \tag{C-17}$$

where

$$I_1 = \int_0^{\frac{1-\gamma}{\gamma}} dq\, N(N+1) \frac{q^{N-1}}{(1+q)^{N+2}} ,$$

$$I_2 = \int_{\frac{1-\gamma}{\gamma}}^{\frac{2-\gamma}{\gamma}} dq\, N(N+1) \frac{q^{N-1}}{(1+q)^{N+2}} \left[1 - (\gamma q + \gamma - 1)^2\right]^{1/2} . \tag{C-18}$$

In integral $I_1$, let $q = \frac{1-\gamma}{\gamma} x$ ; then (reference 7, 15.3.1, 15.3.3)

$$\begin{aligned} I_1 &= N(N+1) \left(\frac{1-\gamma}{\gamma}\right)^N \int_0^1 dx\, x^{N-1} \left(1 + \frac{1-\gamma}{\gamma} x\right)^{-N-2} \\ &= (N+1) \left(\frac{1-\gamma}{\gamma}\right)^N F\left(N+2,\ N;\ N+1;\ -\frac{1-\gamma}{\gamma}\right) \\ &= (N+1) \left(\frac{1-\gamma}{\gamma}\right)^N \left(1 + \frac{1-\gamma}{\gamma}\right)^{-N-1} F\left(-1,\ 1;\ N+1;\ -\frac{1-\gamma}{\gamma}\right) \\ &= (1-\gamma)^N (N\gamma + 1) . \end{aligned} \tag{C-19}$$

In integral $I_2$, let $1 + q = \frac{2/\gamma}{1+x}$ ; then (reference 7, 15.3.1)

$$\begin{aligned} I_2 &= N(N+1) \frac{\gamma^2}{2} \left(1 - \frac{\gamma}{2}\right)^{N-1} \int_0^1 dx\, x^{\frac{1}{2}} \left(1 - \frac{\gamma}{2-\gamma} x\right)^{N-1} \\ &= N(N+1) \frac{\gamma^2}{3} \left(1 - \frac{\gamma}{2}\right)^{N-1} F\left(1-N,\ \frac{3}{2};\ \frac{5}{2};\ \frac{\gamma}{2-\gamma}\right) . \end{aligned} \tag{C-20}$$

Combining the above results we have

$$P_F = (1-\gamma)^N (1+N\gamma) + N(N+1)\frac{\gamma^2}{3}\left(1-\frac{\gamma}{2}\right)^{N-1} F\left(1-N, \frac{3}{2}; \frac{5}{2}; \frac{\gamma}{2-\gamma}\right), \qquad (C\text{-}21)$$

$$0 \leq \gamma \leq 1 .$$

The final results for $P_F$ are given by (C-21) and (C-16) for the complete range $[0, 2]$ of $\gamma$. In table C-1 the required values of threshold $\gamma$ are presented.

Table C-1. Threshold Values $\gamma$ for EA Processor with M = 2

| N | $P_F$ | $\gamma$ |
|---|---|---|
| 0 | .01 | 1.999 949 998 75 |
| 0 | .001 | 1.999 999 500 |
| 1 | .01 | 1.951 327 448 |
| 1 | .001 | 1.989 581 459 |
| 2 | .01 | 1.796 631 253 |
| 2 | .001 | 1.920 106 594 |
| 3 | .01 | 1.618 190 584 |
| 3 | .001 | 1.805 310 077 |
| 4 | .01 | 1.454 698 805 |
| 4 | .001 | 1.678 251 895 |
| 6 | .01 | 1.194 404 233 |
| 6 | .001 | 1.442 868 746 |
| 10 | .01 | .867 343 947 |
| 10 | .001 | 1.100 639 981 |
| 20 | .01 | .509 052 420 |
| 20 | .001 | .676 673 936 |

## Appendix D

## SIMULATION METHOD AND RESULTS FOR EA PROCESSOR

A total of T trials is conducted for the random variable associated with the EA processor (see (24) and (B-1)),

$$\frac{\left(\sum_{k=1}^{M} B_k\right)^2}{\sum_{k=1}^{M} B_k^2 + \sum_{j=1}^{N} \tilde{B}_j^2} , \tag{D-1}$$

by taking G groups, each of the size S, where T = GS. In the g-th group, an estimate $\hat{q}_g$ of the particular quantile of interest is made, based upon S samples. The sample variance of the G quantile estimates is then

$$\hat{V} \equiv \frac{1}{G-1} \sum_{g=1}^{G} \left[ \hat{q}_g - \frac{1}{G} \sum_{j=1}^{G} \hat{q}_j \right]^2 = \frac{1}{G-1} \left[ \sum_{g=1}^{G} \hat{q}_g^2 - \frac{1}{G} \left( \sum_{g=1}^{G} \hat{q}_g \right)^2 \right] . \tag{D-2}$$

Now according to Cramér, reference 8, sect. 28.5, the standard deviation of a quantile estimate based upon a sample of size S is proportional to $S^{-1/2}$ for large S. We estimate the proportionality constant K by setting

$$\frac{\hat{K}}{\sqrt{S}} = \sqrt{\hat{V}} \ ; \tag{D-3}$$

that is, estimate

$$\hat{K} = \left\{ \frac{S}{G-1} \left[ \sum_{g=1}^{G} \hat{q}_g^2 - \frac{1}{G} \left( \sum_{g=1}^{G} \hat{q}_g \right)^2 \right] \right\}^{1/2} . \tag{D-4}$$

The estimate of the quantile from the total of T trials is obtained by combining all group members and making the standard selection of the quantile. Its standard deviation is then approximately

$$\frac{\hat{K}}{\sqrt{T}} = \left\{ \frac{1}{G(G-1)} \left[ \sum_{g=1}^{G} \hat{q}_g^2 - \frac{1}{G} \left( \sum_{g=1}^{G} \hat{q}_g \right)^2 \right] \right\}^{1/2} . \tag{D-5}$$

Notice that we have not used a Gaussian assumption for the quantile estimates, but only the inverse square-root decay of the standard deviation of the quantile estimate with sample size.

The random variable associated with the EA processor in (D-1) is compared with a threshold (scale factor) $\gamma$ for decisions about signal presence or absence. We let $\hat{\gamma}$ be the estimated threshold. Table D-1 presents $\hat{\gamma}$ and its estimated standard deviation. (The thresholds for $M = 1$, $N \geq 1$ are derivable from the threshold table for the UA processor; accordingly no results for this particular case are presented here.) A computer program for the estimation of the threshold is given on p. D-4.

As $N \to \infty$ for the EA processor, GLR test (24) tends to

$$\sum_{k=1}^{M} |z_k| \gtrless \text{Threshold} . \tag{D-6}$$

The characteristic function of the summation random variable in (D-6) is

$$\prod_{k=1}^{M} \left\{ \int_0^\infty dx \exp(i\xi x) \, x \exp\left( - \frac{x^2 + d_k^2}{2} \right) I_o(d_k x) \right\} . \tag{D-7}$$

This quantity can be evaluated for many values of real $\xi$ (for any M and $\{d_k\}$) via M fast Fourier transforms. (For equal signal amplitudes, only one FFT is needed.) Then $P_D$ is available via the techniques in reference 9. However, this technique has not been pursued in this report; hence the results for $N = \infty$ are not presented in figures 37-53 for the EA processor.

Table D-1. Estimated Thresholds and Standard Deviations for the EA Processor

| M | N | $P_F = .01$ | | $P_F = .001$ | |
|---|---|---|---|---|---|
| | | $\hat{\gamma}$ | Estimated Standard Deviation of $\hat{\gamma}$ | $\hat{\gamma}$ | Estimated Standard Deviation of $\hat{\gamma}$ |
| 2 | 0 | 1.99995 (exact) | -- | 1.9999995 (exact) | -- |
| | 1 | 1.95133 | -- | 1.98958 | -- |
| | 2 | 1.79663 | -- | 1.92011 | -- |
| | 3 | 1.61819 | -- | 1.80531 | -- |
| | 4 | 1.45470 | -- | 1.67825 | -- |
| | 6 | 1.19440 | -- | 1.44287 | -- |
| | 10 | .86734 | -- | 1.10064 | -- |
| | 20 | .50905 | -- | 0.67667 | -- |
| 3 | 0 | 2.99414 | .00036 | 2.99935 | .00018 |
| | 1 | 2.8887 | .0029 | 2.9660 | .0032 |
| | 2 | 2.6856 | .0049 | 2.8564 | .0072 |
| | 3 | 2.4600 | .0072 | 2.6881 | .0093 |
| | 4 | 2.2574 | .0088 | 2.552 | .013 |
| | 6 | 1.9061 | .0090 | 2.245 | .015 |
| | 10 | 1.4452 | .0100 | 1.781 | .020 |
| | 20 | .8874 | .0048 | 1.118 | .016 |
| 4 | 0 | 3.9657 | .0012 | 3.99152 | .00070 |
| | 1 | 3.8052 | .0045 | 3.9249 | .0034 |
| | 2 | 3.5351 | .0064 | 3.7849 | .0088 |
| | 3 | 3.3015 | .0080 | 3.619 | .012 |
| | 4 | 3.0730 | .0091 | 3.430 | .016 |
| | 6 | 2.6587 | .0124 | 3.039 | .020 |
| | 10 | 2.0394 | .0095 | 2.454 | .020 |
| | 20 | 1.2996 | .0059 | 1.608 | .018 |
| 5 | 0 | 4.9150 | .0019 | 4.9756 | .0018 |
| | 1 | 4.6969 | .0041 | 4.8757 | .0065 |
| | 2 | 4.4389 | .0069 | 4.6854 | .0099 |
| | 3 | 4.1575 | .0080 | 4.497 | .013 |
| | 4 | 3.8707 | .0095 | 4.272 | .023 |
| | 6 | 3.4358 | .0112 | 3.885 | .025 |
| | 10 | 2.7378 | .0106 | 3.151 | .030 |
| | 20 | 1.7744 | .0101 | 2.180 | .026 |
| 10 | 0 | 9.4364 | .0085 | 9.685 | .012 |
| | 1 | 9.069 | .010 | 9.413 | .019 |
| | 2 | 8.732 | .011 | 9.176 | .019 |
| | 3 | 8.404 | .013 | 8.898 | .026 |
| | 4 | 8.031 | .015 | 8.541 | .026 |
| | 6 | 7.390 | .018 | 8.006 | .031 |
| | 10 | 6.319 | .024 | 6.973 | .036 |
| | 20 | 4.514 | .017 | 5.165 | .042 |

## PROGRAM FOR DETERMINING QUANTILES

```
      PARAMETER GROUPS=40, MEMBRS=1000, TRIALS=GROUPS*MEMBRS
      INTEGER OHM, OTM, OHT, OTT
      LOGICAL REALS
      DIMENSION R(TRIALS), TH(GROUPS), TT(GROUPS)
      DEFINE IRAND=I*K+((1-SIGN(1, I*K))/2)*34359738367
      DEFINE RAND=FLOAT(I)/34359738367.
      M=10
      REALS=.FALSE.
      K=5**15
      I=5281
      OHM=MEMBRS/100
      OTM=MEMBRS/1000
      OHT=TRIALS/100
      OTT=TRIALS/1000
      DO 1 IA=0, 7
      N=IA
      IF (IA.EQ.5) N=6
      IF (IA.EQ.6) N=10
      IF (IA.EQ.7) N=20
      DO 21 IB1=1, GROUPS
      ISTART=1+(IB1-1)*MEMBRS
      ISTOP=IB1*MEMBRS
      DO 2 IB2=1, MEMBRS
      SL=0.
      SS=0.
      ST=0.
      DO 3 IC=1, M
      I=IRAND
      RSQ=-LOG(1.-RAND)
      SL=SL+SQRT(RSQ)
3     SS=SS+RSQ
      IF(N.EQ.0) GO TO 2
      DO 4 IC=1, N
      I=IRAND
      RSQ=-LOG(1.-RAND)
4     ST=ST+RSQ
2     R(ISTART-1+IB2)=SL*SL/(SS+ST)
      CALL SORT(R, ISTART, ISTOP, REALS)
      TH(IB1)=.5*(R(ISTOP-OHM)+R(ISTOP-OHM+1))
```

```
21      TT(IB1)=.5*(R(ISTOP-OTM)+R(ISTOP-OTM+1))
        AVH=0.
        SDH=0.
        AVT=0.
        SDT=0.
        DO 22 IB1=1,GROUPS
        AVH=AVH+TH(IB1)
        AVT=AVT+TT(IB1)
        SDH=SDH+TH(IB1)**2
22      SDT=SDT+TT(IB1)**2
        SDH=SQRT((SDH-AVH**2/GROUPS)/((GROUPS-1)*GROUPS))
        SDT=SQRT((SDT-AVT**2/GROUPS)/((GROUPS-1)*GROUPS))
        CALL SORT(R,1,TRIALS,REALS)
        INTH=TRIALS-OHT
        INTT=TRIALS-OTT
        QH=.5*(R(INTH)+R(INTH+1))
        QT=.5*(R(INTT)+R(INTT+1))
        PRINT 23, M,N,QH,SDH,QT,SDT
        PUNCH 23, M,N,QH,SDH,QT,SDT
23      FORMAT(2I10,4E15.9)
1       CONTINUE
        END
```

## REFERENCES


1. A. H. Nuttall and P. G. Cable, Operating Characteristics for Maximum Likelihood Detection of Signals in Gaussian Noise of Unknown Level. I. Coherent Signals of Unknown Level, NUSC Technical Report 4243, 27 March 1972.

2. H. M. Finn, "Adaptive Detection in Clutter," Proceedings of the National Electronics Conference, vol. 22, 1966, pp. 562-567.

3. C. W. Helstrom, Statistical Theory of Signal Detection, second edition, Pergamon Press, New York, 1968.

4. H. L. Van Trees, Detection, Estimation, and Modulation Theory, Part 1, John Wiley and Sons, Inc., New York, 1968.

5. D. Middleton, An Introduction to Statistical Communication Theory, McGraw-Hill Book Co., Inc., New York, 1960.

6. I. S. Gradshteyn and I. M. Ryzhik, Table of Integrals, Series, and Products, Academic Press, New York, 1965.

7. Handbook of Mathematical Functions, U. S. Department of Commerce, National Bureau of Standards, Applied Mathematics Series No. 55, U. S. Government Printing Office, Washington, D. C., June 1964.

8. H. Cramér, Mathematical Methods of Statistics, Princeton University Press, Princeton, New Jersey, 1961.

9. A. H. Nuttall, "Alternative Forms for Numerical Evaluation of Cumulative Probability Distributions Directly from Characteristic Functions," Proceedings of the IEEE, vol. 58, no. 11, November 1970, pp. 1872-1873.

INITIAL DISTRIBUTION LIST

| Addressee | No. of Copies |
|---|---|
| DDR & E | 1 |
| ONR (Code 102-OS, 427, 466, 468, 480) | 5 |
| CNO (Op-098, -098T, -201G, -942U, -96, -96C1(2), -981G, -981H) | 9 |
| CNM (MAT-03, -03L, -03L4, -03P2) | 4 |
| NUC, Pasadena | 1 |
| NRL | 1 |
| NOO (Code 02, 7200) | 2 |
| NAVELEX (Code 03, PME-124) | 2 |
| NAVORD (ORD-93, -05121) | 2 |
| NAVSHIPS (SHP-03, -031, -0371, -2052(4), PMS-302, -302-4, -302-41, -302-5) | 11 |
| NADC, Warminster | 1 |
| NWC, China Lake | 1 |
| NSRDL, Bethesda | 1 |
| NCSL, Panama City | 1 |
| NOL, White Oak | 1 |
| NELC, San Diego | 1 |
| NUC, San Diego | 2 |
| FLTSONARSCOL, Key West | 2 |
| NAVPGSCOL, Monterey | 1 |
| NWC, Newport | 1 |
| APL/UW, Seattle | 1 |
| ARL/Penn State, State College | 1 |
| CENA | 1 |
| DIAST-2B | 1 |
| IRIA | 1 |
| MPL/Scripps | 1 |
| National Research Council | 1 |
| WHOI | 1 |
| NISC | 1 |
| DDC, Alexandria | 12 |